Structure and Bonding

Article *in* Structure and Bonding · November 2013

DOI: 10.1007/430_2013_128

CITATIONS
0

READS
12,486

1 author:

Hanna Lewandowska
Instytut Chemii i Techniki Jądrowej
36 PUBLICATIONS **373** CITATIONS

SEE PROFILE

Struct Bond
DOI: 10.1007/430_2013_102

Coordination Chemistry of Nitrosyls and Its Biochemical Implications

Hanna Lewandowska

Abstract A comprehensive overview is presented of the biologically relevant coordination chemistry of nitrosyls and its biochemical consequences. Representative classes of metal nitrosyls are introduced along with the structural and bonding aspects that may have consequences for the biological functioning of these complexes. Next, the biological targets and functions of nitrogen (II) oxide are discussed. Up-to-date biochemical applications of metal nitrosyls are reviewed.

Keywords Biological action · Electronic structure · Iron proteins · Metal nitrosyls · Nitric oxide · Non-innocent ligands

Contents

H. Lewandowska (✉)
Institute of Nuclear Chemistry and Technology, Centre for Radiobiology and Biological Dosimetry, 16 Dorodna Str., 03-195 Warsaw, Poland

Abbreviations

5C	Five-coordinate
AAA+	ATPases associated with diverse cellular activities
ATP	Adenosine triphosphate
Bax	Bcl-2-associated X protein
BIPM	2,2′-(phenylmethylene)*bis*(3-methylindole)
Bu	Butyl
Cbl	Cobalamin
cGMP	Cyclic guanosine monophosphate
Cp	Cyclopentadienyl
CPMAS	Cross polarization magic angle spinning
CuFL	Fluorescein-copper (II) complex
Cys	Cysteine
DETC	Diethyl thiocarbamate
DFT	Density functional theory
DMSO	Dimethyl sulfoxide
DNDGIC	Dinitrosyl–diglutathionyl–iron complex
DNIC	Dinitrosyl iron complex
DTC	Dithiocarbamate
EDRF	Endothelium-derived relaxing factor
ENDOR	Electron nuclear double beam resonance
eNOS	Endothelial nitrogen (II) oxide synthase
EPR	Electron paramagnetic resonance
Et	Ethyl
FL	Fluorescein
GAF domain	cGMP-specific phosphodiesterases, adenylyl cyclases, and FhlA characteristic domain
GC	Guanylate cyclase
GSH	Glutathione
GSNO	Nitrosoglutathione
GST	Glutathione transferase
GTP	Guanosine triphosphate
H_2bpb	*N*,*N*′-*bis*(bipyridine-2-carboxamido)-1,2-diaminobenzene
Hb	Hemoglobin
HiPIP	High-potential iron–sulfur protein
His	Histidine
HOMO	Highest occupied molecular orbital
HTH	Helix–turn–helix
iNOS	Cytokine-inducible nitrogen (II) oxide synthase

IR	Infrared
IRE	Iron responsive element
IRP	Iron regulatory protein
IUPAC	International Union of Pure and Applied Chemistry
LIP	Labile iron pool
LMW	Low molecular weight
LUMO	Lowest unoccupied molecular orbital
Me	Methyl
metHb	Methemoglobin
MNIC	Mononitrosyl iron complex
MNIP	4-Methoxy-2-(1*H*-naptho[2,3-*d*]imidazol-2-yl)phenol
MorDTC	Morpholyldithiocarbamate
MRP1	Multidrug resistance-associated protein1; iron regulatory protein1
MT	Metallothionein
MTP1	Ferroportin1
NAD	Nicotinamide adenine dinucleotide
naphth-enH_2	2-Hydroxy-1-naphthaldehyde and ethylenediamine
naphth-mphH_2	4-Methyl-*o*-phenylenediamine
naphth-phH_2	*o*-Phenylenediamine
NHase	Nitrile hydratase
NHE	Normal hydrogen electrode
NIR	Nitric oxide reductase
NMR	Nuclear magnetic resonance
nNOS	Neuronal nitrogen (II) oxide synthase
NO	Nitrogen (II) oxide
NorR	Anaerobic nitric oxide reductase transcription regulator
NOS	Nitrogen (II) oxide synthase
NRVS	Nuclear resonance vibrational spectroscopy
OEP	Octaethylporphyrin
$PaPy_3H$	*N*,*N*-*bis*(2-pyridylmethyl)amine-*N*-ethyl-2-pyridine-2-carboxamide
PeT	Photoinduced electron transfer
Ph	Phenyl
porph	Porphyrin
$PPDEH_2$	Protoporphyrin IX diester
PPh_3	Triphenylphosphine
PPN	3-Phenyl-2-propynenitrile
RBS	Roussin's black salt
RRE	Roussin's red salt ester
RRS	Roussin's red salt
RSNO	*S*-nitrosothiol
S_2-o-xyl	Dianion of 1,2-phenylenedimethanethiol
SCE	Saturated calomel electrode
Ser	Serine

sGC	Soluble guanylate cyclase
SNP	Sodium nitroprusside
SoxR	Superoxide response DNA-binding transcriptional dual regulator
SoxS	Activator of superoxide stress genes
TCPP	meso-*tetrakis* (4-carboxyphenyl) porphyrin
TMPyP	meso-*tetrakis* (4-N-methylpyridinium) porphyrin
TPE	Two photon excitation
TPP	Tetraphenylporphyrin
TPRR′	*tris*(pyrazolyl) borato ligand
TTMAPP	meso-*tetrakis* [4-(N,N,N-trimethyl) aminophenyl] porphyrin
Tyr	Tyrosine
UTR	Untranslated region of RNA
UV–VIS	Ultraviolet–visible spectroscopy

1 Introduction

The investigation of transition metal nitrosyl complexes has gained in importance, since the role of nitric oxide (NO) in various physiological processes was discovered. Non-innocent nature of nitric oxide as a ligand and the associated ambiguity in assignment of metal and NO–ligand oxidation states in metal nitrosyls complicate their classification and the interpretation of their electronic spectra and redox properties, chemical behavior, and biological activity. The chemistry of nitrosyl compounds is important, because of the structural, synthetic, and mechanistic implications. This review focuses attention particularly on those nitrosyl complexes that are of direct relevance to biology and medicine. The structural aspects of representative classes of metal nitrosyls of biological significance are reviewed, with particular emphasis on their biological functions and sources, as well as some of their biochemical applications.

2 Structural Aspects for Metal Nitrosyls

NO is a diatomic, stable free radical with an N–O bond length of 1.154 Å and a $^2\Pi$ ground state [1]. Simple molecular orbital theory predicts a bond order of 2.5, consistent with its bond length between those of N_2 (1.06 Å) and O_2 (1.18 Å). The singly occupied MO is a π^* orbital, but polarized toward nitrogen in a manner opposing the polarization of the lower energy π^b orbitals. The result is a relatively nonpolar diatomic molecule; consequently, the ν(NO) stretching vibration, at 1,875 cm^{-1} (15.9 mdynes/cm), has a very low intensity in the infrared absorption spectrum. Because of spin–orbit coupling of the unpaired electron with its π-orbital (~121 cm^{-1}), NO exhibits P, Q, and R rotational branches in its gas-phase vibrational spectrum [2, 3]. The increase in the population of the π^* orbital in the row:

NO^+, NO^0, NO^- leads to the increase in the bond length (1.06 Å, 1.154 Å, 1.26 Å, respectively) and to the decrease in the IR stretching frequencies of ν(NO) from 2,377 for NO^+ to 1,470 cm^{-1} for NO^- [4, 5]. More information on the NO molecule bonding and electronic structure can be found in the chapter by Mingos.

2.1 Bonding in Metal Nitrosylates

Bonding of NO to transition metals usually occurs via the nitrogen atom. Other types of bonding occur in some rare cases and include: twofold and threefold nitrosyl bridges σ/π-dihaptonitrosyls (so-called side-on nitrosyls) and isonitrosyls (M–O–N bound), as reviewed in [6].

Table 1 illustrates a variety of possible NO bonding patterns for which structural data are available. It also gives the IUPAC notations and other ones encountered in the literature [23]. The typical values of the most important structural parameters for the species listed in Table 1 are quoted according to [6]. Structural aspects for each of the group of compounds have recently been reviewed and can be found in the cited reference.

Apart from the above, in biological and biomimetic systems, metals usually bind one or two terminal NO groups. The M–N–O bond angles may be essentially linear or bent, up to ca. 120°. The bridging mode of NO coordination is rarely found in biomimetic systems but is encountered in organometallic and cluster chemistry. In the *molecular orbital* approach, the bonding of NO to a metal can be generally presented as the superposition of two components: The first one involves donation of electron density from the N atom of NO to the metal, involving a σ molecular orbital; the second component is back-donation from metal dπ orbitals to the π* orbitals of NO (π backbonding[1]). The bond order within the ligand is decreased by this process, while the metal–ligand bond order is increased [24]. It is often formally assumed that the NO ligands of metal–nitrosyl moiety are derivatives of the nitrosyl cation, NO^+. The nitrosyl cation is isoelectronic with carbon monoxide; thus, the bonding between a nitrosyl ligand and a metal follows the same principles as the bonding in carbonyl complexes. Yet, the formal description of nitric oxide as NO^+ does not match certain measureable and calculated properties. In an alternative description, nitric oxide serves as a 3-electron donor, and the metal–nitrogen interaction is a triple bond. Both these approaches are presented in the literature. Despite the general analogy between metal carbonyls and nitrosyls, it is noteworthy that NO is even stronger π-acceptor than CO. This manifests itself in the relatively

[1] According to the definition of IUPAC: A description of the bonding of π-conjugated ligands to a transition metal which involves a synergic process with donation of electrons from the filled π-orbital or lone electron pair orbital of the ligand into an empty orbital of the metal (donor–acceptor bond), together with release (back-donation) of electrons from an *n*d orbital of the metal (which is of π-symmetry with respect to the metal–ligand axis) into the empty π*-antibonding orbital of the ligand [7].

Table 1 Classification of metal nitrosyls in terms of the bonding mode of nitrosyl group; according to [6]

Structure diagram	Nomenclatures [7]	Typical structural parameters (according to [6])	Exemplary complex (reference)
M–N–O	*Linear nitrosyl* IUPAC: σ-NO M(NO)	r(NO) = 1.14–1.20 Å r(MN) = 1.60–1.90 Å α(MNO) = 180–160 Å	Manganium porphyrinates [8, 9] $\{Fe(NO)_2\}^9$, e.g., $[Fe(NO)_2(CO)_2]$ $[Co(NO)(CO)_3]$ [10] $[PPN][S_5Fe(NO)_2]$ [11]
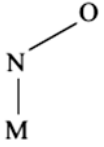	*Bent nitrosyl* IUPAC: σ-NO M(NO)	r(NO) = 1.16–1.22 Å r(MN) = 1.80–2.00 Å α(MNO) = 140–110 Å	Nitrosyl halides, alkanes, and arenes, four-coordinate complexes of Co [12], Os [13], $Fe(NO)_4$ (two of four NO groups) [14] $[Pt(NO)(NO_2)_2(Cl)_3][K]_2$ [15]
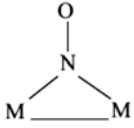	*Normal twofold nitrosyl bridge* IUPAC: μ_2-NO $M_2(\mu_2\text{-NO})$ $M_2(NO)$	r(MM) = 2.30–3.00 Å r(NO) = 1.18–1.22 Å r(MN) = 1.80–2.00 Å α(MNM) = 90–70 Å	$[Mn_2(NO)(X)(\mu_2\text{-NO})_2(Cp)_2]$ (X=Cp [16] or NO_2 [17]) $Ru_3(CO)_{10}(NO)_2$ [18]
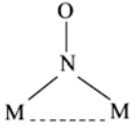	*Long twofold nitrosyl bridge* IUPAC: μ_2-NO $M_2(\mu_2\text{-NO})$	r(M···M) = 3.10–3.40 Å r(NO) = 1.20–1.224 Å r(NM) = 1.90–2.10 Å α(MNM)= 130–110 Å	$Cp_2Mn_2(\mu\text{-NO})_2(NO)_2$ [19]
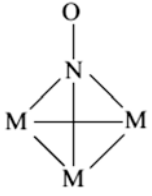	*Threefold nitrosyl bridge* IUPAC: μ^3-NO $M^3(\mu^3\text{-NO})$ $M^3(NO)$	r(NO) = 1.24–1.28 Å r(MN) = 1.80–1.90 Å	$Cp^3Co^3(\mu^3\text{-NO})^2$ [20]

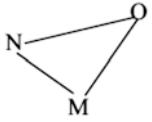	σ/π-*Dihaptonitrosyl* IUPAC: η^2-NO σ/π-NO M(η^2-NO)	r(MN) = 1.70–1.90 Å r(MO) = ca. 1.90–2.00 Å	
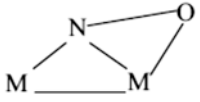	σ/π-*dihaptonitrosyl bridge* IUPAC: η^2, μ_2-NO M_2(η^2, μ_2-NO) M(NO)/M		Metastable states of $2H_2O{\cdot}[Fe(\eta^2\text{-NO})(CN)_5][Na]_2$ (sodium nitroprusside) [21]
M – O – N	*Linear isonitrosyl* IUPAC: σ-ON M(ON)		BrON (metastable state, UV irradiation of BrNO) [22]
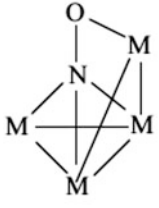 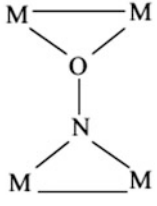	*Isonitrosyl bridges* IUPAC: η^2, μ^4-NO M_4(η^2, μ^4-NO) M_3(NO)M IUPAC: η^2, μ^4-NO M_4(η^2, μ^4-NO) M_2(NO)M_2		Metastable states of $2H_2O{\cdot}[Fe(\eta^2\text{-NO})(CN)_5][Na]_2$ (sodium nitroprusside) [21]

PPN 3-Phenyl-2-propynenitrile, *Cp* Cyclopentadienyl

strong metal–nitrogen bonding, lowering of the bond order within the ligand, and hence the high degree of electron density delocalization in this triatomic fragment. Therefore, in accordance with the Enemark and Feltham notation, MNO is treated as a covalently bound functional group [25] represented as $\{M(NO)_x\}^n$, in which n denotes the total number of electrons associated with the metal d and π* (NO) orbitals. The structure becomes disturbed by the coordination of additional ligands. Energies of π* orbitals of NO are close to d orbitals of transition metals. Therefore, the relative charge distribution in M–N bonding orbitals may vary to a great extent for the two isoelectronic complexes, and very small changes in metal or ligand properties may cause substantial changes in the character of the nitrosyl moiety (NO^+, NO, or NO^-), and consequently, in the NO-donating properties of the complex. Despite the difficulty in assigning formal oxidation states to the metal and the NO in nitrosyl complexes, the charge distribution within this residue, which is comprised between $\{M^{z-1}(NO^+)\}$ $\{M^z(NO)\}$ and $\{M^{z+1}(NO^-)\}$ remains an important issue, particularly with respect to the electronic and magnetic behavior of complexes, as reflected in the chemical properties of the nitrosyls.

A good indicator of the backbonding and bond polarization degree is IR spectroscopy; the NO vibrations are usually observed in the broad region: ~1,300–1,900 cm^{-1}, the higher for the linear, the medium for bent and the lower being characteristic for the bridging mode of NO coordination (see Table 1), as summarized in the chapter on spectroscopy by Lewandowska and in the chapter of Mingos. As noted by McCleverty [5], these three ranges overlap significantly and are strongly dependent on the multiple electronic factors, thus no simple correlation can be seen between the position of ν(NO) and the M–N–O bond angle, unless these factors are allowed for a certain adjustments [6, 13] (see spectroscopic chapter by Lewandowska). The typical N–O and M–N bond distances and M–N–O bond angles for the linear and bent nitrosyls are: 1.14–1.20 Å/1.60–1.90 Å/180–160 Å and 1.16–1.22 Å/1.80–2.00 Å/140–110 Å, respectively [6]. Apart from the vibrational spectroscopy, among other tools applied in the determination of the structure of nitrosyls especially useful are: Mössbauer spectroscopy, nuclear resonance vibrational spectroscopy, and in case of the paramagnetic forms, EPR and ENDOR. Some easily available information on the electronic structure and the geometry of electronic transitions can be found by UV–VIS and magnetic circular dichroism. For even-electron MNO fragments also NMR chemical shifts can give some additional information on the electron charge distribution [26–32]. However, in order to obtain definitive data on the structure it is necessary to complement the results with theoretical methods. Conclusions on nitrosyl structures, which can be drawn from the spectroscopic data will be discussed in the next chapter by Lewandowska.

Comprehensive analyses of the electron charge of metal nitrosyls based on theoretical methods including spectroscopic data have been carried out by Ghosh and coworkers [33–38]. The results of their work are summarized in the chapter by Mingos. In the search of new tools that would allow simple and unambiguous way to determine the electronic nature of transition metal nitrosyl complexes, it has recently been proposed by Sizova et al. [39] to use the quantum chemical bond order indices

deconvoluted into σ-, π-, and δ-contributions, for some organometallic nitrosyls of ruthenium and rhodium with bent and linear configurations of the MNO groups. The new (as regards nitrosyls) approach, considering bond order a good characteristic of electron distribution in molecules, implemented in parallel with the classical structural theory proved useful for structural analysis of nitrosyl complexes. The charges of the NO moieties and the π- and σ-contributions to the bond order were calculated. Unusually large values of through-atom indices confirmed the delocalization of the π-electron density over the linear Ru–N–O fragment. Changes in the electron charge distribution in a series of $\{Ru–N–O\}^{6–7–8}$ complexes were analyzed in terms of the bond order, the metal charge, and the nature of the nitrosyl moiety. This approach allowed the authors [39] to explain the mechanistic aspects of the metal–metal bond destruction in the paddlewheel-type dimetal complexes $M_2(L)_4(NO)_2$ caused by the coordination of nitric oxide.

2.2 Linear Versus Bent Nitrosyl Ligands

Typical ranges for the values of internuclear N–O and M–N bond distances and M–N–O bond-angles are: 1.14–1.20 Å/1.60–1.90 Å/180–160 Å for linear nitrosyls and 1.16–1.22 Å/1.80–2.00Å/140–110 Å, for bent nitrosyls. It should be noted that in some early papers mononitrosyl compounds containing linear M–N–O groups were assumed to contain bound NO^+, whereas those having bent M–N–O arrangements were regarded as containing NO^-, but this has subsequently been found misleading [5]. When applying a *valence bond* approach to a linear M–N–O arrangement, it is convenient to regard the N and O atoms in the NO^+ group as being sp hybridized.

According to the Enemark-Feltham approach, the factor that determines the bent vs. linear NO ligands in octahedral complexes is the sum of electrons of π-symmetry. Complexes with π-electrons in excess of 6 tend to have bent NO ligands. Thus, $[Co(ethylenediamine)_2(NO)Cl]^+$, with seven electrons of π-symmetry (six in t_{2g} orbitals and one on NO), adopts a bent NO ligand, whereas $[Fe(CN)_5(NO)]^{3-}$, with six electrons of π-symmetry, adopts a linear nitrosyl [40].

According to Scheme 1, the electronic configuration for $\{M(NO)\}^6$ will be $(e_1)^4(b_2)^2(e_2)^0$. In such an arrangement, or in any other with fewer metal d electrons (for six-coordinated complex), the population of the strongly bonding (e_1) and nearly nonbonding metal centered (b_2) orbitals, and the vacancy at the antibonding e_2 orbital explain the multiple bond order along the linear MNO moiety. An addition of one more electron, giving the configuration $(e_1)^4(b_2)^2(e_2)^1$ would result in occupation of a totally antibonding π-type orbital. This enforces bending according to Walsh's rules, distortions of the M–N–O bond angle, and a change in symmetry. Mixing of the a_1 and the x component of the previously designated e_2 orbital (see Scheme 1b) affords a more bonding a' level, mainly π*(NO) admixed with d_{z2}, and an equivalent antibonding level which is mainly d_{z2} in

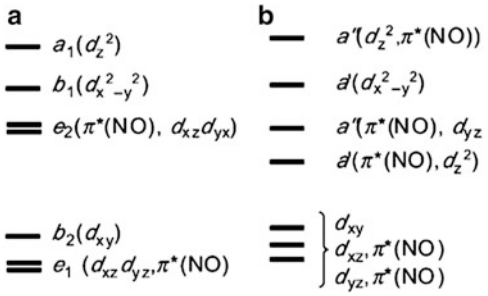

Scheme 1 Arrangement of molecular orbitals in six-coordinate $\{M(NO)\}^n$ when M–N–O is (**a**) 180° and (**b**) 120°. The MNO bond defines the *z*-axis [5]

character. Consequent on the bending of the M–N–O bond, the electronic configuration of the frontmost orbitals in $\{M(NO)\}^7$ will be $(a')^1(a'')^0$. This is equivalent to describing the coordinated nitric oxide as NO•. In $\{M(NO)\}^8$, the electronic configuration in this MO system will be $(a')^2(a'')^0$, representing the coordination of singlet NO^-. The molecular orbital scheme shown in Scheme 1 assumes a relatively strong ligand field, in which the separation of the "t_{2g}" and "e_g" levels is significant [5].

Linear and bent NO ligands can be distinguished using infrared spectroscopy. Linear M–N–O groups absorb in the range 1,650–1,900 cm^{-1}, whereas bent nitrosyls absorb in the range 1,525–1,690 cm^{-1} (please note that these regions overlap). The differing vibrational frequencies reflect the differing N–O bond orders for linear (triple bond) and bent NO (double bond). Application of amendment factors to ν(NO) values proposed by De La Cruz et al. [6], depending on the environment of the central ion and electron configuration, allows a more unambiguous differentiation of the spectral characteristics of nitrosyls (see also the spectroscopic chapter by Lewandowska).

3 Representative Classes for Metal Nitrosyls of Biological Significance

3.1 Homoleptic Nitrosyl Complexes

In contrast to metal carbonyls, homoleptic nitrosyls are rare and include $[M(NO)_4]$ (where M= Cr, Mo, W, the premier member being $Cr(NO)_4$ [25]), $[Co(NO)_3]$, $[Rh(NO)_3]$, $[Ir(NO)_3]$, as well as transient copper and iron nitrosyls [41]. The structure of the latter has been solved just recently, in the work of Lin et al. [14]. The iron teranitrosyl displays three nitrosyl bands, at 1,776, 1,708, and 1,345 cm^{-1} in KBr, and the band at 1,345 cm^{-1} is assigned to the bent N−O vibration. The slightly lower-energy NO bands of complex 1 shifted by ~4 cm^{-1} from those of $[(NO_2)_2Fe(NO)_2]$ (1,782, 1,712 cm^{-1} in KBr) reflect the similar electron-donating ability and

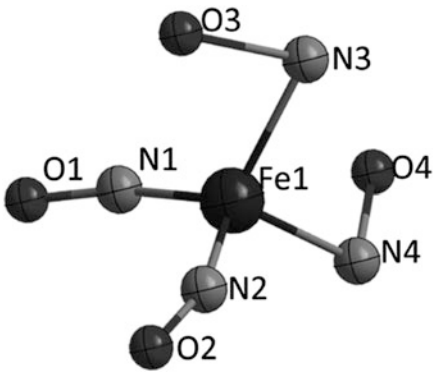

Fig. 1 Spatial structure of dinitroxyldinitrosyl iron. Reprinted from [14], with the permission of the American Chemical Society, copyright 2012

the binding affinity of NO^- and $NO^{2\bullet-}$ ligands toward the $\{Fe(NO)_2\}^9$ motif. The various character of the two coordination modes is explicitly seen in the X-ray structure as the difference between the M–N–O angles (see Fig. 1). Its electronic structure thus is best described as a $\{Fe(NO)_2\}^9$ motif coordinated by two nitroxyl (NO^-) ligands. The infrared and Raman spectra of homoleptic nitrosyls together with DFT calculations are helpful in solving nitrosyl structures of biological importance, as will be shown in the chapter on spectroscopy by Lewandowska.

3.2 Roussin's Red and Black Salts

Roussin's red and black salts were among the earliest synthesized nitrosyl complexes. These iron–sulfur nitrosyls were discovered by Roussin while studying the action of sulfur on solutions of sodium nitroprusside and described in 1858 [42].

Roussin's red salt, $K_2[Fe_2S_2(NO)_4]$ is a historically important complex of a great interest for biochemists, being the first synthetic model of iron–sulfur cluster, analogical to those present widely in proteins (*vide infra*). Moreover, it is already a nitrosylated form of such a cluster, and the cluster nitrosylation just recently has been widely studied, since this process is associated with the regulatory action of many non-heme iron–sulfur enzymes.

Roussin's red salt anion is an edge-shared bitetrahedron, wherein a pair of $Fe(NO)_2$ units are bridged by a pair of sulfide ligands (Scheme 2). The Fe–NO bonds are close to linear indicating that NO is acting as a three-electron donor. The diamagnetic compound obeys the 18-electron rule, and each iron center is assigned the oxidation state of Fe(−I). It is formed during the nitrosylation of the dinucleated Rieskie-type clusters in proteins [43].

Roussin's black salt has a more complex cluster structure. The $[Fe_4(NO)_7S_3]^-$ displays an incomplete cubane geometry of the anion cluster and consists of a tetrahedron of iron atoms with sulfide ions on three faces of the tetrahedron (see Scheme 3). The point group symmetry of the anion is C_{3v}. Three iron atoms

Scheme 2 Roussin's red salt

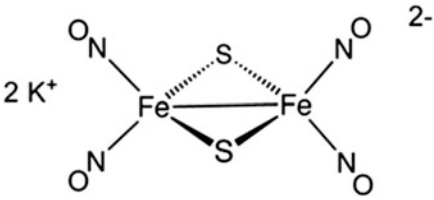

Scheme 3 Roussin's black salt

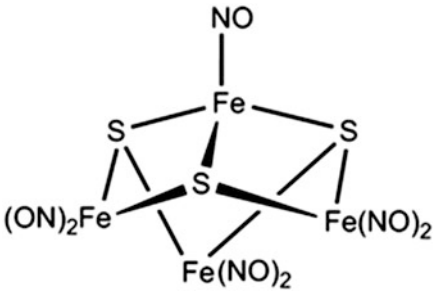

are bonded to two nitrosyl groups. The iron atom on the threefold symmetry axis has a single nitrosyl group which also lies on that axis. Roussin's red and black salts can interconvert among each other upon the change of the pH, according to the reaction given below:

Roussin's Black Salt with the formula $\mathbf{NaFe_4S_3(NO)_7}$ displays an incomplete cubane geometry of the anion cluster. The point group symmetry of the anion is C_{3v} and possesses one $\{FeNO\}^7$ and three $\{Fe(NO)_2\}^9$ units. RBS and RRS interconvert among each other, depending on the pH, from RBS in acidic, to RRS in alkaline solution. Roussin's red salt and its esters (RREs, $Fe_2(SR)_2(NO)_4$, where "R" is an alkyl group) are dinuclear forms of dinitrosyl iron complexes (DNICs, *vide infra*). They are diamagnetic and EPR silent due to the antiferromagnetic coupling between the dinuclear irons. The esters are being investigated as nitric oxide donors in biology and medicine, due to the relatively low toxicity and good stability. In addition, Roussin's salts are discussed in the fields of microbiology and food science due to their mutagenic properties. Their bactericidal effect on the food-spoilage bacteria was demonstrated (see, e.g., [44]). It is known that RREs act as promoters for the carcinogenic properties of other substances for a long period of time (see, e.g., [45]). At the same time attempts to use them against melanoma cancer cells have proven promising [46]. Photolysis of the compounds induced the release of NO, thereby sensitizing target cells to exposure to radiation. Both black and red roussinate anions undergo photodecomposition in aerobic solution to give, eventually, ferric precipitates plus NO, the red roussinate anion being more photoactive. This property of roussinates enables developing photochemical strategies for delivering NO to biological targets on demand [47, 48].

3.3 Mononitrosyl Iron Complexes

Mononuclear mononitrosyl iron complexes (MNIC), designated as $\{Fe(NO)\}^7$ in the Enemark-Feltham notation, have an S = 3/2 ground state in contrast to heme-type $\{Fe(NO)\}^7$ species for which S = 1/2. EPR spectra pointing to formation of MNIC are obtained upon NO treatment of various non-heme iron proteins, such as rubredoxins and mammalian ferritins; yet, these nitrosyls are of transitory character and readily disproportionate into DNICs and Fe(III) thiolates [49]. Reaction of aquated Fe^{2+} salts with NO affords a six-coordinate iron nitrosyl, $[Fe(NO)(H_2O)_5]^{2+}$, an $\{Fe(NO)\}^7$ species. This complex also is formed in the so-called brown ring test for NO_2^- used in simple qualitative analysis [50]. Four-coordinate mononitrosyl iron complexes such as $[Fe(NO)(SR)_3]^-$ are rare but have been known for several decades [51, 52]. Nitrosylation of the biomimetic reduced- and oxidized-form rubredoxin was shown to give the extremely air- and light-sensitive mononitrosyl *tris*(thiolate) iron complexes. Transformation of $[Fe(NO)(SR)_3]^-$ into dinitrosyl iron complexes (DNICs) $[(RS)_2Fe(NO)_2]^-$ and Roussin's red ester $[Fe_2(\mu\text{-}SR)_2(NO)_4]$ occurred rapidly under the addition of 1 equivalent of NO(g) and $[NO]^+$, respectively [53]. Chemistry of the Fe(III) thiolate, $[Fe(SR)_4]^-$, with NO also proceeds to the DNIC through the MNIC, like in case of the Fe(II) complex [53] (Scheme 4). The reactivity of these iron thiolates demonstrates that RS− ligands play a role of reductants during the process of transformation of Fe(II) or Fe(III) to $\{Fe(NO)_2\}^9$ species.

3.4 Dinitrosyl Iron Complexes

An important and representative group of biologically significant nitrosyls are dinitrosyl iron complexes (DNICs). Their occurrence has been observed in many kinds of organisms and in a wide spectrum of physiological conditions associated with inflammation, Parkinson's disease, and cancer. Accumulation of DNICs coincides with intensified production of nitric oxide in macrophages, spinal cord, endothelial cells, pancreatic islet cells, and hepatocytes [55–57]. DNICs are also important in NO-dependent regulation of cellular metabolism and signal transduction [58–61]. Dinitrosyl iron complexes (DNICs) and *S*-nitrosothiols (RSNO) have been known to be two possible forms for storage and transport of NO in biological systems [61]. Depending on the micro-environment, the low molecular weight (LMW) DNICs can provide at least two types of nitrosylating modification of proteins, forming either protein-*S*-nitrosothiols or protein-bound DNICs. Also, DNICs were shown to mediate the iron-catalyzed degradation and formation of *S*-nitrosothiols [53, 62]. Abstracting from the subtitle of this section it is worth to note that the reversible degradation of S-nitrosothiols also was shown to be catalyzed by copper ions [63]. The interaction of NO with $Cu(DTC)_2{\cdot}3H_2O$ (DTC: dithiocarbamate) was studied and the formation of two stable nitrosyl complexes, $Cu(DTC)_2NO$

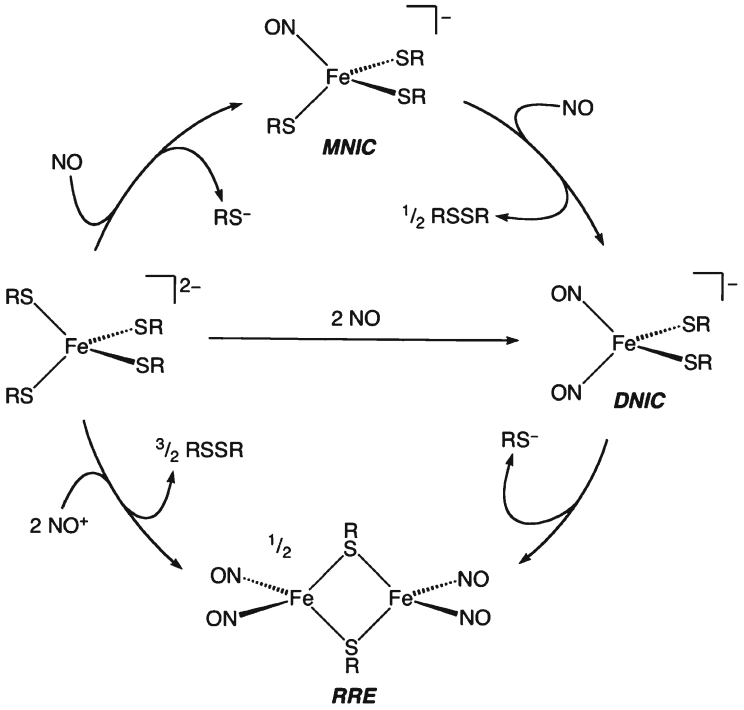

Scheme 4 Redox interconversions between MNIC, DNIC, and RREs. Reprinted from [54], with permission of the American Chemical Society, copyright 2010

and $Cu(DTC)_2(NO)_2$, was proven. The complexes were air-stable and were not disrupted by purging the solution with an inert gas. $Cu(MorDTC)_2NO{\cdot}3H_2O$ was isolated in the solid state and its NO (IR) band was observed at 1,682 cm^{-1}. The latest results by Lim et al., concerning the mechanism of reduction of the 2,9-dimethyl-1,10-phenanthroline copper(II) complex by NO, support an inner sphere mechanism, where the first step involves the formation of a copper–nitrosyl (Cu(II)–NO or Cu(I)–NO^+) adduct, and argue against an outer sphere electron transfer pathway, which was assumed earlier [64]. LMW-DNICs may release NO to various targets. As observed in cells or tissues, LMW-DNICs exerting cyclic GMP-independent effects were attributed to the nitrosylating modification of proteins via transfer of NO or $Fe(NO)_2$ unit, thus yielding protein *S*-nitrosothiols or protein-bound DNICs [65, 66]. The transfer of the $Fe(NO)_2$ motif of LMW-DNIC resulting in the formation of protein-bound DNIC serving as an NO-storage site also was demonstrated in isolated arteries, although the persistent *S*-nitrosylation of protein is another mechanism of formation of releasable NO-storage site in arteries [67–70]. LMW-DNICs elicited an NO release-associated relaxant effect in isolated arteries [71]. Also, it has been proposed

that free thiols/thiolates can displace the proteins of the protein-bound DNICs via thiolate exchange to LMW-DNICs [72, 73]. Protein-bound DNICs are stable for hours and can accumulate in high concentrations in tissues, their stability being lower in the presence of LMW-thiols, due to transnitrosylation [72–74]. The complex relationship between iron and NO and the putative biological role of DNIC have been reviewed by Richardson and Lok [75] and Lewandowska et al. [76]. Although DNICs chemistry has been studied since early 1960s, determination of the electronic structure of the core complex is still a matter of research and discussion [77]. Among the very few dinitrosyl complexes of well-defined structural and spectral parameters are metal dinitrosyl halides [78, 79], $[Fe(NO)_2(CO)_2]$ [80], osmium and ruthenium phenylophosphinates [13, 81–83].

The ON–M–NO angles for DNICs lie between 180° in the *trans* case and 90° in the *cis* case. This has further spectroscopic implications, as further discussed in this volume, in the chapter on spectroscopy. When the two equivalent bent NO groups are attached to the same metal atom in four-coordinate complexes, they can conform either with the NO moieties slightly bent towards each other, or shooting out in opposite directions, in other words N–O–M–O–N fragment can adopt either the *attracto* or the *repulso* conformation. Martin and Taylor [84] concluded that the *attracto* form is characteristic for those dinitrosyls, where N–M–N angle is less than ∼130°, and *repulso* form occurs in complexes with α(NMN) greater than ∼130°.

Regarding the electronic structure of the $\{Fe(NO)_2\}$ core present in DNICs, the known stable DNICs can be classified into three groups: the paramagnetic mononucleated $\{Fe(NO)_2\}^9$ DNICs, the dimerized forms of $\{Fe(NO)_2\}^9$, which are diamagnetic due to electron pairing, and the diamagnetic $\{Fe(NO)_2\}^{10}$ DNICs. Ligands contained in $\{Fe(NO)_2\}^9$ type complexes are (1) thiol groups of amino acids or inorganic sulfur (II) atoms in sulfur clusters, (2) imidazole rings present, e.g., in histidine and purines, (3) pyrole rings of heme-type prosthetic groups [58, 61, 68, 70, 85]. The $\{Fe(NO)_2\}^{10}$ DNICs are coordinated by CO, PPh_3, and N containing ligands [86]. Prototypical DNICs, which contain a single iron atom, are paramagnetic low spin $S = ½$ $\{Fe(NO)_2\}^9$ species. The doublet ground state gives rise to a characteristic axial EPR signal at $g_{av} = 2.03$ [85]. This common spectroscopic signature was a hallmark of DNICs occurrence in both synthetic and biological contexts, dating back several decades to early studies on cancerous liver samples [87]. DNICs typically take the form of an $[Fe(NO)_2(X)_2]^-$ anion, where, in the case of biological milieu, X is a ligand such as a protein-based cysteinate residue or an LMW thiol, like glutathione. The nature of the non-nitrosyl ligands in tissue-derived DNICs is uncertain, and it is assumed that beside thiolate ligands, also imidazole rings present in residues, such as histidine or purines, can form LMW-DNICs. In high molecular weight complexes, thiols are responsible for DNIC formation in non-heme iron proteins, whereas histidine participates in the formation of iron complexes containing heme ligands [76]. A single example of a crystallographically characterized, protein-bound DNIC contains a tyrosinate ligand [88]. Thus, the similarity of the EPR spectra

of thiol- and histidine-derived dinitrosyl complexes in aqueous media precludes unequivocal assignment of their biological role [57, 77, 89]. While dinitrosyl-dithiol iron (II) complexes are well-characterized species in which iron is coordinated by two sulfur atoms and two NO molecules [57], the biological importance of complexes of histidine, NO, and iron has scarcely been investigated. In the very early publication of Woolum [90], it was proposed that the N7 atom of histidine imidazole ring is responsible for coordination of iron and DNIC formation in non-thiol proteins.

According to several authors, the toxicity of DNIC's components seems to be mutually dependent on each other, but the reported results give an ambiguous picture. Bostanci et al. [91, 92] reported attenuation of iron-induced neurotoxicity by nitric oxide synthase inhibitors. On the other hand, the presence of NO donors was reported to protect against iron-induced nephrotoxicity [93, 94]. The reported ability of iron ions to rescue tumor cells from the pro-apoptotic effects of NO is in line with these results, showing a mutual interrelationship of nitric oxide and iron toxicity [95]. Another effect is attributed to coinciding active transport of iron and glutathione outside the cells [96] that was proven to be dependent on MRP1 [97]. The dependence of iron release on glutathione provides evidence that intracellular iron might be depleted via MRP1 in the form of DNIC. It was also shown that depletion of glutathione rendered the cells vulnerable to NO donors [98]. Recently more and more data have been collected on the regulatory functions that DNICs may have in proteins. In addition to the positive regulatory roles of DNICs that are described in the following sections, DNICs are also known for their toxic effects [99]. In particular, diglutathionyl DNIC is a potent and irreversible inhibitor of glutathione reductase [100, 101]. At the same time the formation of DNICs may play a protective role due to their higher stability than that of NO [102]. Denninger et al. found that the formation of DNICs decreases the labile iron pool (LIP[2]) and therefore makes the cell less susceptible to oxidative stress [105]. Several works suggested that LIP is a target for •NO complexation [97, 106, 107]. These findings imply the role of DNICs in the cellular mechanisms of protection against a labile iron surge during inflammation.

DNICs can exist in equilibrium with their dimeric analogs, Roussin's red esters [108]. Several factors including solvent polarity, concentration, and the nature of the thiolate ligand can influence which species predominates in solution [49, 68, 109–112]. In the case of LMW thiolate DNICs, an excess of ligand (usually ca. 20-fold) is required to maintain the mononucleated form. If the concentration of thiol compound is low, the ions are promptly condensed into a binuclear RRE structure via formation of two RS-bridges and release of other two RS-ligands, according to Eq. (1).

[2] The labile iron pool has recently been defined by Cabantchik et al. [103] as the pool of iron labilly bound to low-molecular complexes available for redox reactions. Typical LIP concentration in the cell does not exceed 1 μM [104].

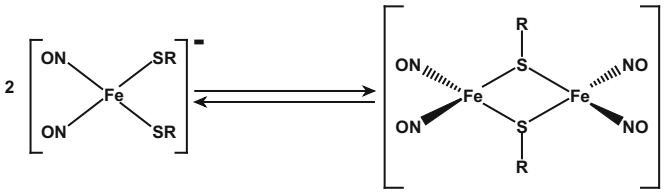

(1)

The above reaction is, in fact, an electrochemically reversible one-electron reduction corresponding to the $\{Fe(NO)_2\}^{9/10}$ couple [113]. In the presence of a different thiol, its S-nitrosation, yielding nitrosothiol and other decomposition products, can also occur [68, 114]. This behavior is responsible for the role of $[(RS)_2Fe(NO)_2]^-$ in the NO storage and NO-transport occurring in vivo [114]. Theoretical explanation of the fact that DNICs tend to form bi-nucleated complexes was presented by Jaworska and Stasicka [115]. According to these authors, the effective overlap of the spatially extensive HOMO orbital (derived from sulfur orbitals) and the LUMO orbital of the d type between two molecules can result in the formation of the RS-bridge. This reaction can be further facilitated by solvent-enhanced polarization of the S–C bond, a contribution of S orbitals to HOMO, and distorted tetrahedral geometry of the complex. A considerable contribution of π^*_{NO} to LUMO and polarization of the NO bond enable the RS nucleophile attack followed by the Fe–NO bond cleavage. Not surprisingly, one-electron reduction of RRE derivatives also gives rise to the corresponding rRREs. Reduced Roussin's red esters have been detected in nitrosylated protein samples that have been subjected to reduction [116]. The $\{Fe(NO)_2\}^9$ units can also occur as a component of several different structures, including a product of [4Fe–3S] cluster nitrosylation known as Roussin's black salt (see above) [51].

As to the geometry of the coordination sphere in DNICs, the anisotropy of the *g* values, determined from the electron spin resonance spectra of frozen solutions, varies considerably from complex to complex. The results are consistent with the view that all these complexes have a distorted tetrahedral geometries, but the extent of the distortion depends on the ligands. As a result of this variation there are changes in the nature of the spin-containing d orbital. Ligands containing hard, nonpolarizable donor atoms such as oxygen or fluorine produce a distortion towards a planar geometry, placing the odd electron in a predominantly $d_{x2\text{-}y2}$ orbital, while those containing softer donor atoms such as phosphorus or sulfur give complexes with a different type of distortion, leading to placement of the odd electron in a predominantly d_{z2} orbital. Nitrogen and halide donor ligands produce smaller distortions, leading to spin-containing molecular orbitals with contributions from a mixture of d orbitals. Bryar et al. [117] suggested that complexes of this type have a structure based on a trigonal bipyramid with a missing ligand. Costanzo et al. [110], based on spectroscopic data, determined the geometry of those complexes as distorted tetrahedral (the electronic configuration $\{Fe\ (NO)_2\}^9$). This conclusion was based on a comparison of the molar extinction coefficients of absorption bands for d–d transitions in typical tetrahedral and octahedral complexes of iron. For

DNICs the extinction coefficients are much higher than those for octahedral complexes and suggest a tetrahedral environment. Since 2001 these predictions have been confirmed in numerous other papers [6, 118–121].

Three electronic states of $\{Fe(NO)_2\}$ are recognized, i.e. paramagnetic $\{Fe(NO)_2\}^9$, diamagnetically coupled $\{Fe(NO)_2\}^9$–$\{Fe(NO)_2\}^9$ ligand-bridged RREs, and $\{Fe(NO)_2\}^{10}$ species [122]. The electronic and geometric structures of paramagnetic iron dinitrosyl complexes were investigated using electron spin resonance, infrared spectroscopy, and X-ray crystallography. It was concluded that these compounds are best described as 17 electron complexes with a d^9 configuration, the unpaired electron being localized mainly around the iron atom. NO groups have partial positive charges (bent nitrosyl groups) and the metal atom charge is close to zero [115]. The earliest conclusion that the electron configuration of iron dinitrosyl complexes is best described as d^9 was formulated in the study of Bryar and Eaton [117], yet proposals for other electronic configurations emerged as well [89], due to the fact that DNICs in solution give characteristic EPR signals implying axial symmetry, while X-ray analyses of DNIC crystals reveal a distorted tetrahedral structure. This inspired Vanin et al. [89, 123, 124] to conclude that in solution d^9 complexes transform into square-planar structures with d^7 configuration, with the unpaired electron localized on the d_{z2} iron orbital. Consequently, taking into consideration the low-spin state of DNICs, d^7 configuration would result in square-planar DNIC spatial structure, whereas the d^9 would imply tetrahedral structure. Crystallographic studies of DNICs with some LMW thiols support the assumption of the deformed tetrahedral configuration with C_{2v} symmetry [110, 111] supporting this suggestion, but it should be noted that (as stated above) the symmetry and coordination of crystalline compounds changes in the solution where their occurrence and metabolism can be observed [89, 123, 124]. Initially it was assumed that DNICs with thiol ligands have octahedral geometries, in which additional ligands, or solvent molecules, are located axially to the plane of the four remaining ligands [123]. The infrared spectroscopy revealed the existence of the inter-isomeric redox equilibrium of the linear and bent NO groups of two forms of $[Ru(NO)_2(PPh_3)_2(Cl)]^+$ [82]. A trigonal bipyramidal form with two linear NO groups has been proposed as the transition state for this process ($E_a < 35$ J mol^{-1}). This is not a unique phenomenon in solution, as shown by the fluxional interconvertibility between the linear NO group of the trigonal bipyramidal structure and the bent NO group of the tetragonal pyramidal structure of a series of compounds of general formulae $[Co(NO)\{P(XY_2)_2\}(Cl)_2]$ [where (X,Y) = (Et/Et), (Bu/Bu), (Me/Ph), (p-Me-C_6H_4) or (Ph/Ph)] [82, 125] (see also spectroscopic chapter by Lewandowska).

The final and decisive conclusion on the electronic configuration and its interchanges among the different isomeric dinitrosyl iron complexes has recently been reviewed by Lu et al. [126]. Their comprehensive research and analysis has unambiguously identified the reduced DNIC as a bimetallic species containing antiferromagnetically coupled $\{Fe(NO)_2\}^9$–$\{Fe(NO)_2\}^{10}$ centers. This electronic configuration gives rise to an S= ½ ground state and an axial EPR signal centered at $g_{av} = 1.99$. The series of papers by Liaw and coworkers [127–132] presents a

thorough and comprehensive analysis of the changes in the electronic structure that occur during the syntheses of DNICs from mononitrosyl complexes, the transformations between four-coordinated and six-coordinated DNICs, as well as the $\{Fe(NO)_2\}^9$–$\{Fe(NO)_2\}^{10}$ interconversions. Changes in the structural properties are illustrated by the spectral shifts and appropriate electronic states have been assigned. An exceptionally interesting example of how the EPR signal geometry changes from axial to rhombic along with the shift between the six-coordinated and four-coordinated $\{Fe\ (NO)_2\}^9$ complex is presented in the paper of Tsai et al. [133]. In contrast to tetrahedral $\{Fe(NO)_2\}^9$ DNICs with an EPR g value of 2.03, the six-coordinate $\{Fe(NO)_2\}^9$ DNIC displays an EPR signal with $g_{av} = 2.013$ (in THF solution). The temperature-dependent reversible transformation occurs between both DNICs. The addition of 2 equivalent of PPh_3 into the hexacoordinate complex promotes O-atom transfer of the chelating nitrito ligand to generate $OPPh_3$, the neutral EPR-silent $\{Fe(NO)_2\}^{10}$ tetracoordinate complex, and NO. Recently, the group of Liaw presented a series of papers on the reversible interconversions between d^9 and d^{10} forms of DNICs. Cyclic voltammetry experiments indicated pseudo-reversibility of the $\{Fe(NO)\}^9 \longleftrightarrow \{Fe(NO)\}^{10}$ redox process, suggesting that the $\{Fe(NO)\}^{10}$ DNICs with thiolate coordination are not as stable as their $\{Fe(NO)\}^9$ counterpart [86]. This finding implies that higher electron density around the Fe center in the $\{Fe(NO)\}^{10}$ DNICs no longer favors an electron-rich coordination sphere by anionic thiolate ligation. According to the EPR Fe K-edge spectroscopic results, the electronic structure of the dimeric d^{10} $[\{Fe(NO)_2\}]_2L_2$ complex is best described as $\{Fe^{II}(NO^-)_2\}^{10}$. The binding affinity of $[SR]^-$ type ligands is greater than that of $[OPh]^-$ in the examined $\{Fe(NO)_2\}^{9/10}$ type complexes, which explains the fact that the most of the DNICs and RREs in living organisms are bound to proteins through cysteinate side chains. As indicated in Scheme 5, the dinuclear DNICs can be classified according to oxidation levels and configurations: the EPR-silent neutral and diamagnetically coupled $\{Fe(NO)_2\}^9\{Fe(NO)_2\}^9$ RRE [134, 135], the EPR-active neutral $\{Fe(NO)_2\}^9\{Fe(NO)_2\}^9$ RRE containing two separate $\{Fe(NO)_2\}^9$ motifs [136], the EPR-silent anionic $\{Fe(NO)_2\}^9\{Fe(NO)_2\}^9$ RRE containing mixed thiolate–sulfide-bridged ligands [137], the EPR-silent $\{Fe(NO)_2\}^9\{Fe(NO)_2\}^9$ Roussin's red salt [138], the EPR active $\{Fe(NO)_2\}^{10}\{Fe(NO)_2\}^9$ reduced RREs [122, 126], and the EPR-silent $\{Fe(NO)_2\}^{10}\{Fe(NO)_2\}^{10}$ dianionic reduced RREs [128]. A direct interconversion between $\{Fe(NO)_2\}^{10}$ DNIC and the $\{Fe(NO)_2\}^9$ DNIC was demonstrated. On the basis of IR ν(NO) stretching frequencies, Fe−N (N−O) bond distances and Fe K-edge pre-edge energy values, the electronic structure of $\{Fe(NO)_2\}^{10}$ core is best described as $\{Fe^{II}(NO^-)_2\}^{10}$. Interconversions were shown to be driven to a specific pathway by the site selective interactions. The distinct S K-edge pre-edge absorption energies and patterns can prove efficient tools for the characterization of the various oxidation-state dinuclear DNICs. The reviewed results indicate that protein-bound $\{Fe(NO)_2\}^{10}$ DNICs dianionic reduced RREs may exist in living organisms. Also, the cysteine-containing $\{Fe(NO)_2\}^{10}$ DNICs, $\{Fe(NO)_2\}^{10}\{Fe(NO)_2\}^{10}$ RREs, and $\{Fe(NO)_2\}^{10}\{Fe(NO)_2\}^9$ reduced RREs may be regarded as the potential species derived from nitrosylation of [Fe−S] proteins. The diversity of DNICs/RREs in

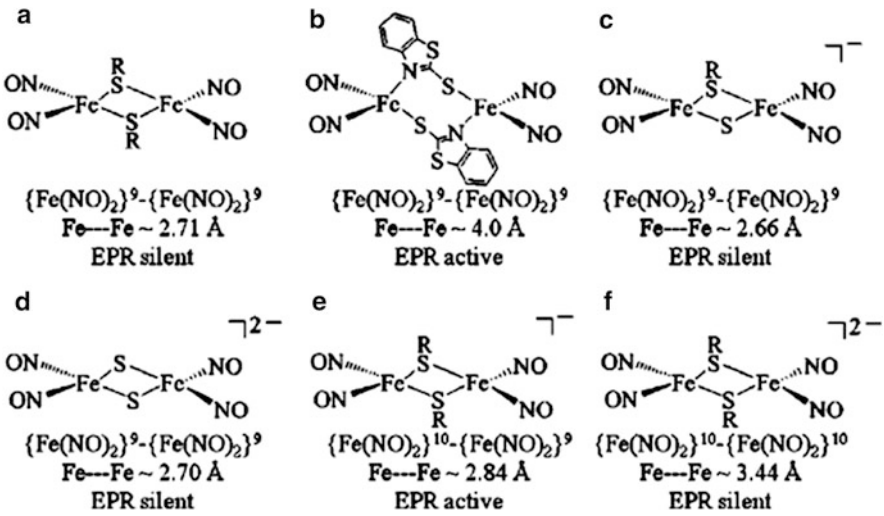

Scheme 5 The various forms of DNICs. Reprinted from [128], with the permission of the American Chemical Society, copyright 2012

biological evolution and bioavailability of a given DNICs/RREs during repair of the modified [Fe−S] proteins remain open questions.

3.5 Iron–Sulfur Cluster Nitrosyls

Iron–sulfur [Fe–S] clusters are ensembles of iron and sulfide centers ubiquitously present in proteins, where they function as prosthetic groups. Fe–S clusters are evolutionary ancient and are involved in sustaining fundamental life processes. The group of known regulatory proteins that contain an iron–sulfur cluster cofactors is growing both in number and in importance, with a range of functions that include electron transfer, sensing of molecular oxygen, stress response, substrate binding/activation, iron regulation and storage, regulation of gene expression. They are involved in a number of enzymatic activities and as well possess structural functions. In some cases, the cluster is required for the protein to attain its regulatory form, while in others the active form requires loss or modification of the cluster [139]. Three main types of [Fe–S] clusters present in biosynthetic systems are presented in Scheme 6. Various synthetic iron sulfur clusters have been synthesized [54, 141].

Most of the research studying the binding of NO to synthetic FeS clusters has been aimed at molecular and/or electronic structural issues and to facilitate the understanding of the reactivity of the coordinated NO group. The reaction of synthetic iron–sulfur clusters (both [2Fe–2S] and [4Fe–4S]) with nitric oxide was

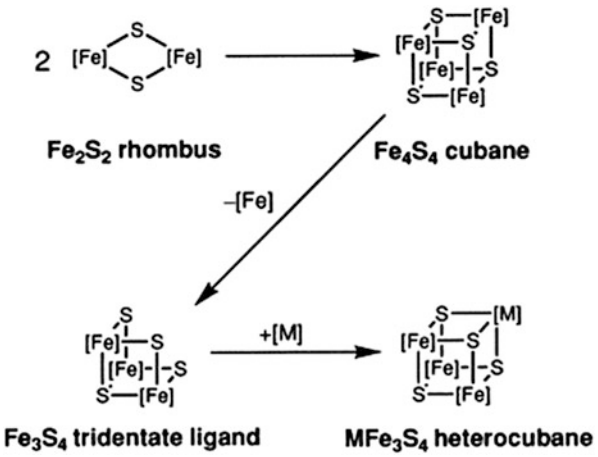

Scheme 6 Some of the important iron–sulfur cluster units found in metalloenzymes. [2Fe–2S] rhombus cluster is characteristic of [2Fe–2S] ferredoxins and Rieskie proteins, [4Fe–4S] cubane – e.g., in [4Fe–4S] ferredoxins, aconitase; [3Fe–4S] clusters are present in the inactive form of aconitase, [3Fe–4S] ferredoxins. The iron vertices, designated as [Fe], have high-spin tetrahedral FeS_4 coordination. Reprinted from [140], with the permission of Elsevier, copyright 2000

first communicated in 1985 [49]. These studies demonstrated the propensity for cluster disassembly by NO and NO^{2-}. Subsequently, it was shown that this process involves the formation of DNICs. The mechanism of cluster nitrosylation was shown to proceed with modification of the sulfur ligands, not thiolates, as in case of homoleptic iron thiolates. An exemplary reaction of that type, for the oxidized synthetic [2Fe–2S] type complex, is given by Eq. (2).

$$\left[Fe_2S_2(SR)_4\right]^{2-} + 4NO \rightarrow 2\left[Fe(NO)_2(SR)_2\right]^{-} + 2S^0 \tag{2}$$

The elemental sulfur that is formed by destruction of the [2Fe–2S] cluster can further react with the DNIC, resulting in oxidation of the thiolate ligands to disulfide and formation of the Roussin's black salt in the reaction of unknown stoichiometry, which can be formally formulated as follows [Eq. (3)].

$$4\left[Fe(NO)_2(SR)_2\right]^{-} + 4S^0 \rightarrow 4RSSR + NO^{-} + S^{2-} \tag{3}$$

The described reaction proceeds slowly for aryl-thiolate DNICs and is fast for alkyl-thiolate complexes. Trapping of the elemental sulfur atoms by phosphine inhibits oxidation [137]. The fate of the sulfide ligands in reactions of biological iron–sulfur clusters with NO remains unknown, although analogically it is expected that sulfur by-products must be sequestered from the vicinity of the iron atoms in order for the DNICs to remain stable. It was shown that the cluster reassembly

proceeds in vivo in aerobically growing *Escherichia coli* cells in the presence of L-cysteine and cysteine desulfurase (thus, via sulfur atom transfer), which is consistent with results using synthetic clusters [142]. The synthetic cluster can be regenerated from the DNIC, in the presence of S_8 and Fe(1,2-benzenedithiolate)$_2$, which serves as a trap for NO [86] or via formation and subsequent reduction of Roussin's red salt in the transnitrosylation reaction with $[Fe(SR)_4]^-$ (this being, however, not relevant to a possible model of [2Fe–2S] repair in vivo). The described processes are affected by O_2, due to nitric oxide oxidation. Consequently, it was shown that a synthetic Rieske-type [2Fe–2S] cluster, $[Fe2(\mu\text{-}S)_2(BIPM)(S_2\text{-}o\text{-}xyl)]^{2-}$(BIPM = 2,2′-(phenylmethylene)*bis*(3-methylindole), S_2-o-xyl = dianion of 1,2-phenylenedimethanethiol), could be nitrosylated to the corresponding *N*-bound and *S*-bound DNICs [143–146]. Unlike DNICs containing thiolate ligands, DNICs containing nitrogen ligands might be expected to undergo redox reactions without decomposition because of a lesser propensity for ligand oxidation. Unlike DNICs, RRE derivatives are EPR silent due to antiferromagnetic coupling between the two $\{Fe(NO)_2\}^9$ units, which gives rise to a diamagnetic ground state. Consequently, tracking the emergence of these species in vivo is more difficult. Presently, a complementary use of UV–vis, Raman, Mössbauer, and nuclear resonance vibrational spectroscopy (NRVS) is employed to aid the identification of protein-bound RREs [147, 148]. A detailed structural characterization of model DNIC-type complexes and mechanistic data on their interconversions are presented by the group of Liaw [14, 53, 86, 122, 126, 127, 136, 149–152]. Of special interest, as regards nitrosylation of proteins, is their recent work on the peptide-bound DNICs and RREs/rRREs [130]. Using aqueous IR, UV–vis, EPR, CD, XAS, and ESI-MS the authors provide data on the dynamic equilibria between high- and LMW DNICs, thus giving insight into the possible mechanisms of interaction between DNICs in nitrosylated proteins. Reaction of [4Fe–4S] clusters from aconitase [116], HiPIP [147], and endonuclease [153] with nitric oxide leads to formation of protein-bound DNICs. As with [2Fe–2S] clusters, the repair of [4Fe–4S] clusters by DNICs has been demonstrated in both protein and synthetic systems [54]. According to the recent results of Crack et al. [145, 154, 155] and Smith et al. [156], the [4Fe–4S] cluster nitrosylation (in *M. tuberculosis* WhiD/WhiB1 proteins, transcription factors in *Actinobacteria*, required for differentiation and sporulation) proceeds via a complex, multiphasic reaction, with a rate at least ~4 orders of magnitude greater than for the reaction with O_2. The first step of the [4Fe–4S] nitrosylation was shown to be first order with respect to NO, and it was concluded that during that process one NO molecule binds to the cluster. This increased the accessibility to further NO binding in the two following steps: these reactions could be observed spectrophotometrically, at 360 nm and 420 nm, respectively. Both were first order for NO, indicating either that a single NO is involved in each one or that NO binding to different irons of the cluster occurs independently, giving an overall first-order dependence. The fluorescence titration data revealed a stable intermediate at a stoichiometry of ~4 NO molecules per [4Fe–4S] cluster. The last step of the reaction was again first order in NO leading to an EPR-silent octa-nitrosylated product(s) with the overall stoichiometry Fe:NO = 1:1.

3.6 *Nitrosylated Porphyrins and Porphyrin Analogues*

The reactions of NO with heme are of great biological significance. The first known physiological target of NO was the soluble guanylate cyclase (sGC). This intracellular NO-sensing enzyme involved in vasodilation is a protein receptor for NO; see Sec. 4.2.1. The generation of NO in vivo is catalyzed by the nitric oxide synthase (NOS) class of enzymes, which belong to the family of heme-thiolate enzymes [157]. NO binds to the ferrous heme in sGC and releases the heme-ligating histidine, resulting in a heme Fe^{2+}–NO complex formation. This reaction triggers a change in heme geometry and a subsequent conformational change of the protein to an enzymatically active form [105]. Hemoglobin nitrosyl complexes are formed with both reduced (Hb(Fe^{2+})) and oxidized (Hb(Fe^{3+}) – metHb) hemoglobin. The iron atom is most often in the reduced state and paramagnetic heme-Fe^{2+}(NO) is formed. The ferrous porphyrin has a greater affinity for NO. In that case the nitrosylation reaction is reversible (see Table 2 for kinetic data). Another heme-type target for NO is cytochrome c oxidase (CcOx, *aliter* Complex IV), the last enzyme in the respiratory electron transport chain of mitochondria (or bacteria) located in the mitochondrial (or bacterial) membrane. Nitrosyl complex formation inhibits cytochrome *c* peroxidase activity due to the impediment of H_2O_2 access to heme Fe. Besides nitrosyl complex formation, cytochrome *c* can participate in redox reactions with NO. Reduction of cytochrome *c* with NO is well known and is analogous to that of Hb [Eqs. (4)–(6)] [167].

$$\text{cyt}\, c^{3+} + \text{NO} \leftrightarrow \text{cyt}\, c^{3+} - \text{NO} \tag{4}$$

$$\text{cyt}\, c^{3+} - \text{NO} \leftrightarrow \text{cyt}\, c^{2+} - \text{NO}^{+} \tag{5}$$

$$\text{cyt}\, c^{2+} - \text{NO}^{+} + 2\text{OH}^{-} \leftrightarrow \text{cyt}\, c^{2+} + \text{NO}_2{}^{-} + \text{H}_2\text{O} \tag{6}$$

The cyt c^{3+}–NO complex can be spontaneously destroyed, and in this case practically the entire NO is converted into nitrite [166]. Besides that, NO can be reduced to nitroxyl anion [NO^-, Eq. (7)], and this reaction is characterized by the rate constant of 200 M^{-1} s^{-1} [166].

$$\text{cyt}\, c^{2+} + \text{NO} \rightarrow \text{cyt}\, c^{3+} + \text{NO}^{-} \tag{7}$$

Both Hb and cytochrome *c* produce stable nitrosyl complexes that in some cases serve as an NO depot in the organism [168–170]. The described nitrosyl complexes are photosensitive and can be destroyed upon irradiation with visible light.

Due to the many biological functions of ferrous heme nitrosyls, many corresponding model complexes have been synthesized and structurally and spectroscopically characterized, viz. tetraphenylporphyrin ($TPPH_2$), octaethylporphyrin ($OEPH_2$) and protoporphyrin IX diester ($PPDEH_2$), meso-*tetrakis* (4-carboxyphenyl) porphyrin (TCPP), meso-*tetrakis* [4-(N,N,N-trimethyl) aminophenyl] porphyrin (TTMAPP),

Table 2 Kinetic and thermodynamic constants for nitric oxide binding to different forms of ferrous and ferric iron

Compound	On rate (M^{-1} s^{-1})	Off rate (s^{-1})	Dissociation constant (M)	Reference
Ferrous compounds				
Hemoglobin (R-state)	2×10^7	1.8×10^{-5}	0.9×10^{-12}	[158]
Hemoglobin (T-state)	2×10^7	3×10^{-3}	1.5×10^{-10}	[158, 159]
Myoglobin	1.7×10^7	1.2×10^{-4}	0.7×10^{-11}	[160, 161]
Cytochrome *c*	8.3×10^0	2.9×10^{-5}	3.5×10^{-6}	[162, 163]
Ferric compounds				
Hemoglobin	4×10^3	1×10^0	2.5×10^{-4}	[144]
Hemoglobin α-chain	3.3×10^3	2.1×10^0	1.4×10^{-4}	[144]
Hemoglobin β-chain	1.3×10^4	3×10^0	2.3×10^{-4}	[144]
Myoglobin (sperm whale)	5.3×10^4	14×10^0	2.6×10^{-4}	[162, 164, 165]
Myoglobin (elephant)	2.2×10^7	40×10^0	1.8×10^{-6}	[144]
Microperoxidase	1.1×10^6	3.4×10^0	3.1×10^{-6}	[165]
Cytochrome *c*	1×10^3	3×10^{-2}	3×10^{-5}	[162, 164, 166]

Adopted from [74], with the permission of Elsevier, copyright 1999

and meso-*tetrakis* (4-N-methylpyridinium) porphyrin (TMPyP) [3, 171–173] (for a more detailed review on the porphyrinate nitrosyls, see also chapter by Lehnert et al.). In addition to these porphyrin-type ligands, there are model chelators mimicking porphyrin binding and geometry designed to obtain certain required spectral or dynamic features. Examples are five-coordinate (5C) Schiff base-type tetradentate macrocyclic ligands. These complexes have structural and vibrational features, which make them good spectroscopic models for 5C ferrous heme-nitrosyls by giving less obscure electronic spectra due to absence of very intense $\pi \rightarrow \pi^*$ transitions of the heme macrocycle [174]. Importantly, vibrational spectroscopy has always been a key technique in examination of heme nitrosyl model complexes, because their vibrational properties are very sensitive to the electronic and spin state of the metal, its coordination number, etc. In the case of ferrous heme nitrosyls, it has been demonstrated that binding of an axial ligand (usually an N- or S-donor) in position *trans* to the NO moiety weakens the Fe–NO and N–O bonds in comparison with the corresponding 5C species. In this way, it increases the amount of radical character (spin density) on the coordinated NO by a *trans*-effect [28, 175]. Other examples of the five-coordinated mononitrosyl Schiff base complexes are those prepared by condensation of 2-hydroxy-1-naphthaldehyde and ethylenediamine (naphth-enH_2), *o*-phenylenediamine (naphth-phH_2), and 4-methyl-*o*-phenylenediamine (naphth-mphH_2) with Co(II) and Fe(II) (in methanol) forming the tetragonal pyramidal mononitrosyls [176]. The iron complexes have temperature-independent magnetic moments corresponding to the high-spin electronic structure (S = 3/2). The cobalt complexes were shown to be diamagnetic $\{Co(NO)\}^8$ species and were shown to contain bent Co–N–O bonds (ca. 125°), as shown by crystallographic studies, and by $^{14/15}N$ NMR spectroscopy in solution and in the solid state [176, 177]. These diamagnetic complexes, like their porphyrinato analogues, are subject to photolysis of the Co–NO bond.

Vibrational methods applied to proteins and model complexes include IR, resonance Raman, and NRVS [173, 178–180]. The interpretation of these vibrational data combined with DFT studies on the reaction mechanisms of heme proteins is frequently based on the porphine approximation, i.e. all porphyrin ring substituents are neglected. Whereas this is intuitively a good approximation for D_{4h}-symmetric macrocycles (e.g., TPP complexes), it is noteworthy that the biologically observed hemes all contain asymmetric substitution patterns on the porphyrin ring [181].

Iron nitrosyl porphyrins may be five- or six-coordinate, the sixth ligand being usually either an N-heterocycle, water, alkyl/aryl, or NO_2^-. The metal–NO bond angles in the diamagnetic $\{Fe(NO)\}^6$ group of complexes lie between 169° and 180°, i.e. are essentially linear, and the Fe–N(O) distances (in the range 1.63–1.67 Å) are generally independent of coordination number. Occasionally, a slight off-axis tilt of the Fe–N–O bond system was observed. The NO stretching frequencies of this group lie between 1,830 and 1,937 cm^{-1}. In model systems, the NO dissociation rates for the complexes of the same heme-type ligand are usually higher for six-coordinated than for five-coordinated species, in line with the negative trans-effect rule. Nevertheless, the electron donating/withdrawing properties of the substituents to the porphyrin ring are critical for the k_{off} rates [160, 173, 182]. Weakening of the FeNO bond resulting from the axial trans base coordination is associated with a lowering of the ν(NO) frequency. Distortions of the porphyrinato ligand do not have any significant effect on the Fe–N–O bond angle [173, 183]. There is a group of complexes consisting major exception to the structural generalities for $\{Fe(NO)\}^6$ porphyrinates referred to above. The most cited are [Fe(NO)(OEP)(C_6H_4F-*p*)], (T(p-OMe)TPP)Ru(NO)Et. In addition to the unexpected bending of the MNO, the nitrosyl group is also tilted off the normal to the porphyrin plane. Analysis of the crystal structure excludes the possibility of steric factors. The tilting of the nitrosyl group was also observed in other nitrosyl metalloporphyrinates. For example, the high-resolution crystal structure for [Co(OEP)(NO)] shows that the axial Co–N (NO) vector is tilted from the normal to the porphyrin plane. The off-axis tilt is correlated with an asymmetry in the equatorial Co–Np bond distances [184]. [Fe(NO)(OEP)(C_6H_4F-*p*)] has an Fe–N–O bond angle of 157° and the Fe–N(O) distance is 1.73 Å, both dimensions more similar to $\{Fe(NO)\}^7$ species, and the Fe–N–O group is tilted significantly off-axis [185]. It was shown early on that this species and its analogues [Fe(NO)(OEP)R] (R = Me, C_6H_5, etc.) are diamagnetic, thus the d^7 configuration is excluded [186]. The NO stretching frequency (1,791 cm^{-1}) and the Mössbauer isomer shift ($\ddot{a}$) 0.14 mm s^{-1} of this complex are significantly different from those of other six-coordinate $\{Fe(NO)\}^6$ species. However, DFT calculations show that the structure of this unusual species represents a minimum energy form. The bending and tilting of the nitrosyl group was proposed to result from the interaction of the NO π* orbital with mixed metal orbitals d_{x2-y2} and d_{xz}. In the $\{Fe(NO)\}^7$ group, the Fe–N–O bond angles are 140–150° and the Fe–N(O) distances 1.72–1.74 Å. The NO stretching frequencies range from 1,625 to 1,690 cm^{-1} and are dependent on the coordination number and the nature of the *trans* axial ligand in the six-coordinate species. These species are paramagnetic ($S = 1/2$), and the Mössbauer spectral isomer shifts vary from 0.22 to

0.35 mm s^{-1} [187]. A comparison of the structures of five-coordinate metal nitrosyl porphyrinato complexes of Mn, Co, Fe, Ru, and Os, based on the $\{MNO\}^6$, $\{MNO\}^7$, and $\{MNO\}^8$, cores reveals that the M–N–O bond angle changes from essentially linear in $\{MNO\}^6$, as exemplified by $[Mn(NO)^-(porph)]$ and $[Fe(NO)(porph)]^+$, through ca. 143° for $\{FeNO\}^7$, to ca. 122° in $\{MNO\}^8$, as in [Co(NO)(porph)] [6, 172, 188]. The M–N–O bond lengths also progressively lengthen, but the displacement of the metal atom out of the N_4 porphyrin plane decreases.

Cobalt nitrosyl porphyrinato-complexes containing the $\{CoNO\}^8$ core are five-coordinate and essentially square pyramidal, the Co–N–O bond angle falling close to 120° [189], although that in [Co(NO)(TPP)] is unexpectedly large (ca. 135°; this may be due to the quality of the X-ray data). This anomaly may be related to the ability of the NO group to swing or rotate about the Co–N–O bond in the solid state, an effect detected by CPMAS NMR spectral studies (see above) [189]. The Co–N(O) bond distances average 1.84 Å, and ν(NO) falls in the range 1,675–1,696 cm^{-1} (KBr or Nujol). Porphyrinato and related (chlorins, isobacteriochlorins) cobalt nitrosyls can be electrochemically oxidized and reduced [190]. In general, oxidation is primarily associated with electron loss from the macrocyclic ligands, affording metal (nitrosyl)-stabilized porphyrin δ-radical cations. Reduction affords mono- and dianionic species which are unstable and readily lose NO. Cobalamin, a precursor of vitamin B_{12}, possessing a corrinoid prosthetic group was shown to inhibit deleterious and regulatory effects of nitric oxide [191–197]. The reduced form of aquacobalamin binds NO under physiological conditions yielding a diamagnetic six-coordinate product with a weakly bound α-dimethylbenzimidazole and a bent nitrosyl coordinated to cobalt at the β-site of the corrin ring. It has also been described as $Co^{III}NO^-$, on the basis of UV–vis, ^1H, ^{31}P and ^{15}N NMR data [198].

Porphyrinato ruthenium complexes contain the $\{Ru(NO)\}^6$ group and are six-coordinate. In ruthenium chemistry, the $\{Ru–NO\}^6$ configuration is generally accepted as NO^+ bound to an Ru(II) center. This is largely based on the high NO stretching frequencies (ν_{NO} = 1,820–1,960 cm^{-1}) noted with $\{Ru–NO\}^6$ nitrosyls, versus that of either free NO (~1,750 cm^{-1}) [199, 200] or bound NO• (1,650–1,750 cm^{-1}) in $\{Ru–NO\}^7$ species [201–205]. Mössbauer [206, 207] and K-edge X-ray absorption spectroscopic data on $\{Fe–NO\}^6$ nitrosyls with similar NO stretches have unequivocally established their formal $\{Fe(II)–NO^+\}$ description. Although similar data on $\{Ru–NO\}^6$ species have not been reported, the $\{Ru(II)–NO^+\}$ formulation best describes most of the $\{Ru–NO\}^6$ nitrosyls. Ruthenium nitrosyls with $\{Ru–NO\}^7$ exhibit lower νNO values (1,650–1,750 cm^{-1}) and a characteristic S = ½ EPR signal of the bound NO• radical near g ≈ 2; their properties, however, have not been fully characterized [200]. With two exceptions, all six-coordinate ruthenium nitrosyl porphyrinato complexes, $[Ru(NO)(porph)L]^+$ (L = neutral ligand), contain an essentially linear Ru–N–O bond angle, the Ru–N(O) bond distance falling in the range 1.74–1.77 Å. The exception to this general rule is $[Ru(NO)(porph)(C_6H_4F\text{-}p)]$ which, like its iron analogue, has a bent Ru–N–O bond angle, 152–155°. The NO stretching frequencies of those species containing linear Ru–N–O range from 1,790 to 1,856 cm^{-1} (KBr), whereas those in the alkyl or aryl species are significantly lower (1,759–1,773 cm^{-1}).

Once again, the *trans* σ-bonding alkyl or aryl ligand exerts a powerful influence on the M–N–O bond angle. Studies on transient intermediates during photolysis of $\{Ru–NO\}^6$ nitrosyls have revealed different modes of binding (and dissociation) of coordinated NO at the ruthenium centers. Metastable NO linkage isomers have been observed for $\{MNO\}^6$ (M = Fe, Ru, Os) and for $\{MNO\}^{10}$ complexes of Ni, as well as for $\{FeNO\}^7$ iron nitrosyl porphyrins [208–212].

3.7 Copper Complexes

Copper-containing enzymes play a central role in denitrification. To date, there have been several types of copper nitrite reductases discovered [213]. These CuNIR are found in many different plants and bacteria. NO_3^- and NO_2^- serve as terminal electron acceptors, ultimately producing NO, N_2O, and/or N_2. All CuNIR contain at least one type 1 copper center in the protein. A copper–NO species has been proposed as a key intermediate in biological nitrogen oxide reduction. The site binding NO_2^- or NO has a distorted trigonal planar molecular geometry that is stabilized by two weaker interactions with a methionine sulfur and a peptide oxygen [214]. The nitrosyl adduct, which has the configuration $\{Cu(NO)\}^{10}$, is described as Cu(I) bound by NO^+. The crystal structure of an intermediate (type 2 copper)-nitrosyl complex formed during the catalytic cycle of CuNIR reveals an unprecedented side-on binding mode in which the nitrogen and oxygen atoms are nearly equidistant from the copper cofactor [215, 216]. The first well-characterized copper nitrosyl coordination compound was derived from a dinucleating ligand (2,6-*bis*[*bis* (2-pyridylethyl)aminomethyl] phenolate) and contains a bridging NO group [217]. The Cu–N–O bond angles are 130°, the N–O bond distance is 1.18 Å, typical of NdO, and $\nu(NO) = 1{,}536\ cm^{-1}$. The coordination around each copper atom is distorted square pyramidal, and the Cu–Cu distance is 3.14 Å, thus nonbonding. Complexes that can be treated as models for the active site of nitrite reductases have been obtained using sterically hindered *tris*(pyrazolyl) borato ligands (TPRR′). The obtained model mononuclear copper–nitrosyl complexes of hydro*tris*(pyrazolyl) borate ligands, with various substituents to the pyrazole ring [Cu(NO)TPRR′], display a pseudotetrahedral coordination geometry, with a terminal N end-on nitrosyl, possessing virtually linear (163.5°–176.4°) M–N–O groups with a short Cu–N(O) bond (1.76 Å). NO addition was reversible, and the complexes reacted with oxygen to form $[Cu^{II}(O_2NO)TPRR']$. It was suggested that these $\{Cu(NO)\}^{11}$ species should be described as Cu(I) coupled to NO• ($S = 1/2$), and so they have one more electron than the proposed active site in nitrite reductase. However, it showed up that very similar structures, varying in the substituted R groups had different magnetic properties. NO(g) dismutation in model complexes is strongly influenced by the nature of the substituents R and R′ on the TPRR′ ligand, as given in the recent review by Gennari [218]. There are various hypotheses on the structure of active complex formed with the copper center during nitrite transmutation to NO: A hypothesis proposed by Averill [219, 220] assumes an initial reduction of the metal center and a subsequent binding of nitrite to Cu(I) by N atom coordination

(analogical binding in model complexes supports this hypothesis). Subsequent protonation of the substrate would give water and an unstable $\{CuNO\}^{10}$ terminal N-bonding nitrosyl. This high-energy complex would promptly release NO and Cu(II), allowing the catalytic cycle to continue. An alternative hypothesis to Averill's proposed mechanism for the catalytic cycle of CuNIR [221–224] considers the initial binding of nitrite to the oxidized copper(II) form, which has the effect of increasing the reduction potential of Cu(II) [225, 226]. This favors the subsequent electron transfer (and dehydration) to give a $\{CuNO\}^{10}$ species that, to minimize structural rearrangements, would display a side-on η^2-NO coordination. For this hypothesis there is that the Cu(II)-nitrito form of CuNIR exhibits η^2-O,O′ coordination of NO_2^- to copper [222, 226] stabilized by hydrogen bond interactions with the protein-matrix side chains. This type of coordination was shown also for some (TPRR′)Cu(II)-nitrito complexes, and it is noteworthy that bulky substituents to the TPRR′ drove an asymmetric coordination mode of NO_2 moiety, like in the active site of CuNIR. Recently it has been discovered that the nitrite ion is bound in a tridentate fashion in the reduced form of CuNIR, with its oxygen atoms coordinated to Cu(I) and an additional weak Cu–N interaction [227], a binding mode promoting minimal structural rearrangements from haptocoordinated NO_2^- towards side-on coordinated NO ($\{CuNO\}^{10}$) species. Side-on coordination of NO to copper was found in the crystal structure of reduced $\{CuNO\}^{11}$ CuNIR [215]. However, it was suggested that this peculiar coordination may be an artifact of the solid state and could not reflect the real situation in solution [228]. The spectroscopic properties of the model complexes, in which NO is end-on bound to the metal, were compared to those of CuNIR [209]. This has allowed for the determination of the binding mode of the $\{CuNO\}^{11}$ species in protein solutions as strongly bent end-on (with a Cu–N–O angle of ~135°), but not side-on [229]. For the detailed review on the copper complexes of NO see the chapter by Tolman et al. in this volume of Structure and Bonding.

4 Nitrosyls in Biology

Probably the first evidence for the formation of nitrosyl complexes of iron in living cells was provided by Commoner and coworkers in 1965 [87]. Using electron paramagnetic resonance spectroscopy, they recorded the signal of the *g* factor 2.04 in the livers of rats with chemically induced cancerous changes [90, 230]. Similar discoveries made simultaneously by Vanin et al. [231, 232] and Maruyama et al. [233]. The EPR signal was correctly interpreted as originating from the complex of iron with two molecules of nitric oxide and other ligands containing sulfhydryl groups. In 1978 Craven proved that nitrosyl–heme complex was involved in activation of guanylate cyclase. Little attention was paid to these findings until 1986, when nitrogen (II) oxide has been identified as an endothelium-derived relaxing factor (EDRF), that is, a chemical responsible for the expansion of the smooth muscle of blood vessels and thus regulating blood

pressure [234–237]. In naturally occurring circumstances nitric oxide is synthesized from L-arginine and oxygen by various NO synthases and by reduction of inorganic nitrate. Formation of DNICs in biological material under the laboratory conditions is observed after the addition of various NO donors, the review on which is presented by Yamamoto et al. [238].

4.1 The Biological Functions of Nitrogen (II) Oxide

Nitrogen (II) oxide, historically referred to as nitric oxide, is now recognized as an important signaling molecule that impacts a wide range of physiological responses, including blood pressure regulation, insulin secretion, airway tone, peristalsis, neurotransmission, immune response, apoptosis; it is also involved in angiogenesis and in the development of nervous system [199]. It is believed to function as a retrograde neurotransmitter and hence is likely to be important in the process of learning [239]. In the living cells NO is enzymatically synthesized from L-arginine by nitric oxide synthases (NOSs) by the stepwise oxidation of L-arginine to citrulline, which is accompanied by the generation of one molecule of NO. Arginine-derived NO synthesis has been identified in mammals, fish, birds, invertebrates, and bacteria [240]. The NO-forming reaction occurs in the oxidase domain of eNOSs, which contains a heme responsible for L-arginine hydroxylation. There is abundant evidence for NO signaling in plants, but plant genomes are devoid of enzyme homologs found in other kingdoms [241]. In mammals, three distinct genes encode NOS isozymes: neuronal (nNOS), cytokine-inducible (iNOS), and endothelial (eNOS) [242]. iNOS and nNOS are soluble and found predominantly in the cytosol, whereas eNOS is membrane associated. eNOS and nNOS take part in the calcium/calmodulin-controlled NO signaling. The inducible isoform iNOS is involved in the immune response and it produces large amounts of NO as a defense mechanism, this being a direct cause of septic shock and playing a role in many autoimmune diseases. It must be noted here that the paramagnetic oxidonitrogen radical is not the only NO form involved in the reactions with diverse biological targets; more and more data bring evidence of the important regulatory functions played by the diamagnetic, one-electron oxidized NO^+ nitrosonium cation, and the one-electron reduced NO^-, the nitroxyl anion (or its protonated form, HNO) [167, 204, 243].

In biological systems nitrogen monoxide is incorporated into its transducers, such as transition metal complexes, in prevailing number of cases, being those of iron and nitrosothiols [61, 244, 245]. The fact that NO is a radical, inspired the idea that incorporation into these biological conveyors determines its existence in biofluids. This supposition was based on the notion that radicals are highly reactive, whereas it was shown that NO can be transported to a distance several-fold exceeding cell sizes [246]. Indeed, free NO can be readily caught by various endogenous cellular scavengers, for example, by exposed heme centers and inorganic ferrous clusters in proteins, oxygen species, and other free radicals [247], the two most obvious NO targets being hemoglobin and superoxide anion. Yet, the NO chemistry is limited.

From the chemical point of view, nitric oxide is a stable free radical, it acts as a σ-donor and π-acceptor. Unpaired electron is localized at 2pπ* orbital, and its loss produces nitrosonium ion NO^+, much more stable than NO. This is seen in the shift of ν vibrations of N–O bond in infrared spectroscopy. ν(NO) of nitrosonium ion is 2,273 cm^{-1}, while these of NO and NO^- are 1,880 cm^{-1} and 1,366 cm^{-1}, respectively. In nitrosyl complexes this band occurs at 1,900–1,500 cm^{-1} [248].

NO is neither readily reduced nor oxidized. Fairly high reduction potential of NO^+ into NO has been estimated to be 1.50 V vs. SCE according to the results of Lee [249], and ca. +1.2 V vs. NHE by Stanbury [250], whereas the recently reexamined reduction of NO to triplet and singlet NO^- was determined to be -0.8 ± 0.2 V for $^3NO^-$ and -1.7 ± 0.2 V for $^1NO^-$, rendering NO inert to direct, one-electron reduction processes under physiological conditions [251]. Conversely, NO^- and its protonated form, HNO show a quite high reactivity towards a broad range of oxidants, reductants, nucleophiles, or metalloproteins, often leading to the formal oxidation of NO^- to NO. Nitrosonium cation, NO^+, is moderately stable in aqueous solutions but highly reactive with nucleophiles or other nitrogen oxides [252]. Both NO^+ and NO^- were shown to display biological activity, distinct from that of NO radical [167]. NO• is isoelectronic with the dioxygen monocation (O_2^+). NO^+ is isoelectronic with CO and CN^-, whereas NO^- is isoelectronic with O_2 and both can exist in singlet and triplet state. This last relationship accounts for the continuing interest in the study of certain types of metal nitrosyl complexes due to their structural and electronic similarity to biological oxygen activators. NO can be an effective probe for examination of spatial and electronic structures and function of metalloenzymes, where a spectroscopic examination of the resting or oxygenated enzyme is difficult or impossible because of instability. Due to that and also to their similar size and hydrophobicity, O_2, CO, and NO have an access to the same cellular iron pools, either labile or protein-bound. They could theoretically compete for binding sites on ferrous iron. Paramagnetic properties of both NO and O_2 result in the addition of unpaired electrons to the system which initiates further interconversions besides simple reversible binding. Nitric oxide affinity for heme-bound Fe^{2+} is much greater than that of CO and O_2. This results mainly from its lower dissociation rate (in some cases $<10^{-5}$ s^{-1}) as compared to O_2 (15 s^{-1} from R-hemoglobin, 1,900 s^{-1} for T-Hb) and CO (ca 10^{-2} s^{-1}; for on-, off-rates and stability constants of NO complexes with ferrous iron in different proteins see [253], see Table 2 for thermodynamics of iron binding to heme). Simultaneously, binding rates of NO are slightly (up to an order of magnitude) higher than those of O_2 and CO. This susceptibility to heme, together with its paramagnetic nature made NO an excellent tool for structural studies of a wide range of heme–iron proteins by means of EPR, as described in the following sections/chapters. Due to this special significance of nitrosyl-iron chemistry, investigations of Fe–NO complexes dominated the literature of nitric oxide interactions with transition metals, although NO complexes with almost all transition metals are known (see references in section 2). NO binding to ferric heme is less reversible than that to ferrous heme due to the possibility of reductive nitrosylation, which yields ferrous iron and nitrite anion [74].

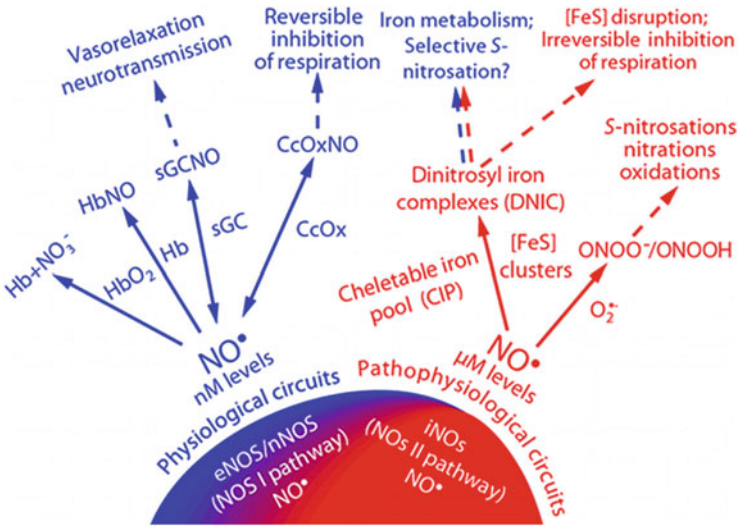

Fig. 2 Nitric oxide signaling relevant to metal nitrosyl chemistry. Reprinted from [254], with the permission of the American Chemical Society, copyright 2012

4.2 The Biological Targets of Nitrogen (II) Oxide

4.2.1 Heme Iron Proteins

Figure 2 illustrates an overview of biological NO signaling pathways relevant to metal nitrosyl chemistry. The two primary targets of NO-mediated regulatory action are: nitric oxide (NO)-sensitive guanylyl cyclase (NO-sensitive GC), the most important NO receptor which catalyzes cGMP formation, and cytochrome *c* oxidase (in the mitochondrial complex IV), which is responsible for mitochondrial O_2 consumption and is inhibited by NO in competition with O_2 [255]. Both these enzymes are hemoproteins and prosthetic heme group is responsible for the regulation of the enzymes by NO [256, 257]. In contrast to other hemoproteins such as hemoglobin or myoglobin, the heme of NO-sensitive GC does not bind oxygen [258]. In the case of cytochrome *c* oxidase inhibition is based upon competitive binding of NO to the O_2 binding site [255].

The soluble guanylate cyclase (sGC) serves as the biological NO sensor/receptor. This enzyme upon its interactions with NO mediates cardiovascular regulation [259–263]. In its active form, sGC contains a five-coordinate (5C) heme with proximal histidine coordination in the ferrous oxidation state [260]. Due to the strong σ-*trans* effect of NO on the axial His ligand, upon binding of NO the Fe(II)–His bond is broken, leading to the corresponding five-coordinated ferrous heme NO complex [28, 175, 264]. Formation of a stable NO–heme complex results in a low-activity species. This is believed to be accompanied by large structural changes that modulate the duration and intensity of the catalytic site of sGC enzyme

activity, which in turn correlates with activation for the conversion of guanosine triphosphate (GTP) to cyclic guanosine monophosphate (cGMP). The latter serves as a secondary messenger molecule involved in relaxation of the vascular smooth muscles, this inducing vasodilation of the arteries, and hence, controlling the blood flow. In the absence of excess NO, GTP accelerates conversion of the transient six-coordinate intermediate to the five-coordinate final species, which is fully active. ATP blocks GTP from accelerating conversion of the intermediate to the final species. When ATP is present together with GTP, both the conversion to the final species and the dissociation of NO from the heme are slow. This species has low activity, and additional NO produces a transient, fully active enzyme [265].

NO binds to ferrous heme iron in a bent mode (i.e., angle between Fe–N–O is 130–150°), whereas in complexes with ferric iron a linear geometry is favored [9, 74]. The bent mode binding is assigned to NO being a one-electron donor, while the linear mode corresponds to NO being a three-electron donor [266]. Dissociation constants of ferric heme complexes fall within the range of 10^{-4}–10^{-7}; this makes them much less stable than the ferrous analogues. For numbers, see [74]. NO penetrates easily through the erythrocyte membrane, and under the action of oxyhemoglobin transforms into non-permeable nitrite ion, which accumulates inside the erythrocyte. Independently, a pool of NO converts to stable S-nitrosothiols with the SH groups of hemoglobin and other proteins. The erythrocyte cell converts into the "depot" of rather stable NO donors [267, 268]. Then, the nitrite ion is easily reduced to NO under the action of deoxyhemoglobin [269, 270]. Therefore, hemoglobin in erythrocytes could be one of the most important elements in the biological transformation of NO donors and NO transport inside the organism. Sanina et al. performed some investigations on the possible interaction of DNICs and hemoglobin and noticed that Hb cannot act as a reductant in the reaction of NO release from DNIC-type complexes [170, 271]. In the case of catalase NO binds to the ferric heme group and thereby inhibits the enzymatic conversion of hydrogen peroxide to water [254, 272]. In this respect, the binding and inhibition of catalase by NO provides a point of cross-talk between the H_2O_2 and NO-mediated redox signaling pathways. The primary site of interaction of NO with mitochondria is the cytochrome c oxidase in the complex IV of the mitochondrial respiratory chain. NO binds to the ferrous iron of heme a_3 in the binuclear site of the enzyme [273] with high affinity ($K_d = 1 \times 10^{-10}$ M) [274] and reaction is very fast with a rate constant of $1 \times 10^8\ M^{-1}\ s^{-1}$ [275].

Nitrite reacts both with oxy- and deoxyhemoglobin. The primary reaction, described in 1981 by Doyle and colleagues, leads to autocatalytic oxidation of HbO_2 to Hb^{3+}, accompanied by the formation of NO and H_2O, and excess nitrite binding weakly to Hb(Fe^{3+}) [276–278]. The affinity of NO to hemoglobin measured at half-saturation is $3 \times 10^{10}\ M^{-1}$, while those of CO and O_2 are 2×10^7 and $6 \times 10^4\ M^{-1}$, respectively. The main reason for such a high affinity is the very slow dissociation of NO from HbNO (mean $t_{1/2} \sim 3$ h) [159, 279] as compared to CO (mean $t_{1/2} \sim 35$ s) and O_2 (mean $t_{1/2} \sim 20$ ms) [280, 281]. It may seem surprising that although it has an exceptionally low off rate from hemoglobin, NO is a fast signal transducer. For example, NO-dependent inhibition of guanylate

cyclase is restored in 50% after less than a minute. This is possible due to preventing bond formation and/or increasing the rate of NO dissociation [74]. In effect, even during endotoxemia in rats (the biological situation where NO production probably is at its maximum) only 2% of the total hemoglobin concentration is trapped as Hb-NO [282]. A complex reaction mechanism has been postulated to prevent the formation of a ferrous-nitrosyl bond during the reaction cycle [219]. It is claimed that heme-proteins' amino acid structure is able to modify the environment of NO–Fe site in a way that allows its much higher dissociation rates. NO dissociation from six-coordinate model heme occurs at least 1,000 times faster than from five-coordinate heme [160]. Another mechanism of NO removal from heme residues can be explained by the reaction of nitrosyl hemoglobin (or myoglobin) with oxygen which generates methemoglobin and nitrate. Different mechanisms have been proposed for this reaction [283]. Binding of NO to ferric heme in many cases leads to reductive nitrosylation. This slow reaction (minutes for hemoglobin in neutral pH) produces ferrous-nitrosyl complex and NO_2^- and can be reversed in the presence of oxygen [164, 284, 285].

4.2.2 Non-Heme Iron Proteins

As described above, the biological properties of NO are generally attributed to its interaction with iron in the heme groups of enzymes. However, NO also interacts with a wide range of other cellular components, many of which do not contain heme [286]. In the case of NO, the ferrous iron frequently remains high spin ($S = 2$) resulting in an EPR signal due to an $S = 3/2$ spin system (when spin coupled to the $S = 1/2$ NO molecule). Similar to iron enzymes, iron storage proteins can react with NO. A complex series of ferritin interactions with NO includes signals from $S = 1/2$ and $S = 3/2$ spin states [287, 288]. It is possible that these interactions are responsible for the ability of NO to release iron from the ferritin stores [287]. Metallothioneins (MTs) are small, sulfur-rich metal-binding polypeptides produced in response to a variety of physiological and environmental stresses. In the presence of iron and NO, both apo-metallothionein and Zn-metallothionein form EPR spectra similar to DNIC [289].

Enzymes that react with oxygen (e.g., monooxygenases, dioxygenases) have the potential to make nitrosyl complexes as shown in the case of lipoxygenase [290, 291]. Alike iron cluster-binding enzymes, iron storage proteins upon the reaction with NO give EPR spectra similar to those of DNICs [288, 292]. One should bear in mind that the EPR-observable DNICs formed with the cellular proteins may not be the only species responsible for nitrosative modification of proteins. Only recently Tinberg et al. [43] reported that in the reaction of NO with Rieske-type [2Fe–2S] clusters dinuclear RRE species instead of mononuclear DNICs are formed. This finding implies that in certain cases RREs may be the primary iron dinitrosyl species responsible for the pathological and physiological effects of nitric oxide.

The electron-transferring iron–sulfur centers in the mitochondrial electron transfer chain are inaccessible to oxygen or NO for steric reasons. However, in iron–sulfur enzymes with non-redox roles [293, 294] it is frequently necessary for LMW compounds (e.g., citrate) to interact with the cluster and therefore, also NO access could not be prevented. These are generally [4Fe–4S] clusters in which three of the iron atoms have cysteine coordination, while the fourth is coordinated by inorganic sulfur. The substrate reacts at the non-cysteine coordinated iron. Most notable of these are mitochondrial and cytoplasmic aconitases.

Mitochondrial aconitase catalyzes isomerization of citrate to isocitrate in the citric acid cycle. It contains a [4Fe–4S] center that is essential for complexing with citrate. $ONOO^-$ has been shown to inhibit the activity of isolated aconitase by a mechanism that is reversed by the addition of iron and thiols [295–297]. Intriguingly, substrate binding seems to prevent this damage [116], suggesting that peroxynitrite cannot access the iron cluster in the presence of citrate in the active site. High concentrations of NO (>100 μM) can also inhibit aconitase activity [295–297] but in contrast to the situation with peroxynitrite, substrate binding did not prevent this inhibition [116].

Cytoplasmic aconitase is identical to the iron regulatory protein 1 (IRP1). When the cellular iron level is low, the enzyme loses its [4Fe–4S] cluster and the apoprotein acquires the ability to bind specific RNA structures called iron responsive elements (IREs) [298–300]. The IRE sequences are located in the mRNA for ferritin (iron-storage protein), the transferrin receptor (cellular iron import protein), and erythroid 5-aminolevulinate synthase (heme biosynthesis catalyzing enzyme) [58, 301]. IRP binding represses the translation of mRNA for ferritin and erythroid 5-aminolevulinate synthase, and protects mRNA for the transferrin receptor against degradation. Described turning on post-transcriptional gene regulation assists the cell in accumulating iron, while preventing high levels of labile iron pool being diverted into storage or heme biosynthesis. The cluster-containing form of the protein has aconitase activity, but does not bind to the IRE, in contradiction to apoprotein. The [3Fe–4S] form of the cluster has neither aconitase activity nor does it bind to the IRE [302]. An interesting issue is interconversion of [4Fe–4S] cluster of this enzyme during formation of DNIC. It is reported that during formation of DNIC in aconitase, cluster is completely or partially removed from the active site. It has been demonstrated that specific NO inactivation of aconitase proceeds by attack at the non-cysteine coordinated iron site and protein-bound iron-sulfur dinitrosyl complexes, giving $g = 2.04$ EPR signals, are formed [100]. Inhibition of mitochondrial aconitase is pH-dependent. No inhibition can be seen in pH 7.5, while a slow inhibition ($\tau_{1/2} = 1$ h) was observed at pH 6.5 for the enzyme at rest [100, 296, 297, 303]. It has been shown that NO may play a role in activating the IRP [58, 304, 305]. When high (μM) levels of NO are produced in activated rodent macrophages and cell lines, the $g = 2.04$ DNIC EPR signal can be detected simultaneously with inhibition of cytoplasmic aconitase activity and activation of the IRP [306, 307]. The mitochondrial aconitase is a constituent of the Krebs cycle; so its inactivation by NO decreases cellular energy metabolism. This inactivation of aconitase may have a protective effect against additional oxidative

stress by acting as a reversible "circuit breaker" [308]. Inactivation results in reduced electron flow through the mitochondrial electron transport chain, and thereby decreases the generation of reactive oxygen species (ROS), the natural by-products of respiration [309, 310]. In fact, it was also suggested, that NO-derived species, like peroxynitrate rather than $NO^{\bullet}$ *per se*, have been proposed to mediate the inactivation of aconitases. Indeed, peroxynitrite reacts vastly with the [4Fe–4S] cluster of aconitase yielding the inactive [3Fe–4S] enzyme [296, 297, 311], yet a number of evidence is also presented for NO-mediated inactivation of iron-sulfur proteins [309–311], the above question being resolved by the group of Drapier [305].

Nitrile hydratase (NHase, EC 4.2.1.84) is a microbial enzyme that catalyzes the hydration of diverse nitriles to their corresponding amides. NHase is a metalloenzyme which contains non-heme Fe(III) or non-corrinoid Co(III) in its catalytic center [312, 313]. Crystallographic studies on Fe-containing NHase from *Rhodococcus* sp. N-771 revealed that the metal center is composed of a cysteine cluster ($C^{109}SLCSC^{114}$) and sulfur atoms from the three cysteine residues Cys109, Cys112, Cys114 and two amide nitrogen atoms of the peptide backbone from Ser113 and Cys114 are coordinated to the iron [314–317]. Interestingly, two cysteine ligands, Cys112 and Cys114, are oxidized to a cysteine sulfinic acid (Cys-SO_2H) and cysteine sulfenic acid (Cys-SOH), respectively. It has been shown that the post-translational oxidation of the Cys-S residues is essential for the catalytic activity of the enzyme [318]. The activity of Fe-NHase is regulated by visible light and dependent on formation of the nitrosyl–iron complex. The active form of the enzyme ($NHase_{light}$) reacts with endogenous nitric oxide to form an $\{Fe–NO\}^6$ complex and yield the inactive form ($NHase_{dark}$). X-ray crystallographic studies of $NHase_{dark}$ reveal an exceptional $N_2S_3Fe–NO$ core with two amido nitrogen donors and three cysteine-derived sulfurs. In the inactive state, an NO molecule occupies the sixth coordination site of the Fe(III) center. Exposure to light causes a rapid loss of NO, and the subsequent binding of water activates the enzyme [319, 320].

Helicases are enzymes that unwind the DNA double helix. They are motor proteins that move directionally along a nucleic acid phosphodiester backbone, separating two annealed nucleic acid strands using the energy derived from ATP hydrolysis. There are many helicases adapted to the great variety of processes in which strand separation must be catalyzed. DinG helicase from *E. coli* plays an important role in recombinational DNA repair and the resumption of replication after DNA damage [321]. The protein contains a redox-active [4Fe–4S] cluster with a midpoint redox potential (E_m) of -390 ± 23 mV (pH 8.0). Reduction of the cluster reversibly switches off helicase activity. The DinG [4Fe–4S] cluster is very stable and the enzyme remains active after exposure to 100-fold excess of H_2O_2, but it can be modified by NO; this results in the formation of the dinitrosyl iron complex and the loss of helicase activity both in vitro and in vivo. It was proposed that modification of the iron–sulfur clusters in DinG and possibly other DNA repair enzymes such as human XPD helicase might contribute to the NO-mediated genomic instability [322].

Gene transcription is a complex process regulated by specific regulatory proteins that bind to the promoter regions of the gene. For example, the [2Fe–2S] centers in

the regulatory protein, SoxR from *E. coli*, are essential for the activation of transcription of a regulon known as SoxS which controls the expression of several genes involved in the defense against activated macrophage-induced oxidative and nitrosative damage [323]. Interestingly, SoxR activation by NO occurs through direct modification of the [2Fe–2S] centers to form protein-bound dinitrosyl-iron-dithiol adducts, which have been observed both in intact bacterial cells and in purified SoxR protein after NO treatment. Another example of a bacterial transcription factor regulated by NO is the NorR protein, a regulatory protein in enteric bacteria known to serve exclusively as an NO-responsive transcription factor. In *E. coli*, NorR activates the transcription of the genes encoding flavorubredoxin and an associated flavoprotein, respectively, which together have NADH-dependent NO reductase activity. The wild-type NorR monomer consists of the three domains: (1) The regulatory, iron-containing N-terminal domain (GAF domain), which was shown to contain a mononuclear non-heme iron center, (2) the central catalytic AAA^+ domain, and (3) carboxy-terminal HTH DNA binding domain. The function of the GAF domain is to sense the signal and inhibit the ATPase activity of the central AAA^+ domain. When exposed to NO, iron center of GAF domain is modified by a single NO molecule to generate a mononitrosyl $\{Fe(NO)\}^7$ ($S = 3/2$) species. Formation of mononitrosyl iron complex triggers a conformational change in the protein that leads to the initiation of transcription: The interaction between the GAF domain and the AAA^+ domain is released, allowing ATP hydrolysis that is further coupled to transcriptional activation [324]. These two examples of functional activation through nitrosylation of iron–sulfur centers contrast with the inactivation typically caused by this modification [325, 326]. In contrast to most dinitrosyl–iron complexes, NO binding is reversible in mononitrosyl systems.

Early papers suggested that DNICs formation with iron–sulfur clusters occurs via transnitrosylation. It was concluded that external iron ions and LMW thiol ligands are necessary in the process of iron–sulfur cluster disruption by NO (see, e.g., [3, 5, 65, 252, 327, 328]). Nevertheless, recent studies on nitrosylation of the biomimetic compounds imply that the most straightforward and facile pathway of the formation of the $\{Fe(NO)_2\}^9$ type DNICs with iron–sulfur proteins is the direct nitrosylation of $[Fe_m(SR)_n]^{x-}$ clusters [118].

4.2.3 Cobalamins

NO is known to react with the cobalt of cobalamins (Cbl). The structure of cobalamin is presented in Scheme 7. Cobalamins containing various axial ligands *trans* to dimethylbenzimidazole moiety are known as vitamin B_{12} and are important cofactors for 5-methyltetrahydrofolate-homocysteine methyltransferase and methylmalonyl-coA mutase playing a key role in the normal functioning of the brain and nervous system and in red blood cell formation [330, 331].

Depending on the axial ligand *trans* to dimethylbenzimidazole, cobalamins differ with their affinity for NO: Aquacobalamin (H_2O-Cbl) and hydroxocobalamin (OH-Cbl) readily react with nitric oxide, unlike cyanocobalamin [CN-Cbl],

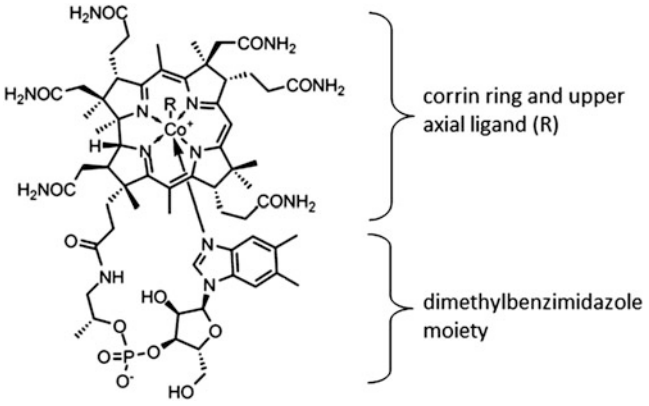

Scheme 7 The structure of cobalamin (α-(5,6-dimethylbenzimidazolyl)cobamidcyanide); R = CN; the axial group R can alternatively be methyl, OH, deoxyadenosyl group [329]

methylcobalamin [Me-Cbl], or adenosylcobalamin [Ado-Cbl] [330]. The reduced form of aquacobalamin binds nitric oxide very effectively to yield a nitrosyl adduct, Cbl(II)−NO [198]. Spectroscopic data suggest that the reaction product under physiological conditions is a six-coordinate complex with a weakly bound dimethylbenzimidazole moiety and a bent nitrosyl coordinated to cobalt at the β-site of the corrin ring. The nitrosyl adduct can formally be described as Cbl(III)−NO^- [198]. The kinetic studies on the binding of NO to Cbl suggested the operation of a dissociative interchange substitution mechanism at the Co(II) center [198]. The laser flash photolysis of cobalamin nitrosyl indicated the formation of water-bound intermediates in the laser flash experiments further supporting the dissociative interchange mechanism.

NO has a high affinity for cobalamin in the 2+ oxidation state [Cbl(II)] but does not react with Cbl(III). NO coordinates to Cbl(II) at all pH values and Cbl(III) does not react with NO at neutral pH. At low pH, however, a two-step process was observed that included the reduction of Cbl(III) to Cbl(II) and Cbl-NO adduct formation [332]. Reduced Cbl (II) with an odd number of outer shell electrons of the central ion is a free radical, and thus EPR spectroscopy can be used to investigate the possible NO interactions with reduced cobalamins [330].

Endogenous cobalamins and cobinamides (Cbi) may play important roles regulating NOS activity in normal and pathological conditions [329]. Regulatory function of cobalamins towards nitric oxide synthases was brought up and discussed by Weinberg et al. [329, 333] and also by Wheatley et al. [334, 335]. Recently, Weinberg et al. [329] reported that OH-Cbl, Cbi, and $(CN)_2$Cbi can potently inhibit the enzymatic function of NOS and thus block the biological formation of NO. It is to be reminded that (as stated above) OH-Cbl can bind and scavenge NO; the same was observed for OH-Cbi; thus, these two agents are able to regulate the NOS/NO system both by decreasing NOS activity and by quenching the existing NO pool. CN_2Cbi, the principal vit. B_{12} form, did not act as NO scavenger (due to the higher affinity of CN for the cobalt center), but it still directly interacted with NOS.

Hydroxocobalamin (OH-Cbl), cobinamide (Cbi), and dicyanocobinamide [$(CN)_2$-Cbi] were shown to potently inhibit ^{14}C-labeled L-arginine to L-citrulline conversion by NOS1, NOS2, and NOS3 [cyanocobalamin, methylcobalamin, and adenosylcobalamin had much less effect, but could be photoactivated (see further in the text)]. OH-Cbl and CN_2-Cbi directly bound to the reduced NOS1 and NOS2 oxygenase domain (as indicated by spectral perturbation analysis) and prevented binding of the oxygen analog carbon monoxide (CO) to heme. NOS inhibition by corrins was rapid and could not be reversed by dialysis with L-arginine (substrate) and tetrahydrobiopterin (a required NOS cofactor). Molecular modeling and UV–vis spectroscopy indicated that corrins could access the unusually large heme and substrate-binding pocket of NOS. The greater ability to inhibit NOS1 than NOS2 relates to the fact that the NOS1 active site pocket is larger than the NOS2 pocket. Best fits were obtained for the "base-off" conformations of the lower axial dimethylbenzimidazole ligand, $(CN)_2$Cbi being the most potent inhibitor.

Application of corrins would allow to regulate both NO and superoxide generation by NOS in circumstances when NO acts in a deleterious fashion (e.g., inflammatory diseases). These agents are well tolerated in high doses, as applied in cyanide poisoning [336, 337]. As high as millimolar blood levels were shown to be accompanied with minimal side effects (red urine and mild, reversible hypertension).

Various cobalamins are known to be light sensitive. Upon irradiation Cbl dissociates the upper (Co[β]) ligand converting to OH-Cbl, a form active as an NOS inhibitor [329]. It was thus proposed that this property of light-activation for NOS inhibition could be useful for site- and time-selective delivery of NOS inhibitors or NO quenchers. As an instance, Me-Cbl and Ado-Cbl are the two corrin derivatives of a very poor inhibitory activity towards NOS. During blue light irradiation of the methylated and adenosylated cobalamin the methyl and adenosyl groups dissociate which results in the formation of OH-Cbl.

Recently it has been reported that cobinamides can act as co-activators of nitric oxide receptor of soluble guanylyl cyclase by direct binding to the catalytic domain of sGC [338]. This offers new possibilities for its therapeutic applications in augmenting the effect of other sGC-targeting drugs.

4.2.4 The Pool of Labile Iron

As mentioned earlier, nitrosyl complexes have been ubiquitously detected in cells and tissues exposed to NO, but the exact origin of the ligands as well as the central ions remains obscure. These complexes are considered to be formed concurrently with low molecular cellular thiol–glutathione and with proteins, but the latter still remain undefined [76, 77, 339, 340]. Dinitrosyl–diglutathionyl–iron complex (DNDGIC) is readily formed in vitro starting from GSH, GSNO, and trace amounts of ferrous ions [341]. The reaction probably occurs after release of nitric oxide through an iron-mediated reaction between GSNO and GSH. DNDGIC may be monitored through the typical EPR spectrum of this complex which shows a

characteristic shape with a maximum at $g = 2.03$. The detection limit of this procedure is about 1 μM concentration for EPR analysis performed at 25°C [59].

A considerable part of labile iron pool (LIP)-formed DNICs originates in lysosomes, since the inhibition of protein disassembly in lysosomes caused up to a 50% decrease in DNIC formation. The process of the DNIC's formation is strictly dependent on lysosomal proteolysis due to the presence of either high levels of labile iron or the free reduced thiols liberated in this process [342]. In addition, the primary iron source for cellular DNICs seems to be LIP and not a prosthetic iron such as iron–sulfur clusters [342, 343]. Nevertheless prosthetic group-bound DNICs were observed and are regarded as modifications having a regulatory role in cellular pathways. Toledo and coworkers found that no DNICs are detectable when cells are treated with very high (10 mM) concentrations of nitrite, ruling out this species as a source of NO ligands in DNIC formation. Comparison of the levels of formed paramagnetic DNICs to the simultaneous consumption of LIP proved that upon addition of close-to-physiological levels of the common NO donors most of the DNICs formed in the cell are paramagnetic [343]. DNICs were shown to emerge under physiologic conditions from low concentrations of •NO (~50 nM) and they formed the largest intracellular fraction of all •NO-derived adducts. At the physiological •NO dose, DNIC concentrations reached slowly (4 h in the conditions of the experiment) a stabile maximum level corresponding to the levels of the labile iron pool (LIP). However, upon exposure to higher steady-state •NO concentrations, DNICs accumulated at levels in two- to threefold excess of the LIP. At cytotoxic concentrations of •NO the LIP no longer was the limiting source of iron for DNIC assembly. It was speculated that, in addition to other, well-known toxic effects of the nitrosyl radical, one consequence of pathologic •NO concentrations may be the accumulation of non-LIP iron in the form of DNICs. Other potential sources of cellular iron, in addition to the LIP, are iron-storage proteins, iron–sulfur clusters, heme, and non-heme iron proteins [344]. These results are consistent with other research, showing high stability in solution and no effect of iron chelators on DNICs decomposition, pointing to an inert character of these complexes [59, 60, 102, 343]. This is confirmed by the analysis of temperature dependence of the EPR signal shape for biological DNICs. The spectra obtained by Watts et al. [97] in •NO-exposed mammary carcinoma cells at 150 K were essentially identical to those obtained at 265 K, implying a large molecular mass of DNICs. Moreover, it was shown that the magnitude of DNIC formation and disappearance in response to changes in O_2 concentrations was much less affected than the overall magnitude of •NO synthesis or •NO degradation in response to changes in O_2. For these reasons the formation of DNIC may function by buffering the dramatic effects of O_2 on •NO synthesis and degradation [344].

4.3 Biological Consequences of DNIC Formation

It is postulated that dinitrosyl iron complexes play an important role in signal transduction pathways regulating the cellular functions [60, 345, 346]. Both low

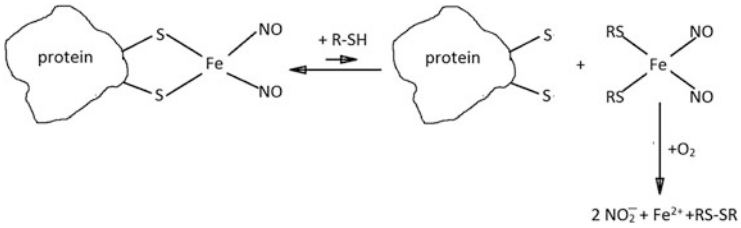

Scheme 8 A proposed model for the LMW-thiol mediated decomposition of protein-bound DNICs. LMW-thiol (e.g., L-Cysteine, glutathione) extrudes the DNIC from the protein-bound DNIC to form LMW-thiol-bound DNIC via thiol ligand exchange. Under anaerobic conditions, both the LMW-thiol-bound DNICs and the protein-bound DNICs are stable, and no DNIC is decomposed. Under aerobic conditions, the LMW-thiol-bound DNIC is rapidly disrupted by oxygen, resulting in eventual decomposition of the protein-bound DNIC [147, 286]

and high molecular DNICs are more stable than the nitrogen (II) oxide and are considered to be its transporters [61, 99]. DNICs also inhibit platelet aggregation, lower blood pressure, dilate blood vessels, induce the formation of proteins in the cellular response to oxidative stress, and modulate the activity of ion channels. Their appearance in cells exposed to NO is closely synchronized with the enzyme activity inhibition of proteins containing iron sulfur centers in the complexes I and II of mitochondrial respiratory chain and of mitochondrial aconitase. DNICs irreversibly inhibit the activity of glutathione reductase, and also reversibly of glutathione transferases. Extremely strong inactivation of these enzymes by DNICs indicates their important role in the metabolism of glutathione [60, 85, 345, 346].

The endogenous production of DNICs has been explained by the binding of NO to iron–sulfur cluster-containing proteins or enzymes in mitochondria and thiol-rich proteins in the presence of free iron [51, 90, 147, 347, 348]. It has been demonstrated that under physiological conditions, DNICs are generated in two forms having LMW thiols or cysteine residues of protein as ligands [68, 69, 90]. Although it has been suggested that an LMW-DNIC with cysteine [DNIC-$(Cys)_2$] possesses activities such as an endothelium-derived relaxing factor (EDRF) [69, 124] and exhibits S-nitrosating activity toward cysteine residues of serum albumin in vitro [61, 68], its physiological role has not been definitely elucidated. One of the reasons may be that in vivo detection of DNICs is very difficult because it can be formed in only a limited quantity under physiological conditions. Investigations of the in vivo distribution and behavior of LMW-DNICs have been conducted by means of EPR spectral measurements on the abdomen of mice treated by the DNIC-$(GS)_2$ [349]. The EPR spectra attributable to DNIC-$(GS)_2$ were detected in the blood, liver, kidney, and spleen; and it was shown that this complex has a relatively high affinity for the liver and kidney [68]. Ueno et al. demonstrated that when an LMW-DNIC-$(GS)_2$ was injected into living mice, different EPR spectral line-shapes were observed emanating from their isolated organs [349]. The appearance of such spectral conversions was explained mainly as the result of chemical modifications by the reaction of LMW-DNICs with thiol-containing compounds such as serum albumin and iron proteins (Scheme 8). It is probable that NO donation from

DNICs to a variety of in vivo targets and their resultant chemical modifications are closely associated with the physiological activities of DNICs.

DNICs have been reported to react with low molecular thiols or protein thiols to yield S-nitrosothiols. Further, DNIC may nitrosate endogenous secondary amines with the formation of nitrosamines [68]. In biological systems, therefore, transnitrosylation by DNIC would be in competition with nitrosation. This is consistent with findings of Ueno et al. [65] that the efficiency of transnitrosylation of Fe-DTC by DNICs is lower in the liver, a thiol-rich organ, than in the kidney.

Apart from their natural biological functions various metal nitrosyls (including organometallic dinitrosyl complexes of Cr and Mo) proved to be very convenient carriers supplying nitric oxide to various biological targets and are presently widely introduced into the therapy as vasodilators and in cancer treatment [350–352], see the chapter by Morris et al. in this volume of S&B.

4.3.1 Interactions of Glutathione Transferases and Dinitrosyl Iron Complexes

Glutathione transferases (GSTs) (EC 2.5.1.18) are a family of enzymes involved in the cellular defense against toxic compounds [353]. GSTs could be involved in the DNIC binding, storage, and detoxification as they can trap these complexes with one subunit, while maintaining their well-known detoxifying *effect* toward dangerous compounds with the other subunit [341]. The human cytosolic GSTs are dimeric proteins grouped into eight classes (Alpha, Kappa, Mu, Omega, Pi, Sigma, Theta, and Zeta) on the basis of amino acid sequence, three-dimensional structure, substrate and inhibitor specificity, and immunological properties [354]. Each subunit contains a binding site for the GSH (G-site) and a second one for the hydrophobic co-substrate (H-site). The most important reaction catalyzed by GSTs is the conjugation of the sulfur atom of GSH to an electrophilic center of many toxic organic compounds; this increases their solubility and enables excretion [353]. Other physiological roles of GSTs include chemical sequestration [355], regulation of Jun kinase[3] [356], inhibition of the proapoptotic action of Bax[4] protein [357], and modulation of calcium channels [358].

Dinitrosyl–diglutathionyl–iron complex binds with extraordinary affinity to the active site of all these dimeric enzymes, showing K_d values of 10^{-10}–10^{-9} M [59, 60, 341]. One of the glutathiones in the iron complex binds to the enzyme G-site, whereas the other GSH molecule is lost and replaced by a tyrosine phenolate in the coordination of the ferrous ion [60] Thus the bound complex is a

[3] c-Jun N-terminal kinases – mitogen-activated protein kinases which are responsive to stress stimuli, such as cytokines, ultraviolet irradiation, heat shock, and osmotic shock, and are involved in T cell differentiation and apoptosis. Kinase (phosphotransferase) – a type of enzyme that transfers phosphate groups from high-energy donor molecules, such as ATP, to specific substrates.

[4] Bcl-2–associated X protein (Bax) is a pro-apoptotic Bcl-2 type protein.

monoglutathionyl species. The binding of DNIC to the first subunit of the dimeric Alpha, Pi, and Mu GSTs triggers intersubunit communication, which lowers the affinity for DNIC of the second subunit that can still bind GSH and maintains the original enzyme activity [341]. In this way, GSTs may protect proteins against the toxic effect of DNIC and simultaneously prevent the extrusion of the free DNIC which would cause iron depletion. Both inactivation and reactivation of GSTs by DNGIC are relatively slow processes, the fastest for GSTA1-1 and the slowest for GSTT2-2. The reactivation is rate-limited by the release of the inactivator from the G-site. K_i values range from 10^{-10} M for GSTA1-1, 10^{-9} M for GSTM2-2, and GSTP1-1 to 10^{-7} M for GSTT2-2 [60]. DNDGIC binds to GSTA1-1, GSTM2-2, and GSTP1-1 with k_{on} values similar to those found for GSH (10^6–10^7 M^{-1} s^{-1}) [359], suggesting that the G-site is open enough to accommodate DNDGIC without gross structural changes. This perfectly agrees with the molecular modeling data that show DNDGIC partially exposed to the solvent and well stabilized in the G-sites of these GSTs. The observed strong affinity is likely due to the coordination of the iron atom to the phenolate group of the conserved Tyr residue of the active site (Tyr-7 in GSTP1-1, Tyr-6 in GSTM2-2, and Tyr-9 in GSTA1-1) which also causes a very slow extrusion of the complex from the G-site (low k_{off} value). A lower k_{on} value for DNDGIC binding appears to be the kinetic determinant of the decreased affinity of the second G-site in the half-saturated GSTs. Thus, negative cooperativity is not caused by a non-optimized geometry of iron ligands in the second G-site (which would cause an increased k_{off} value) but probably by an increased rigidity or shielding of the second G-site triggered by DNDGIC binding to the first subunit. Interestingly, the spectrum of the GST-bound dinitrosyl-iron complexes changes appreciably according to the GST isoform used. The A1-1 and M2-2 GSTs give essentially axial spectra, whereas P1-1 and T2-2 give strongly rhombic spectra; these differences concern the geometry of the ligand arrangement around the iron or the nature of the ligands themselves but not the number of ligands (four), thus indicating a four-coordinated iron with the ligand set [N, N, S^-, O^-] in the bound complex. Because the A1-1, M2-2, and P1-1 show similar K_d values for the dinitrosyl diglutathionyl iron complex, the actual conformation of the bound complex is not important for stability, as long as the iron is coordinated efficiently to both the glutathione and the tyrosine residue.

De Maria et al. noticed that from an evolutionary point of view it appears that the GST superfamily is under selective pressure in the direction of the optimization of the DNIC binding process as more recently evolved classes (Alpha, Mu, Pi) show a higher affinity for DNIC than the Theta class, which is close to the ancestral precursor of all GSTs [60].

4.3.2 The Role of Multidrug Resistance-Associated Protein 1 in the Efflux of DNIC-Bound Iron from Cells

It was shown by Watts et al. that GSH-bound nitrosyl iron takes part in NO-mediated iron mobilization from cells [96]. According to their results, NO-donors induced

an increase in iron release from cells and a decrease in intracellular iron–ferritin levels. GSNO additionally decreased the mobilization of iron from cells and of the intracellular ferritin-iron levels. This decrease was a function of both time and increasing concentrations of nitrosoglutathione. The depletion of GSH prevented an NO-mediated iron efflux from cells, and the decrease in intracellular ferritin-iron levels seen in the presence of GSNO. Iron depletion was caused by a variety of permeable iron chelators. Extracellular high affinity Fe-binding proteins and the extracellular Fe chelators did not enhance NO-mediated iron efflux. GSNO, in contrast to desferrioxamine, did not mobilize iron from cytosolic lysates, while being more effective than DFO at mobilizing iron from intact cells. Finally, Fe mobilization was increased by incubating cells with D-glucose due to the subsequent generation of GSH [96, 97]. Taken together these results allowed the authors to conclude that the NO-mediated Fe efflux occurred as a GS–Fe–NO complex, which was exported from cells by the energy-dependent transport. Furthermore, the authors gave strong evidence that the iron and GSH efflux was the result of metabolic processes, by showing that these processes were dependent on the temperature and ATP. This inspired the authors to investigate the dependence of iron mobilization on the activity of a GSH transporter, multidrug resistance-associated protein 1 (MRP1). And so, the NO-mediated iron efflux was found to be greater in MRP1-hyperexpressing cell lines, while MRP1 inhibitors decreased NO-mediated iron efflux and induced DNIC accumulation in cells. The resulting outline of the interdependence of Fe, NO, GSH, and MRP1 is presented in the report by Watts et al. [97].

4.4 Biochemical Applications of Metal Nitrosyls

4.4.1 Nitric Oxide Donors

The rate of NO release and stability of metal nitrosyls depends mainly on the electron density of the metal centers and the nature of the ancillary ligands. Transition metal ions bind to ligands via interactions that are often strong and selective and the charge of the ion can be manipulated depending on the coordination environment. The thermodynamic and kinetic properties of metal–ligand interactions influence ligand exchange reactions. A partially filled d-shell confers unique electronic and magnetic properties, allows a range of coordination geometries (depending on the resulting electronic structure), and enables 1-electron oxidation and reduction reactions. The potential for designing transition metal nitrosylates with specific thermodynamic parameters makes them an interesting class of NO donors for biochemical and medical applications [360–362]. Some exemplary NO donors are depicted in Scheme 9. Attempts to design agents that deliver NO to a desired target in a controlled manner promise the prospect of obtaining new, NO-based

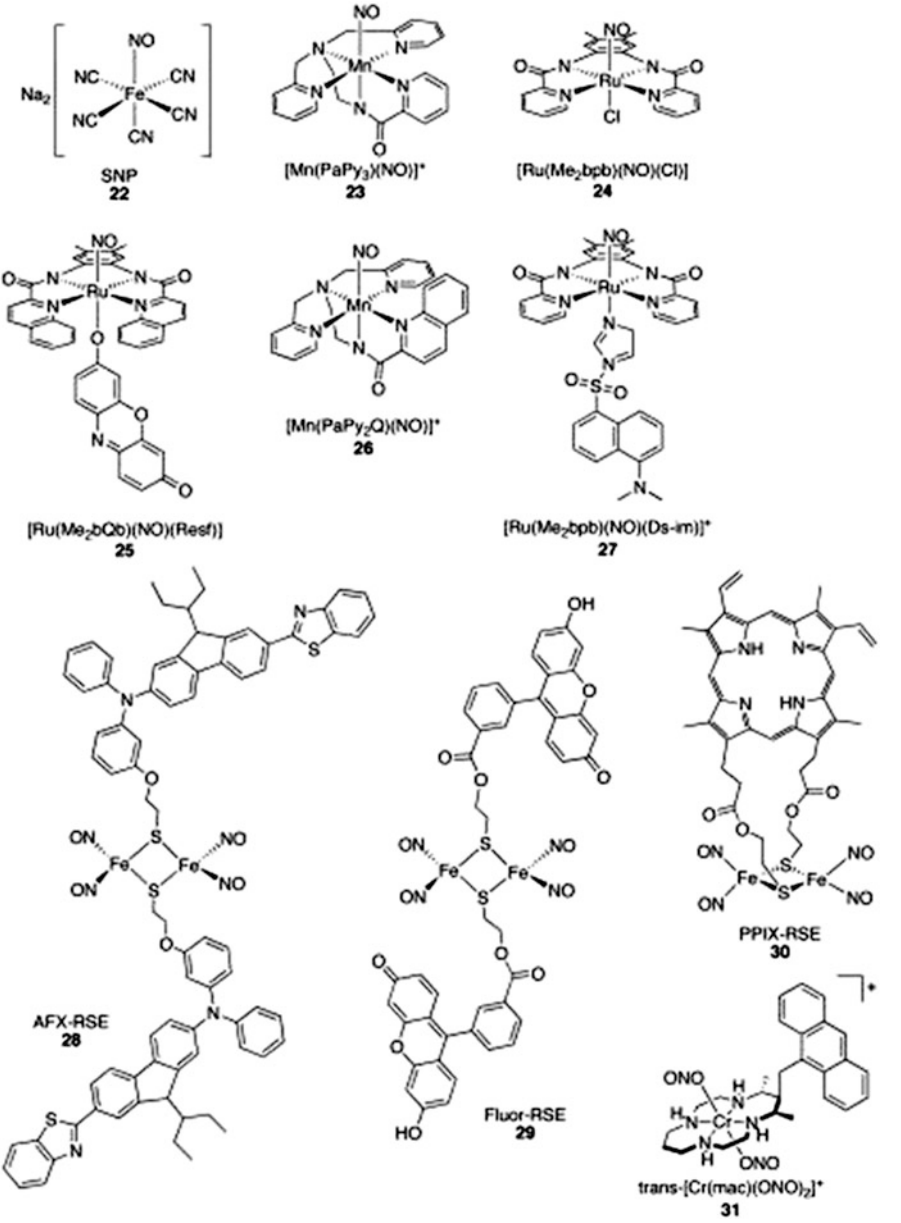

Scheme 9 The chosen NO-releasing metal complexes. Reprinted from [363], with permission of the American Chemical Society, copyright 2009

anti-infectious agents and γ-radiation sensitizers for photodynamic therapy. The known photosensitivity of many metal nitrosyl compounds makes light an attractive stimulus to release NO from a metal center.

The nitroprusside anion, $[Fe(CN)_5NO]^{2-}$, a seemingly simple octahedral coordination complex of Fe(II) with one NO and five cyanide ligands was the first metal-containing NO-donor identified and until recently used as a slow release agent for NO^+. Recently also DNICs have been considered as a potential new class of NO-donating drugs [364]. Depending on the ligand's electron properties DNICs' NO-donating ability can be easily modulated [86] which enables the controlling of DNICs' NO storage and transporting action in biological systems. Syntheses of such preparations are being conducted and initial toxicity tests have already been carried out [86, 89, 150, 365, 366]. Biological levels of NO are quantified by chelators containing iron, such as the iron complex of diethyldithiocarbamate (DETC) [73]. DETC administered to living animals can be visualized by EPR imaging in vivo and ex vivo for MNIC occurrence and thus NO distribution [65, 99, 367]. Another complex that can be used in NO imaging is the NO–Fe complex of N-(dithiocarboxy) sarcosine [368]. Pharmacokinetic methods with the use of EPR X-band imaging were elaborated [369]. The study allowed to evaluate the stability of NO–Fe(II)–DTCS in biological systems and the pharmacokinetic parameters were calculated on the basis of the two-compartment and hepatobiliary transport models. It was revealed that the compound is widely distributed in the peripheral organs and partially excreted into the bile. Also the organotransition–metal mononitrosyl complexes, $CpCr(NO)_2Cl$ and $CpMo(NO)_2Cl$, were examined and proposed as a new class of nitric oxide donors [351].

Photoactive Nitrosyl Donors

Several photosensitive metal nitrosyls including SNP, Roussin's salts, and simple Ru complexes like $[Ru(NO)Cl_5]^{2-}$ have been used as controlled sources of NO to elucidate the biological and neurophysiological roles of NO in cells and tissues. The disadvantages connected with the use of these simple salts include: production of toxic by-products like cyanide, the uncontrolled NO decay (due to pH and thermal instability, spontaneous disproportionation, or oxidation to NO_x) or the undesired reactions of the released metal with biomolecules as in the case of Ru forming DNA adducts [145, 200]. Some effort has been put into designing alternative multidentate ligands that support photoactive Mn and Ru nitrosyl adducts [145, 200, 363], as well as water-soluble Fe complexes [370, 371]. The photoactive metal nitrosylates can be divided into several groups, as described below. The applications of the various metal nitrosyls in therapy are discussed in the chapter by Morris in this volume of Structure and Bonding.

Two-Photon-Excitation-Sensitive NO Donors

The concept of two-photon excitation is based on the idea that two photons of comparably approximately half the energy necessary to excite the molecule also excite a fluorophore in one quantum event. NO donors coupled with the two-photon

excitation sensitive fluorophores should be thermally stable but reactive under excitation at visible (vis) or near-infrared wavelengths where tissue transmission is optimal [372]. In order to enhance the light-gathering capability of light-sensitized NO donors, such as Roussin's red salt esters, Ford and coworkers have attached chromophores with high single- or two-photon absorption cross-sections to several photochemical NO precursors, including aminofluorene chromophore (AFX-RSE, RS = 2-thioethyl ester of N-phenyl-N-(3-(2-ethoxy)phenyl)-7-(benzothiazol-2-yl)-9,9-diethyl-fluoren-2-yl-amine) [373], fluorescein (Fluor-RSE) [374, 375], and protoporphyrin IX (PPIX-RSE) [376]. About 85% of the fluorescence intensity is quenched in these compounds, indicating energy transfer from the antenna to the Fe–NO cluster, ultimately inducing photochemical release of NO. The most commonly used fluorophores have excitation spectra in the 400–500 nm range, whereas the laser used to excite the two-photon fluorescence lies in the ~700–1,000 nm (infrared) range [360]. The probability of the near-simultaneous absorption of two photons is extremely low. Therefore a high flux of excitation photons is typically required, usually a femtosecond laser. Two-photon excitation (TPE) is of special interest, since the use of focused laser pulses to activate release could provide three-dimensional spatial control in therapeutic applications [377].

NO Donors Sensitive to Visible and Near-Infrared Light

Metalloporphyrins, being prone to photolysis-induced release of NO, were promptly recognized as bioregulatory compounds that could deliver NO to a target in a selective manner. Nevertheless, although having intense long-wavelength absorptions, the porphyrinate metal nitrosyls proved to be thermally unstable and oxygen sensitive. Ru–NO porphyrins, being relatively stable and convenient NO donors sensitive to light, suffer from complicated back and side reactions, such as rapid recombination of the photoproducts [360, 378–380]. In contrast, the nitrosyls with non-porphyrin ligands, such as amines, Schiff bases, thiolates, and ligands with carboxamide groups, readily release NO upon illumination and generate controlable photoproducts. For instance, complexes of Fe, Ru, and Mn with pentadentate ligand $PaPy_3H$ (*N,N-bis* (2-pyridylmethyl)amine-*N*-ethyl-2-pyridine-2-carboxamide) providing four nitrogen atom chelation around the equatorial plane of the metal and an additional chelating carboxamide group *trans* to NO proved promising, again the most stable and controllable being complexes of Mn and Ru [379–382]. The strong σ-donor character of the negatively charged carboxamide being *trans* to NO is a key feature in the photolability of these complexes, with the nature of the metal center dictating the wavelength of light required to achieve photo-release. Apart from being light-activated NO donors, these complexes allow the study of fast reactions of NO with heme proteins [383]. The Mn complex is promising with regard to therapeutic applications, as it is activated by visible light (500–650 nm) to release NO and the resulting photoreaction gives the Mn(II) complex, $[Mn(PaPy_3)(H_2O)]^+$, H_2O-substituted in place of NO [384]. Both the Mn and the Ru compounds stimulate soluble guanylate cyclase activity in vitro in a light- and concentration-dependent

manner. They also elicit a concentration-dependent increase in cGMP in the vascular smooth muscle cells, demonstrating that the complexes release NO intracellularly under the control of light. Furthermore, the compounds showed light-dependent vasorelaxant activity in a rat thoracic aortic ring [385].

The photoactivity of metal nitrosyls requires promotion of an electron from a metal-based molecular orbital to a π*(NO) antibonding orbital. Therefore the sensitivity to light depends on the energy of the M→π*(NO) electronic transition [259, 382]. The therapeutic application of these complexes would be facilitated if it proved possible to downshift the activation absorption towards infrared because it would be able to reach deeper into the tissue (light penetration through mammalian tissue is mostly restricted to the 700–1,100 nm region). The bathochromic shift the M-NO bands can be achieved either by changing the metal or the field-strength of the ligand or by attaching light-harvesting chromophores to the complex. A good example is the series of modifications to the bipiridyl ligand, *N*,*N*′-*bis*(bipyridine-2-carboxamido)-1,2-diaminobenzene (H_2bpb); formation of a ruthenium nitrosyl complex with its dimethyl derivative yields a complex, which is only sensitive to low-intensity UV light. However, replacing the pyridal arms with quinolines red shifts the Ru–NO photoband from 380 nm to 455 nm, thereby accessing visible light photoactivation [386]. As the four-coordinate H_2bpb allows an additional coordination *trans* to NO, it is possible to attach a light-harvesting dye directly to the metal, and thus additional sensitization is achieved [387, 388]. The effects of the quinoline arms on the ligand and the dye attached to the metal are additive.

Trackable NO Donors

In addition to acting as light harvesters to increase the photosensitization of NO-donors, the incorporation of fluorescent dyes into NO-releasing compounds can provide a tracking signal to monitor the cellular distribution of the donor. Resorufin or dansyl-containing diamagnetic ruthenium nitrosyls [389] are species that retain appreciable fluorescence intensity of the coordinated dansyl or resorufin dyes. Photoinduced loss of NO gives paramagnetic Ru(III) species that quench fluorescence of the coordinated dyes to an extent related to the amount of NO released [387]. Cell culture studies in human breast cancer cells demonstrated the ability to track the visible light-triggered NO release from these compounds [387, 389].

4.4.2 Nitrosyl Formation-Based NO Sensors

Over the last decade, a number of metal complexes have appeared that give a fluorescence change in response to NO [390]. These include systems based on iron (II) [391, 392], cobalt (II) [393], ruthenium (II) [394, 395], rhodium (II) [396, 397], and copper (II) [398–401].

Metal-based NO probes, in contrast to their organic-based counterparts, take advantage of either direct NO reactivity at the metal center or reactivity at chelated ligand atoms. These probes provide an opportunity to explore direct and reversible sensing, because metals can interact reversibly with nitric oxide. Typically, metal-ligand constructs are assembled where the fluorophore is part of the ligand. In the NO-probe complex the fluorophore emission is quenched by one of the several PeT mechanisms [54]. There are three main strategies for eliciting a fluorescence response from these quenched systems in response to NO: In the first possible instance, resumption of fluorophore emission is accomplished by fluorophore displacement from the quenching site either by releasing the ligand entirely or by removing a chelating arm to a sufficient distance from the metal. In both cases, ligand displacement accompanies NO binding to form a metal nitrosyl. Many metal-based NO-probes utilize this approach, including those containing Co(II) [393], Fe(II) [391, 392], Ru(II) [394], or Rh(II) [396, 397].

Reduction of the metal to form a diamagnetic species can alleviate quenching caused by the paramagnetic metal ions [402]. Typically, this mechanism operates in protic solvents (ROH) and results in transfer of NO to the solvent to form an alkyl nitrite (RONO). This strategy has been employed primarily with Cu(II) probes, which are readily reduced by NO but fail to form stable Cu(I)–NO species [399, 401]. Copper(II) has also been incorporated into conjugated polymers to fashion NO-sensitive films with the use of the intrinsic fluorescence of the polymer as the emitter [400, 403, 404]. Certain modifications, such as incorporating water-soluble functional groups to facilitate biological compatibility, can be applied according to the requirements of the experiment [405].

A third mechanism for restoring fluorescence emission relies both on displacement of the fluorophore and on reductive nitrosylation of the paramagnetic metal center. In this process, NO can either coordinate to the metal [396, 405], as in case of paramagnetic cobalt (II) complex of dansyl fluorophore appended aminotroponiminate [406], or nitrosate either the ligand or solvent, when the latter is protic. In the first case, reaction with NO forms Co(I)–dinitrosyl adducts simultaneously inducing dissociation of a fluorescent ligand, thereby providing an ~8-fold emission enhancement. Secondly, a method recently gaining popularity is determination of nitric oxide using fluorescein-based copper (II) complex (CuFL) that allows the visualization of NO in living cells [407]. The FL ligand coordinates Cu(II) with a K_d of 1.5 μM at pH 7.0 to give a non-fluorescent complex that reacts rapidly and selectively with NO to give an 11-fold increase in fluorescence [408]. It was shown that fluorescence derives from the *N*-nitrosated product FL-NO and also is induced by reacting of FL with S-nitrosothiols. FL-NO no longer binds to Cu(II) or Cu(I) and has a 7.5-fold higher quantum yield than FL itself, indicating that it is the species responsible for the observed fluorescence signal. Neither removal of Cu(II) from the CuFL complex nor addition of Cu(I) to FL gives the dramatic fluorescence enhancement, providing further assurance that the response is NO-dependent and doesn't result of metal release or simple reduction of the probe compound. The advantage of this method of NO determination is also that CuFL easily permeates cell membranes [408]. Another Cu(II)-based NO sensor has also appeared recently

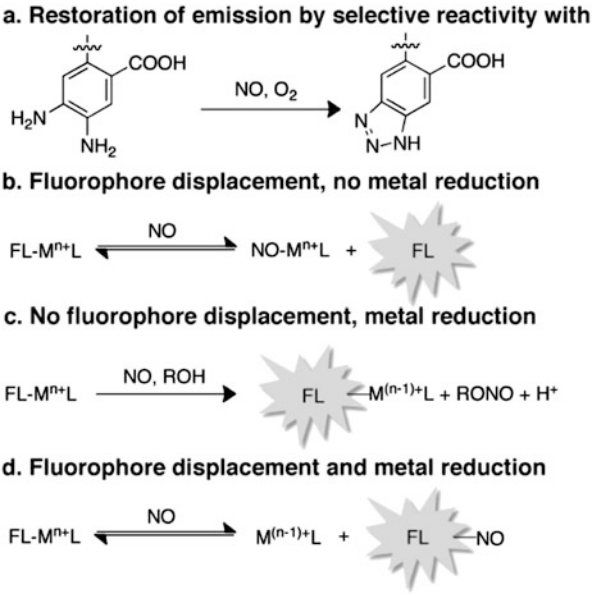

Fig. 3 Possible mechanisms of action for fluorescent NO-sensing probes. Reprinted from [54], with the permission of the American Chemical Society (ACS), copyright 2010

along with the in vivo imaging data. The fluorescent compound, 4-methoxy-2-(1*H*-naptho[2,3-*d*]imidazol-2-yl)phenol (MNIP), binds Cu(II) with 1:1 stoichiometry to give non-fluorescent Cu-MNIP with an apparent K_d in pH 7.4 water/DMSO of 0.6 μM. MNIP-Cu reacts rapidly and specifically with NO to generate a product with blue fluorescence that can be used in vitro and in vivo. The fluorescence enhancement was determined to be a reductive nitrosylation process, where Cu(I) is released from the complex and one of the nitrogen ligands is nitrosylated [409]. The described mechanisms are schematically illustrated in Fig. 3.

5 Conclusions

Nitric oxide (II) is a common free radical produced in living cells through the enzymatic degradation of L-arginine. It displays a number of regulatory functions: it is involved in the processes of neural conduction, regulation of cardiac function and immune defense, it triggers the pathways leading to the controlled cell death – apoptosis. One of the most important and earliest discovered function of NO was to stimulate vasodilation. At the same time, being a free radical, NO is deleterious to the components of living cells.

NO in the unbound form has a very short lifetime in the cell but can be stabilized by the formation of complexes, i.e. metal–porphyrin nitrosyls, dinitrosyl–iron complexes and S-nitrosothiols, which are considered to be its biological transporters. Nitric oxide has a very high affinity for iron contained in the active sites of proteins [74].

Basically one can distinguish three main binding sites of $Fe(NO)_2$ complexes in biological systems (1) the sulfhydryl groups of amino acids and inorganic sulfur atoms, (2) the iron–sulfur centers, (3) the imidazole rings present among others in histidine and purines, (4) the pyrole rings in heme type prosthetic groups. While thiols are responsible for iron binding in non-heme proteins, histidine binds globin to the heme iron of hemoglobin. Proteins containing iron–sulfur centers are the first molecules that undergo nitrosylation under conditions of increased NO production in biological systems [57]. The major protein targets of NO are heme-containing proteins, non-heme iron–sulfur proteins, proteins containing free thiol groups and protein radicals. Among DNICs forming non-protein ligands in living organisms are: the tripeptide glutathione and the amino acids cysteine and homocysteine. Nitrosylation of proteins occurs via direct binding of NO to thiol groups of the peptide chain or by binding of the nitrosylated iron to protein sulfhydryl and imidazole residues. Heme or iron–sulfur centers in proteins exhibit high affinity for nitric oxide. Much of the data indicate that this phenomenon has a significant regulatory function [57]. Nitric oxide and its complexes with biological conveyors are involved in neural conduction, cardiac function, and regulation of immune defense, as well as in directing pathways to the controlled cell death – apoptosis. Therefore, it appears worthwhile to collect spectral data that could clarify the question of metal nitrosyls' electronic structures and affinity of the MNO core to the various ligands of biological importance.

It is postulated that dinitrosyl complexes of iron play an important role in signal transduction pathways by regulating the cell homeostasis [410]. Yet, there is a lack of evidence which of the available thiol ligands in the cell form physiologically active iron nitrosyls; recent reports, however, indicate that a significant portion of these complexes is formed by proteins of high molecular weight [55, 70]. DNICs, both of low and high molecular weight are more stable than the nitrogen (II) oxide and are considered to be its transporters [410]. DNICs also inhibit platelet aggregation, lower the blood pressure, dilate the blood vessels, induce the formation of proteins in the cell response to oxidative stress, and modulate the activity of ion channels. Their appearance in cells exposed to NO is closely synchronized with the enzyme activity inhibition of iron sulfur centers in the complex I and complex II of the mitochondrial respiratory chain and of mitochondrial aconitase. DNICs irreversibly inhibit the activity of glutathione reductase, and reversibly that of glutathione transferases. The extremely strong inactivation of these enzymes by DNICs indicates their important role in the metabolism of glutathione [345, 411]. One- and bi-nucleated dinitrosyl iron complexes induce activation of the oxidative shock response (soxA) gene and cell division inhibiting gene sfiA in *E. coli*. Activation of these genes occurs as a result of DNICs action and is not caused by iron ions or nitric oxide alone [412]. Another proposed function of DNICs is to regulate the amount of labile iron in cells [97, 105]. Labile iron pool (LIP) was defined by Cabantchik et al. as the iron present in the cell in the form of highly dissociable complexes with low molecular weight ligands, and accessible in redox reactions [103]. In addition to these revealed and partially explored functions metal nitrosyls have within the organisms, there may yet be other potentially to be discovered. A putative new function of the $\{Fe(NO)_2\}^{10}$

type DNIC has recently been proposed by Tran et al. [413], who has reported the dioxygen-related reactivity of a bidentate N-ligand bound $\{Fe(NO)_2\}^{10}$ nitrosyl. In the presence of O_2, an unstable complex was formed being presumably a peroxynitrite [Fe(L)(NO)(ONOO)]. The complex exhibited nitrating properties towards 2,4,-di-tert-butylphenol, which suggests that DNIC-type d^{10} complexes might be involved in the processes of nitration of biological phenols, among which protein tyrosine nitration is an important posttranslational modification associated with various pathological conditions including inflammatory, neurodegenerative, and cardiovascular diseases.

The molecular and electronic structure of DNICs continues to be actively studied and discussed [77]. Most of the classification and theoretical structure predictions for nitrosyl complexes of iron and other transition metals are based on diagrams developed by Enemark and Feltham [25]. The construction of nitrosyl complexes proposed by these authors assumed $M(NO)_x$ to be a group of covalently bound atoms, whose structure is modified by the coordination of additional ligands. The energies of transition metal d orbitals are close to the π^* orbital energy of nitric oxide. Thus, the relative charge distribution between the metal and NO group at the M and N binding orbitals may be significantly different between the two isoelectronic complexes, and relatively small changes in the properties of metal or ligand can cause a significant change in the properties of the complex.

Formation of iron nitrosyl complexes is a major biological mechanism that allows direct detection of nitric oxide in cells [414]. Nitrosyl complexes of iron, due to their paramagnetic properties, were the first identified nitric oxide compounds in living organisms long before their numerous regulatory functions were discovered [87]. Currently, research is being conducted aimed at the synthesis of new dinitrosyl iron complexes, which would be applicable in biochemistry and medicine, as donors of nitrogen (II) oxide, mimicking the action of natural NO conveyors (see, e.g., [54, 119]).

Acknowledgments The author wishes to thank Professor I. Szumiel from the Institute of Nuclear Chemistry and Technology for her invaluable meritorical and editorial remarks.

References

1. Greenwood NN, Earnshaw A, Earnshaw A (1997) Chemistry of the elements. Butterworth-Heinemann, Oxford
2. Laane J, Ohlsen JR (1980) Characterization of nitrogen oxides by vibrational spectroscopy. In: Progress in inorganic chemistry. Wiley, New York
3. Ford PC, Lorkovic IM (2002) Mechanistic aspects of the reactions of nitric oxide with transition-metal complexes. Chem Rev 102:993–1018
4. Richter-Addo GB, Legzdins P (1992) Metal nitrosyls. Oxford University Press, Oxford
5. McCleverty JA (2004) Chemistry of nitric oxide relevant to biology. Chem Rev 104:403–418
6. De La Cruz C, Sheppard N (2011) A structure-based analysis of the vibrational spectra of nitrosyl ligands in transition-metal coordination complexes and clusters. Spectrochim Acta A Mol Biomol Spectrosc 78:7–28

7. McNaught AD, Wilkinson A (2012) IUPAC. Compendium of chemical terminology, Version 2.3.2 (the "Gold Book"). Blackwell Scientific, Oxford
8. Scheidt WR, Barabanschikov A et al (2010) Electronic structure and dynamics of nitrosyl porphyrins. Inorg Chem 49:6240–6252
9. Zavarine IS, Kini AD et al (1998) Photochemistry of nitrosyl metalloporphyrins: mechanisms of the photoinduced release and recombination of NO. J Phys Chem B 102:7287–7292
10. Brockway LO, Anderson JS (1937) The molecular structures of iron nitrosocarbonyl Fe $(NO)_2$ $(CO)_2$ and cobalt nitrosocarbonyl $Co(NO)(CO)_3$. Trans Faraday Soc 33:1233–1239
11. Dai RJ, Ke SC (2007) Detection and determination of the Fe(NO)2 core vibrational features in dinitrosyl-iron complexes from experiment, normal coordinate analysis, and density functional theory: an avenue for probing the nitric oxide oxidation state. J Phys Chem B 111:2335–2346
12. Brock CP, Collman JP et al (1973) Bent vs. linear nitrosyl paradox. Infrared and X-ray photoelectron spectra of dichloronitrosylbis (L)cobalt (II) and crystal structure with L = diphenylmethylphosphine. Inorg Chem 12:1304–1313
13. Haymore BL, Ibers JA (1975) Linear vs. bent nitrosyl ligands in four-coordinate transition metal complexes. Structure of dinitrosylbis (triphenylphosphine)osmium (−II) hemibenzene, Os $(NO)_2$ (P $(C_6H_5)_3)_2 \cdot 1/2C_6H_6$. Inorg Chem 14:2610–2617
14. Lin ZS, Chiou TW et al (2012) A dinitrosyliron complex within the homoleptic $Fe(NO)_4$ anion: NO as nitroxyl and nitrosyl ligands within a single structure. Inorg Chem 51:10092–10094
15. Peterson ES, Larsen RD, Abbott EH (1988) Crystal and molecular structures of potassium aquatetrakis (nitrito)nitrosylplatinate (IV), a blue, mononuclear platinum complex with a bent nitrosyl group, and of potassium trichlorobis (nitrito)nitrosylplatinate (IV). Inorg Chem 27:3514–3518
16. Calderon JL, Fontana S et al (1976) The crystal structure of tris-cyclopentadienyldimanganese trisnitrosyl; a compound containing unsymmetrically bonded bridging nitrosyl groups. Inorg Chim Acta 17:L31–L32
17. Calderon JL, Cotton FA et al (1971) Molecular structure of an unusual binuclear manganese complex with highly unsymmetrical nitrosyl bridges. J Chem Soc D 1476–1477
18. Norton JR, Collman JP et al (1972) Preparation and structure of ruthenium and osmium nitrosyl carbonyl clusters containing double-nitrosyl bridges. Inorg Chem 11:382–388
19. Yan B, Xie Y et al (2009) (Cyclopentadienyl)nitrosylmanganese compounds: the original molecules containing bridging nitrosyl groups. Eur J Inorg Chem 2009:3982–3992
20. Müller J, Manzoni de Oliveira G, Sonn I (1988) Reaktionen von Nitrosylkomplexen: VIII. Ein alternativer Weg zu $Cp_3Co_3(\mu 3NO)_2$ sowie Synthese des isoelektronischen clusters $Cp_3Co_2Fe(\mu_3NH)(\mu_3NO)$. J Organomet Chem 340:C15–C18
21. Terrile C, Nascimento OR et al (1990) On the electronic structure of metastable nitroprusside ion in $Na_2[Fe(CN)_5NO] \cdot 2H_2O$. A comparative single crystal ESR study. Solid State Commun 73:481–486
22. Maier G, Reisenauer HP, De Marco M (2000) Isomerizations between nitrosyl halides X-N=O and isonitrosyl halides X-O-N: a matrix-spectroscopic study. Chem Eur J 6:800–808
23. Connelly NG, Hartshorn RM et al (2005) Nomenclature of inorganic chemistry. In: IUPAC recommendations, 1990. N. G. Con. Royal Society of Chemistry, London
24. Reginato N, McCrory CTC et al (1999) Synthesis, X-ray crystal structure, and solution behavior of Fe $(NO)_2$ $(1\text{-MeIm})_2$: implications for nitrosyl non-heme-iron complexes with g = 2.03. J Am Chem Soc 121:10217–10218
25. Enemark JH, Feltham RD (1974) Principles of structure, bonding, and reactivity for metal nitrosyl complexes. Coord Chem Rev 13:339–406
26. Ozawa S, Fujii H, Morishima I (1992) NMR studies of iron (II) nitrosyl Pi-cation radicals of octaethylchlorin and octaethylisobacteriochlorin as models for reaction intermediate of nitrite reductase. J Am Chem Soc 114:1548–1554

27. Afshar RK, Patra AK et al (2004) Syntheses, structures, and reactivities of (Fe-NO)$_6$ nitrosyls derived from polypyridine-carboxamide ligands: photoactive NO-donors and reagents for S-nitrosylation of alkyl thiols. Inorg Chem 43:5736–5743
28. Praneeth VKK, Nather C et al (2006) Spectroscopic properties and electronic structure of five- and six-coordinate iron (II) porphyrin NO complexes: effect of the axial N-donor ligand. Inorg Chem 45:2795–2811
29. Eroy-Reveles AA, Hoffman-Luca CG, Mascharak PK (2007) Formation of a triply bridged Mu-Oxo Diiron (III) core stabilized by two deprotonated carboxamide groups upon photorelease of NO from a [Fe-NO]$_6$ iron nitrosyl. Dalton Trans 5268–5274
30. Hoffman-Luca CG, Eroy-Reveles AA et al (2009) Syntheses, structures, and photochemistry of manganese nitrosyls derived from designed Schiff base ligands: potential NO donors that can be activated by near-infrared light. Inorg Chem 48:9104–9111
31. Horsken A, Zheng G et al (1998) Iron dinitrosyl complexes of TCNE: a synthetic, X-ray crystallographic, high field NMR and electrochemical study. J Organomet Chem 558:1–9
32. Rose MJ, Mascharak PK (2009) Photosensitization of Ruthenium nitrosyls to red light with an isoelectronic series of heavy-atom chromophores: experimental and density functional theory studies on the effects of O-, S- and Se-substituted coordinated dyes. Inorg Chem 48:6904–6917
33. Sandala GM, Hopmann KH et al (2011) Calibration of DFT functionals for the prediction of Fe Mossbauer spectral parameters in iron-nitrosyl and iron-sulfur complexes: accurate geometries prove essential. J Chem Theory Comput 7:3232–3247
34. Conradie J, Hopmann KH, Ghosh A (2010) Understanding the unusually straight: a search for MO insights into linear {FeNO}^{7} units. J Phys Chem B 114:8517–8524
35. Hopmann KH, Ghosh A, Noodleman L (2009) Density functional theory calculations on mossbauer parameters of nonheme iron nitrosyls. Inorg Chem 48:9155–9165
36. Ghosh P, Bill E et al (2007) The molecular and electronic structure of the electron transfer series [$Fe_2(NO)_2(S_2C_2R_2)_3$] (z) (z = 0, -1, -2; R = phenyl, p-tolyl, p-tert-butylphenyl). Inorg Chem 46:2612–2618
37. Conradie J, Ghosh A (2006) Iron (III)-nitro porphyrins: theoretical exploration of a unique class of reactive molecules. Inorg Chem 45:4902–4909
38. Wondimagegn T, Ghosh A (2001) A quantum chemical survey of metalloporphyrin-nitrosyl linkage isomers: insights into the observation of multiple FeNO conformations in a recent crystallographic determination of nitrophorin 4. J Am Chem Soc 123:5680–5683
39. Sizova OV, Sokolov AY et al (2007) Quantum chemical study of the bond orders in the ruthenium, diruthenium and dirhodium nitrosyl complexes. Polyhedron 26:4680–4690
40. Feltham RD, Nyholm RS (1965) Metal nitrosyls. VI. Some new six-coordinate mononitrosyl complexes of cobalt. Inorg Chem 4:1334–1339
41. Herberhold M, Razavi A (1972) Tetranitrosylchromium[$Cr(NO)_4$]. Angew Chem Int Ed Engl 11:1092–1094
42. Roussin ML (1858) Recherches sur les Nitrosulfures Doubles de Fer. (Nouvelle classe de sels.). Ann Chim Phys 52:285
43. Tinberg CE, Tonzetich ZJ et al (2010) Characterization of iron dinitrosyl species formed in the reaction of nitric oxide with a biological Rieske center. J Am Chem Soc 132: 18168–18176
44. Wang R, Camacho-Fernandez MA et al (2009) Neutral and reduced Roussin's red salt ester [Fe_2 μ-RS)$_2(NO)_4$] (R = N-Pr, T-Bu, 6-Methyl-2-Pyridyl and 4,6-Dimethyl-2-Pyrimidyl): synthesis, X-ray crystal structures, spectroscopic, electrochemical and density functional theoretical investigations. Dalton Trans 777–786
45. Liu JG, Li MH (1989) Roussin red methyl ester, a tumor promoter isolated from pickled vegetables. Carcinogenesis 10:617–620
46. Janczyk A, Wolnicka-Glubisz A et al (2004) NO-dependent phototoxicity of Roussin's black salt against cancer cells. Nitric Oxide 10:42–50

47. Mitchell JB, Wink DA et al (1993) Hypoxic mammalian cell radiosensitization by nitric oxide. Cancer Res 53:5845–5848
48. Bourassa J, DeGraff W et al (1997) Photochemistry of Roussin's red salt, $Na_2[Fe_2S_2(NO)_4]$, and of Roussin's black salt, $NH_4[Fe_4S_3(NO)_7]$. in situ nitric oxide generation to sensitize γ-radiation induced cell death. J Am Chem Soc 119:2853–2860
49. Butler AR, Glidewell C et al (1985) Formation of paramagnetic mononuclear iron nitrosyl complexes from diamagnetic di- and tetranuclear iron-sulphur nitrosyls: characterisation by EPR spectroscopy and study of thiolate and nitrosyl ligand exchange reactions. Polyhedron 4:797–809
50. Wanat A, Schneppensieper T et al (2002) Kinetics, mechanism, and spectroscopy of the reversible binding of nitric oxide to aquated iron (II). An undergraduate text book reaction revisited. Inorg Chem 41:4–10
51. Butler AR, Glidewell C, Li MH (1988) Nitrosyl complexes of iron-sulfur clusters. In: Sykes AG (ed) Advances in inorganic chemistry, vol 32. Academic, London
52. Connelly NG, Gardner C (1976) Simple halogenonitrosyl anions of iron. J Chem Soc Dalton Trans 1525–1527
53. Lu TT, Chiou SJ et al (2006) Mononitrosyl tris(thiolate) iron complex $[Fe(NO)(SPh)_3]^-$ and dinitrosyl iron complex $[(EtS)_2Fe(NO)_2]^-$: formation pathway of dinitrosyl iron complexes (DNICs) from nitrosylation of biomimetic rubredoxin $[Fe(SR)_4]^{2-/1-}$ (R = Ph, Et). Inorg Chem 45:8799–8806
54. Tonzetich ZJ, McQuade LE, Lippard SJ (2010) Detecting and understanding the roles of nitric oxide in biology. Inorg Chem 49:6338–6348
55. Henry Y, Ducrocq C et al (1991) Nitric oxide, a biological effector. Electron paramagnetic resonance detection of nitrosyl-iron-protein complexes in whole cells. Eur Biophys J 20:1–15
56. Singel DJ, Lancaster JR Jr (1996) Electron paramagnetic resonance spectroscopy and nitric oxide biology. In: Feelisch M, Stamler JS (eds) Methods in nitric oxide research. Wiley, Chichester
57. van Faassen E, Vanin AF (2007) Radicals for life: the various forms of nitric oxide. Elsevier, Amsterdam
58. Bouton C, Drapier JC (2003) Iron regulatory proteins as NO signal transducers. Sci STKE 182:pe17
59. Turella P, Pedersen JZ et al (2003) Glutathione transferase superfamily behaves like storage proteins for dinitrosyl-diglutathionyl-iron complex in heterogeneous systems. J Biol Chem 278:42294–42299
60. De Maria F, Pedersen JZ et al (2003) The specific interaction of dinitrosyl-diglutathionyl-iron complex, a natural NO carrier, with the glutathione transferase superfamily: suggestion for an evolutionary pressure in the direction of the storage of nitric oxide. J Biol Chem 278:42283–42293
61. Vanin AF (1998) Dinitrosyl iron complexes and S-nitrosothiols are two possible forms for stabilization and transport of nitric oxide in biological systems. Biochemistry 63:782–793
62. Vanin AF, Malenkova IV, Serezhenkov VA (1997) Iron catalyzes both decomposition and synthesis of S-nitrosothiols: optical and electron paramagnetic resonance studies. Nitric Oxide 1:191–203
63. Stubauer G, Giuffre A, Sarti P (1999) Mechanism of S-nitrosothiol formation and degradation mediated by copper ions. J Biol Chem 274:28128–28133
64. Lim MD, Capps KB et al (2005) Further evidence supporting an inner sphere mechanism in the NO reduction of the copper (II) complex $Cu(dmp)_2^{2+}$ (dmp= 2,9-dimethyl-1,10-phenanthroline). Nitric Oxide 12:244–251
65. Ueno T, Suzuki Y et al (2002) In vivo nitric oxide transfer of a physiological NO carrier, dinitrosyl dithiolato iron complex, to target complex. Biochem Pharmacol 63:485–493
66. Wiegant FA, Malyshev IY et al (1999) Dinitrosyl iron complexes with thiol-containing ligands and S-nitroso-D, L-penicillamine as inductors of heat shock protein synthesis in H35 hepatoma cells. FEBS Lett 455:179–182

67. Manukhina EB, Smirin BV et al (2002) [Nitric oxide storage in the cardiovascular system]. Izv Akad Nauk Ser Biol 585–596
68. Boese M, Mordvintcev PI et al (1995) S-nitrosation of serum albumin by dinitrosyl-iron complex. J Biol Chem 270:29244–29249
69. Mulsch A, Mordvintcev P et al (1991) The potent vasodilating and guanylyl cyclase activating dinitrosyl-iron (II) complex is stored in a protein-bound form in vascular tissue and is released by thiols. FEBS Lett 294:252–256
70. Henry Y, Lepoivre M et al (1993) EPR characterization of molecular targets for NO in mammalian cells and organelles. FASEB J 7:1124–1134
71. Alencar JL, Chalupsky K et al (2003) Inhibition of arterial contraction by dinitrosyl-iron complexes: critical role of the thiol ligand in determining rate of nitric oxide (NO) release and formation of releasable NO stores by S-nitrosation. Biochem Pharmacol 66:2365–2374
72. Mulsch A (1994) Nitrogen monoxide transport mechanisms. Arzneimittelforschung 44:408–411
73. Vanin AF, Mordvintcev PI et al (1993) The relationship between L-arginine-dependent nitric oxide synthesis, nitrite release and dinitrosyl-iron complex formation by activated macrophages. Biochim Biophys Acta 1177:37–42
74. Cooper CE (1999) Nitric oxide and iron proteins. Biochim Biophys Acta 1411:290–309
75. Richardson DR, Lok HC (2008) The nitric oxide-iron interplay in mammalian cells: transport and storage of dinitrosyl iron complexes. Biochim Biophys Acta 1780:638–651
76. Lewandowska H, Stepkowski TM et al (2012) Coordination of iron ions in the form of histidinyl dinitrosyl complexes does not prevent their genotoxicity. Bioorg Med Chem 20:6732–6738
77. Lewandowska H, Kalinowska M et al (2011) Nitrosyl iron complexes-synthesis, structure and biology. Dalton Trans 40:8273–8289
78. Hieber W, Nast R (1940) Uber Stickoxydverbindungen von Nickel[I]- und Eisen [I]-halogeniden. Z Anorg Allg Chem 244:23–47
79. Cotton FA (2013) Progress in inorganic chemistry. Wiley, New York
80. Herberhold M, Kremnitz W et al (1982) Solution and matrix photochemistry of the isoelectronic series of a 'half -sandwich' carbonyl (η_5-Cyclopentadienyl)nitrosyl complexes of manganese, chromium, and vanadium, [M (η_5-C_5H_5)$(CO)_3$(NO)] (n= 0, M = Mn; n= 1, M = Cr; n= 2, M = V). J Chem Soc Dalton Trans 1261–1273
81. Haller KJ, Enemark JH (1978) Structural chemistry of the $\{CoNO\}^8$ Group. III. The structure of N, N′-Ethylenebis (salicylideneiminato)nitrosylcobalt (II), Co(NO)(salen). Acta Crystallogr B 34:102–109
82. Collman JP, Farnham P, Dolcetti G (1971) Intramolecular redox equilibriums of cobalt-nitrosyl complexes. J Am Chem Soc 93:1788–1790
83. Pierpont CG, Van Derveer DG et al (1970) Ruthenium complex having both linear and bent nitrosyl groups. J Am Chem Soc 92:4760–4762
84. Martin RL, Taylor D (1976) Bending of linear nitric oxide ligands in four-coordinate transition metal complexes. Crystal and molecular structure of dinitrosyldithioacetylacetonatocobalt(−I), $Co(NO)_2$. Inorg Chem 15:2970–2976
85. Henry Y, Giussani A, Ducastel B (1997) Nitric oxide research from chemistry to biology: EPR spectroscopy of nitrosylated compounds. Springer, Berlin
86. Tsai FT, Chiou SJ et al (2005) Dinitrosyl iron complexes (DNICs) $[L_2Fe(NO)_2]$- (L = Thiolate): interconversion among $\{Fe(NO)_2\}^9$ DNICs, $\{Fe(NO)_2\}^{10}$ DNICs, and [2Fe-2S] clusters, and the critical role of the thiolate ligands in regulating NO release of DNICs. Inorg Chem 44:5872–5881
87. Vithayathil AJ, Ternberg JL, Commoner B (1965) Changes in electron spin resonance signals of rat liver during chemical carcinogenesis. Nature 207:1246–1249
88. Cleare MJ, Fritz HP, Griffith WP (1972) Vibrational spectra of nitrosyl and carbonyl complexes: nitrosylpentahalogeno complexes of osmium, ruthenium and iridium. Spectrochim Acta A Mol Spectrosc 28:2013–2018

89. Vanin AF, Sanina NA et al (2007) Dinitrosyl-iron complexes with thiol-containing ligands: spatial and electronic structures. Nitric Oxide 16:82–93
90. Woolum JC, Tiezzi E, Commoner B (1968) Electron spin resonance of iron-nitric oxide complexes with amino acids, peptides and proteins. Biochim Biophys Acta 160:311–320
91. Bostanci MO, Bagirici F (2007) Neuroprotection by 7-nitroindazole against iron-induced hippocampal neurotoxicity. Cell Mol Neurobiol 27:933–941
92. Bostanci MO, Bagirici F (2008) Nitric oxide synthesis inhibition attenuates iron-induced neurotoxicity: a stereological study. Neurotoxicology 29:130–135
93. Gupta A, Sharma S, Chopra K (2008) Reversal of iron-induced nephrotoxicity in rats by molsidomine, a nitric oxide donor. Food Chem Toxicol 46:537–543
94. Kadkhodaee M, Gol A (2004) The role of nitric oxide in iron-induced rat renal injury. Hum Exp Toxicol 23:533–536
95. Feger F, Ferry-Dumazet H et al (2001) Role of iron in tumor cell protection from the pro-apoptotic effect of nitric oxide. Cancer Res 61:5289–5294
96. Watts RN, Richardson DR (2002) The mechanism of nitrogen monoxide (NO)-mediated iron mobilization from cells. NO intercepts iron before incorporation into ferritin and indirectly mobilizes iron from ferritin in a glutathione-dependent manner. Eur J Biochem 269:3383–3392
97. Watts RN, Hawkins C et al (2006) Nitrogen monoxide (NO)-mediated iron release from cells is linked to NO-induced glutathione efflux via multidrug resistance-associated protein 1. Proc Natl Acad Sci USA 103:7670–7675
98. Fass U, Panickar K et al (2004) The role of glutathione in nitric oxide donor toxicity to SN56 cholinergic neuron-like cells. Brain Res 1005:90–100
99. Ueno T, Yoshimura T (2000) The physiological activity and in vivo distribution of dinitrosyl dithiolato iron complex. Jpn J Pharmacol 82:95–101
100. Boese M, Keese MA et al (1997) Inhibition of glutathione reductase by dinitrosyl-iron-dithiolate complex. J Biol Chem 272:21767–21773
101. Becker K, Savvides SN et al (1998) Enzyme inactivation through sulfhydryl oxidation by physiologic NO-carriers. Nat Struct Biol 5:267–271
102. Vlasova MA, Vanin AF et al (2003) Detection and description of various stores of nitric oxide store in vascular wall. Bull Exp Biol Med 136:226–230
103. Kakhlon O, Cabantchik ZI (2002) The labile iron pool: characterization, measurement, and participation in cellular processes (1). Free Radic Biol Med 33:1037–1046
104. Lipinski P, Drapier JC et al (2000) Intracellular iron status as a hallmark of mammalian cell susceptibility to oxidative stress: a study of L5178Y mouse lymphoma cell lines differentially sensitive to H_2O_2. Blood 95:2960–2966
105. Denninger JW, Marletta MA (1999) Guanylate cyclase and the NO/cGMP signaling pathway. Biochim Biophys Acta 1411:334–350
106. Kubrina LN, Mikoyan VD et al (1993) Iron potentiates bacterial lipopolysaccharide-induced nitric oxide formation in animal organs. Biochim Biophys Acta 1176:240–244
107. Vanin AF, Men'shikov GB et al (1992) The source of non-heme iron that binds nitric oxide in cultivated macrophages. Biochim Biophys Acta 1135:275–279
108. Riley RF, Ho L (1962) Evidence for a pentacyanonitrosyl complex of molybdenum. J Inorg Nuclear Chem 24:1121–1127
109. Szaciłowski K, Oszajca J et al (2001) Photochemistry of the $[Fe(CN)_5N(O)SR]^{3-}$ complex: a mechanistic study. J Photochem Photobiol A 143:93–262
110. Costanzo S, Ménage S et al (2001) Re-examination of the formation of dinitrosyl–iron complexes during reaction of S-nitrosothiols with Fe (II). Inorg Chim Acta 318:1–7
111. Baltusis LM, Karlin KD et al (1980) Synthesis and structure of $Fe(L'H)(NO)_2$, a tetracoordinate complex having a twelve-membered chelate ring, and its conversion to pentacoordinate FeL′ (NO) through formal loss of "HNO" (L′ = SCH2CH2NMeCH2CH2CH2NMeCH2CH2S-). Inorg Chem 19:2627–2632

112. Szaci+éowski K, Macyk W et al (2000) Ligand and medium controlled photochemistry of iron and ruthenium mixed-ligand complexes: prospecting for versatile systems. Coord Chem Rev 208:277–297
113. Crayston JA, Glidewell C, Lambert RJ (1990) Redox properties of iron-sulphur-nitrosyl complexes: exploratory electrochemistry of mononuclear, dinuclear and tetranuclear complexes. Polyhedron 9:1741–1746
114. Wang PG, Xian M et al (2002) Nitric oxide donors: chemical activities and biological applications. Chem Rev 102:1091–1134
115. Jaworska M, Stasicka Z (2004) Structure and UV–vis spectroscopy of nitrosylthiolatoferrate mononuclear complexes. J Organomet Chem 689:1702–1713
116. Kennedy MC, Antholine WE, Beinert H (1997) An EPR investigation of the products of the reaction of cytosolic and mitochondrial aconitases with nitric oxide. J Biol Chem 272:20340–20347
117. Bryar TR, Eaton DR (1992) Electronic configuration and structure of paramagnetic iron dinitrosyl complexes. Can J Chem 70:1917–1926
118. Harrop TC, Tonzetich ZJ et al (2008) Reactions of synthetic [2Fe-2S] and [4Fe-4S] clusters with nitric oxide and nitrosothiols. J Am Chem Soc 130:15602
119. Sanina NA, Rakova OA et al (2004) Structure of the neutral mononuclear dinitrosyl iron complex with 1,2,4-triazole-3-thione[$Fe(SC_2H_3N_3)(SC_2H_2N_3)(NO)_2$]·0.5 H_2O. Mendeleev Commun 14:7–8
120. Sanina NA, Aldoshin SM (2004) Functional models of [Fe–S] nitrosyl proteins. Russ Chem Bull Int Ed 53:2428
121. Davies SC, Evans DJ et al (2002) J Chem Soc Dalton Trans 2473
122. Tsou CC, Lu TT, Liaw WF (2007) EPR, UV–vis, IR, and X-ray demonstration of the anionic dimeric dinitrosyl iron complex[$(NO)_2Fe(micro\text{-}S(t)Bu)_2Fe(NO)_2]^-$: relevance to the products of nitrosylation of cytosolic and mitochondrial aconitases, and high-potential iron proteins. J Am Chem Soc 129:12626–12627
123. Vanin AF, Stukan RA, Manukhina EB (1996) Physical properties of dinitrosyl iron complexes with thiol-containing ligands in relation with their vasodilator activity. Biochim Biophys Acta 1295:5–12
124. Vanin AF (1991) Endothelium-derived relaxing factor is a nitrosyl iron complex with thiol ligands. FEBS Lett 289:1–3
125. Michael D, Mingos P, Sherman DJ (1989) Transition metal nitrosyl complexes. In: Sykes AG (ed) Advances in inorganic chemistry, vol 34. Academic, London
126. Lu TT, Tsou CC et al (2008) Anionic Roussin's Red Esters (RREs) syn-/anti-$[Fe(\mu\text{-}SEt)(NO)_2]^{2-}$: the critical role of thiolate ligands in regulating the transformation of RREs into dinitrosyl iron complexes and the anionic RREs. Inorg Chem 47:6040–6050
127. Hung MC, Tsai MC et al (2006) Transformation and structural discrimination between the neutral $\{Fe(NO)_2\}^{10}$ dinitrosyliron complexes (DNICs) and the anionic/cationic $\{Fe(NO)_2\}^9$ DNICs. Inorg Chem 45:6041–6047
128. Yeh SW, Lin CW et al (2012) Insight into the dinuclear $\{Fe(NO)_2\}^{10}\{Fe(NO)_2\}^{10}$ and mononuclear $\{Fe(NO)_2\}^{10}$ dinitrosyliron complexes. Inorg Chem 51:4076–4087
129. Tsou CC, Liaw WF (2011) Transformation of the {Fe (NO)2}9 dinitrosyl iron complexes (DNICs) into S-nitrosothiols (RSNOs) triggered by acid–base pairs. Chemistry 17:13358–13366
130. Lin ZS, Lo FC et al (2011) Peptide-bound dinitrosyliron complexes (DNICs) and neutral/reduced-form Roussin's Red Esters (RREs/rRREs): understanding nitrosylation of [Fe-S] clusters leading to the formation of DNICs and RREs using a de novo design strategy. Inorg Chem 50:10417–10431
131. Lu TT, Lai SH et al (2011) Discrimination of mononuclear and dinuclear dinitrosyl iron complexes (DNICs) by S K-edge X-ray absorption spectroscopy: insight into the electronic structure and reactivity of DNICs. Inorg Chem 50:5396–5406

132. Tsai FT, Chen PL, Liaw WF (2010) Roles of the distinct electronic structures of the $\{Fe(NO)_2\}^9$ and $\{Fe(NO)_2\}^{10}$ dinitrosyliron complexes in modulating nitrite binding modes and nitrite activation pathways. J Am Chem Soc 132:5290–5299
133. Tsai FT, Kuo TS, Liaw WF (2009) Dinitrosyl iron complexes (DNICs) bearing O-bound nitrito ligand: reversible transformation between the six-coordinate $\{Fe(NO)_2\}^9$[$(1\text{-MeIm})_2$(eta(2)-ONO)$Fe(NO)_2$] (g = 2.013) and four-coordinate $\{Fe(NO)_2\}^9$[(1-MeIm)(ONO)$Fe(NO)_2$] (g = 2.03). J Am Chem Soc 131:3426–3427
134. Harrop TC, Song D, Lippard SJ (2006) Interaction of nitric oxide with tetrathiolato iron (II) complexes: relevance to the reaction pathways of iron nitrosyls in sulfur-rich biological coordination environments. J Am Chem Soc 128:3528–3529
135. Thomas JT, Robertson JH, Cox EG (1958) The crystal structure of Roussin's red ethyl ester. Acta Crystallogr 11:599–604
136. Tsai ML, Hsieh CH, Liaw WF (2007) Dinitrosyl iron complexes (DNICs) containing S/N/O ligation: transformation of Roussin's red ester into the neutral $\{Fe(NO)_2\}^{10}$ DNICs. Inorg Chem 46:5110–5117
137. Lu TT, Huang HW, Liaw WF (2009) Anionic mixed thiolate-sulfide-bridged Roussin's red esters $[(NO)_2Fe(\mu\text{-SR})(\mu\text{-S})Fe(NO)_2]^-$ (R = Et, Me, Ph): a key intermediate for transformation of dinitrosyl iron complexes (DNICs) to [2Fe-2S] clusters. Inorg Chem 48:9027–9035
138. Sanina NA, Filipenko OS et al (2000) Influence of the cation on the properties of binuclear iron nitrosyl complexes. Synthesis and crystal structure of $[Pr_4nN]_2[Fe_2S_2(NO)_4]$. Russ Chem Bull 49:1109–1112
139. Collins DJ, Zhou HC (2011) Iron-sulfur models of protein active sites. In: Encyclopedia of inorganic and bioinorganic chemistry. Wiley, New York
140. King RB, Bitterwolf TE (2000) Metal carbonyl analogues of iron–sulfur clusters found in metalloenzyme chemistry. Coord Chem Rev 206–207:563–579
141. Noodleman L, Pique ME et al (2007) Iron-sulfur clusters: properties and functions. In: Wiley encyclopedia of chemical biology. Wiley, New York
142. Kurihara T, Mihara H et al (2003) Assembly of iron-sulfur clusters mediated by cysteine desulfurases, IscS, CsdB and CSD, from Escherichia coli. Biochim Biophys Acta Proteins Proteomics 1647:303–309
143. Ballmann J, Albers A et al (2008) A synthetic analogue of Rieske-type [2Fe-2S] clusters. Angew Chem Int Ed 47:9537–9541
144. Sharma VS, Traylor TG et al (1987) Reaction of nitric oxide with heme proteins and model compounds of hemoglobin. Biochemistry 26:3837–3843
145. Pavlos CM, Xu H, Toscano JP (2005) Photosensitive precursors to nitric oxide. Curr Top Med Chem 5:637–647
146. Tonzetich ZJ, Do LH, Lippard SJ (2009) Dinitrosyl iron complexes relevant to Rieske cluster nitrosylation. J Am Chem Soc 131:7964–7965
147. Foster MW, Cowan JA (1999) Chemistry of nitric oxide with protein-bound iron sulfur centers. Insights on physiological reactivity. J Am Chem Soc 121:4093–4100
148. Mitra D, Pelmenschikov V et al (2011) Dynamics of the [4Fe-4S] cluster in pyrococcus furiosus D14C ferredoxin via nuclear resonance vibrational and resonance Raman spectroscopies, force field simulations, and density functional theory calculations. Biochemistry 50:5220–5235
149. Huang HW, Tsou CC et al (2008) New members of a class of dinitrosyliron complexes (DNICs): interconversion and spectroscopic discrimination of the anionic $\{Fe(NO)_2\}^9$[$(NO)_2Fe(C_3H_3N_2)_2]^-$ and$[(NO)_2Fe(C_3H_3N_2)(SR)]^-$ ($C_3H_3N_2$ = deprotonated imidazole; R = tBu, Et, Ph). Inorg Chem 47:2196–2204
150. Tsai ML, Liaw WF (2006) Neutral $\{Fe(NO)_2\}^9$ dinitrosyliron complex (DNIC)[(SC_6H_4-o-NHCOPh)(Im)$Fe(NO)_2$] (Im = Imidazole): interconversion among the anionic/neutral $\{Fe(NO)_2\}^9$ DNICs and Roussin's red ester. Inorg Chem 45:6583–6585
151. Chen TN, Lo FC et al (2006) Dinitrosyl iron complexes $[E_5Fe(NO)_2]^-$ (E = S, Se): a precursor of Roussin's black salt $[Fe_4E_3(NO)_7]^-$. Inorg Chim Acta 359:2525–2533

152. Chen HW, Lin CW et al (2005) Homodinuclear iron thiolate nitrosyl compounds [(ON)Fe (S, S-C_6H_4)$_2$Fe(NO)$_2$]- and [(ON)Fe(SO_2, S-C_6H_4)(S, S-C_6H_4)Fe(NO)$_2$]$^-$ with {Fe(NO)}^{7}-{Fe (NO)}$^{2-9}$ electronic coupling: new members of a class of dinitrosyl iron complexes. Inorg Chem 44:3226–3232
153. Rogers PA, Eide L et al (2003) Reversible inactivation of E. coli endonuclease III via modification of its [4Fe-4S] cluster by nitric oxide. DNA Repair 2:809–817
154. Crack JC, Smith LJ et al (2010) Mechanistic insight into the nitrosylation of the [4Fe-4S] cluster of WhiB-like proteins. J Am Chem Soc 133:1112–1121
155. Crack JC, den Hengst CD et al (2009) Characterization of [4Fe-4S]-containing and cluster-free forms of Streptomyces WhiD. Biochemistry 48:12252–12264
156. Smith LJ, Stapleton MR et al (2010) Mycobacterium tuberculosis WhiB1 is an essential DNA-binding protein with a nitric oxide-sensitive iron-sulfur cluster. Biochem J 432:417–427
157. Alderton WK, Cooper CE, Knowles RG (2001) Nitric oxide synthases: structure, function and inhibition. Biochem J 357:593–615
158. Cassoly R, Gibson QH (1975) Conformation, cooperativity and ligand binding in human hemoglobin. J Mol Biol 91:301–313
159. Sharma VS, Ranney HM (1978) The dissociation of NO from nitrosylhemoglobin. J Biol Chem 253:6467–6472
160. Kharitonov VG, Sharma VS et al (1997) Kinetics of nitric oxide dissociation from five- and six-coordinate nitrosyl hemes and heme proteins, including soluble guanylate cyclase. Biochemistry 36:6814–6818
161. Moore EG, Gibson QH (1976) Cooperativity in the dissociation of nitric oxide from hemoglobin. J Biol Chem 251:2788–2794
162. Hoshino M, Ozawa K et al (1993) Photochemistry of nitric oxide adducts of water-soluble iron (III) porphyrin and ferrihemoproteins studied by nanosecond laser photolysis. J Am Chem Soc 115:9568–9575
163. Ascenzi P, Coletta M et al (1994) Nitric oxide binding to ferrous native horse heart cytochrome c and to its carboxymethylated derivative: A spectroscopic and thermodynamic study. J Inorg Biochem 53:273–280
164. Hoshino M, Maeda M et al (1996) Studies on the reaction mechanism for reductive nitrosylation of ferrihemoproteins in buffer solutions. J Am Chem Soc 118:5702–5707
165. Sharma VS, Isaacson RA et al (1983) Reaction of nitric oxide with heme proteins: studies on metmyoglobin, opossum methemoglobin, and microperoxidase. Biochemistry 22:3897–3902
166. Sharpe MA, Cooper CE (1998) Reactions of nitric oxide with mitochondrial cytochrome C: a novel mechanism for the formation of nitroxyl anion and peroxynitrite. Biochem J 332 (Pt 1):9–19
167. Osipov AN, Borisenko GG, Vladimirov YA (2007) Biological activity of hemoprotein nitrosyl complexes. Biochemistry 72:1491–1504
168. Khrapova NV, Malenkova IV, Vanin AF (1995) S-nitrosothiols and dinitrosothiol iron complexes as a source of nitric oxide in animals. Biofizika 40:117–121
169. Shumaev KB, Kosmachevskaya OV et al (2008) Dinitrosyl iron complexes bind with hemoglobin as markers of oxidative stress. Methods Enzymol 436:445–461
170. Timoshin AA, Vanin AF et al (2007) Protein-bound dinitrosyl-iron complexes appearing in blood of rabbit added with a low-molecular dinitrosyl-iron complex: EPR studies. Nitric Oxide 16:286–293
171. Kadish KM, Smith KM, Guillard R (2000) Binding and activation of nitric oxide by metalloporphyrins and heme. In: Kadish KM, Smith KM, Guillard R (eds) The porphyrin handbook. Academic, New York
172. Wyllie GR, Scheidt WR (2002) Solid-state structures of metalloporphyrin NO_x compounds. Chem Rev 102:1067–1090
173. Goodrich LE, Paulat F et al (2010) Electronic structure of heme-nitrosyls and its significance for nitric oxide reactivity, sensing, transport, and toxicity in biological systems. Inorg Chem 49:6293–6316

174. Sulok CD, Bauer JL et al (2012) A detailed investigation into the electronic structures of macrocyclic iron (II)-nitrosyl compounds and their similarities to ferrous heme-nitrosyls. Inorg Chim Acta 380:148–160
175. Praneeth VK, Neese F, Lehnert N (2005) Spin density distribution in five- and six-coordinate iron (II)-porphyrin NO complexes evidenced by magnetic circular dichroism spectroscopy. Inorg Chem 44:2570–2572
176. Larkworthy LF, Sengupta SK (1991) Mononitrosyl derivatives of iron and cobalt complexes of quadridentate ligands from 2-hydroxy-1-naphthaldehyde and ethylenediamine, O-phenylenediamine, and 4-methyl-O-phenylenediamine. Inorg Chim Acta 179:157–160
177. Groombridge CJ, Larkworthy LF et al (1992) Synthesis and ^{15}N nuclear magnetic resonance shift tensors of bent nitrosyl complexes with N-substituted salicylideneiminate coligands; the shift tensor as a criterion of MNO bond angle. J Chem Soc Dalton Trans 3125–3131
178. Zeng W, Silvernail NJ et al (2005) Direct probe of iron vibrations elucidates NO activation of heme proteins. J Am Chem Soc 127:11200–11201
179. Sage JT et al (2001) Nuclear resonance vibrational spectroscopy of a protein active-site mimic. J Phys Condens Matter 13:7707
180. Wolfgang S (2004) Nuclear resonant spectroscopy. J Phys Condens Matter 16:S497
181. Lehnert N, Galinato MG et al (2010) Nuclear resonance vibrational spectroscopy applied to [Fe (OEP) (NO)]: the vibrational assignments of five-coordinate ferrous heme-nitrosyls and implications for electronic structure. Inorg Chem 49:4133–4148
182. Ellison MK, Schulz CE, Scheidt WR (2000) Structural and electronic characterization of nitrosyl (octaethylporphinato)iron (III) perchlorate derivatives. Inorg Chem 39:5102–5110
183. Ellison MK, Schulz CE, Scheidt WR (2002) Nitrosyliron (III) porphyrinates: porphyrin core conformation and FeNO geometry. Any correlation? J Am Chem Soc 124:13833–13841
184. Ellison MK, Scheidt WR (1998) Tilt/asymmetry in nitrosyl metalloporphyrin complexes the cobalt case. Inorg Chem 37:382–383
185. Richter-Addo GB, Wheeler RA et al (2001) Unexpected nitrosyl-group bending in six-coordinate$[M(NO)]^6$ sigma-bonded aryl (iron) and -(ruthenium) porphyrins. J Am Chem Soc 123:6314–6326
186. Guilard R, Lagrange G et al (1985) Reactions of sigma-bonded alkyl- and aryliron porphyrins with nitric oxide. Synthesis and electrochemical characterization of six-coordinate nitrosyl sigma-bonded alkyl- and aryliron porphyrins. Inorg Chem 24:3649–3656
187. Nasri H, Ellison MK et al (1997) Sharing the π-bonding. An iron porphyrin derivative with trans, π-accepting axial ligands. Synthesis, EPR and Mössbauer spectra, and molecular structure of two forms of the complex nitronitrosyl(α, α, α, α-tetrakis(o-pivalamidophenyl)-porphinato)ferrate(II). J Am Chem Soc 119:6274–6283
188. Wyllie GR, Schulz CE, Scheidt WR (2003) Five- to six-coordination in (nitrosyl)iron (II) porphyrinates: effects of binding the sixth ligand. Inorg Chem 42:5722–5734
189. Mason J, Larkworthy LF, Moore EA (2002) Nitrogen NMR spectroscopy of metal nitrosyls and related compounds. Chem Rev 102:913–934
190. Kadish KM, Caemelbecke EV (2007) Electrochemistry of metalloporphyrins in nonaqueous media. In: Encyclopedia of electrochemistry. Wiley-VCH, New York
191. Li CG, Rand MJ (1993) Effects of hydroxocobalamin and haemoglobin on NO-mediated relaxations in the rat anococcygeus muscle. Clin Exp Pharmacol Physiol 20:633–640
192. Rajanayagam MAS, Li CG, Rand MJ (1993) Differential effects of hydroxocobalamin on NO-mediated relaxations in rat aorta and anococcygeus muscle. Br J Pharmacol 108:3–5
193. Rand MJ, Li CG (1993) Differential effects of hydroxocobalamin on relaxations induced by nitrosothiols in rat aorta and anococcygeus muscle. Eur J Pharmacol 241:249–254
194. Jenkinson KM, Reid JJ, Rand MJ (1995) Hydroxocobalamin and haemoglobin differentiate between exogenous and neuronal nitric oxide in the rat gastric fundus. Eur J Pharmacol 275:145–152

195. De Man JG, Boeckxstaens GE et al (1995) Comparison of the pharmacological profile of S-nitrosothiols, nitric oxide and the nitrergic neurotransmitter in the canine ileocolonic junction. Br J Pharmacol 114:1179–1184
196. Akinori A, Yutaka T et al (1993) Protective effects of a vitamin B12 analog, methylcobalamin, against glutamate cytotoxicity in cultured cortical neurons. Eur J Pharmacol 241:1–6
197. Greenberg SS, Xie J et al (1995) Hydroxocobalamin (vitamin B_{12a}) prevents and reverses endotoxin-induced hypotension and mortality in rodents: role of nitric oxide. J Pharmacol Exp Ther 273:257–265
198. Wolak M, Zahl A et al (2001) Kinetics and mechanism of the reversible binding of nitric oxide to reduced cobalamin B_{12r} (Cob(II)alamin). J Am Chem Soc 123:9780–9791
199. Ignarro L (2000) Nitric oxide: biology and pathobiology. Academic, San Diego
200. Rose MJ, Mascharak PK (2008) Photoactive ruthenium nitrosyls: effects of light and potential application as NO donors. Coord Chem Rev 252:2093–2114
201. McGarvey BR, Ferro AA et al (2000) Detection of the EPR spectra of NO in ruthenium (II) complexes. Inorg Chem 39:3577–3581
202. Callahan RW, Meyer TJ (1977) Reversible electron transfer in ruthenium nitrosyl complexes. Inorg Chem 16:574–581
203. Videla M, Jacinto JS et al (2006) New ruthenium nitrosyl complexes with tris(1-pyrazolyl) methane (tpm) and 2,2′-bipyridine (bpy) coligands. Structure, spectroscopy, and electrophilic and nucleophilic reactivities of bound nitrosyl. Inorg Chem 45:8608–8617
204. Roncaroli F, Videla M et al (2007) New features in the redox coordination chemistry of metal nitrosyls {M-NO^+; M-NO; M-NO^- (HNO)}. Coord Chem Rev 251:1903–1930
205. Roncaroli F, Ruggiero ME et al (2002) Kinetic, mechanistic, and DFT study of the electrophilic reactions of nitrosyl complexes with hydroxide. Inorg Chem 41:5760–5769
206. Patra AK, Mascharak PK (2003) A ruthenium nitrosyl that rapidly delivers NO to proteins in aqueous solution upon short exposure to UV light. Inorg Chem 42:7363–7365
207. Serres RG, Grapperhaus CA et al (2004) Structural, spectroscopic, and computational study of an octahedral, non-heme $[Fe\text{-}NO]^{6–8}$ series: $[Fe(NO)\ (cyclam\text{-}ac)]^{2+/+/0}$. J Am Chem Soc 126:5138–5153
208. Coppens P, Novozhilova I, Kovalevsky A (2002) Photoinduced linkage isomers of transition-metal nitrosyl compounds and related complexes. Chem Rev 102:861–884
209. Cheng L, Novozhilova I et al (2000) First observation of photoinduced nitrosyl linkage isomers of iron nitrosyl porphyrins. J Am Chem Soc 122:7142–7143
210. Schmitt F, Govindaswamy P et al (2008) Ruthenium porphyrin compounds for photodynamic therapy of cancer. J Med Chem 51:1811–1816
211. Xu N, Yi J, Richter-Addo GB (2010) Linkage isomerization in heme-NO_x compounds: understanding NO, nitrite, and hyponitrite interactions with iron porphyrins. Inorg Chem 49:6253–6266
212. Fomitchev V, Coppens P et al (1999) Photo-induced metastable linkage isomers of ruthenium nitrosyl porphyrins. Chem Commun 2013–2014
213. Adman ET, Murphy ME (2001) Copper nitrite reductase. In: Encyclopedia of inorganic and bioinorganic chemistry. Wiley, New York
214. Kroneck PMH, Beuerle J, Schumacher (1992) Metal-dependent conversion of inorganic nitrogen and sulfur compounds. In: Sigel A, Sigel H (ed) Metal ions in biological systems: degradation of environmental pollutants by microorganisms and their metalloenzymes. Marcel Dekker, New York
215. Tocheva EI, Rosell FI et al (2004) Side-on copper-nitrosyl coordination by nitrite reductase. Science 304:867–870
216. Tocheva EI, Rosell FI et al (2007) Stable copper-nitrosyl formation by nitrite reductase in either oxidation state. Biochemistry 46:12366–12374
217. Paul PP, Tyeklar Z et al (1990) Isolation and X-ray structure of a dinuclear copper-nitrosyl complex. J Am Chem Soc 112:2430–2432

218. Gennari M, Marchio L (2009) Cu-complexes with scorpionate ligands as models for the binding sites of copper proteins. Curr Bioact Compounds 5:244–263
219. Averill BA (1996) Dissimilatory nitrite and nitric oxide reductases. Chem Rev 96:2951–2964
220. Hulse CL, Tiedje JM, Averill BA (1989) Evidence for a copper-nitrosyl intermediate in denitrification by the copper-containing nitrite reductase of Achromobacter cycloclastes. J Am Chem Soc 111:2322–2323
221. Adman ET, Godden JW, Turley S (1995) The structure of copper-nitrite reductase from achromobacter cycloclastes at five pH values, with NO-2 bound and with type II copper depleted. J Biol Chem 270:27458–27474
222. Murphy MEP, Turley S, Adman ET (1997) Structure of nitrite bound to copper-containing nitrite reductase from Alcaligenes faecalis: mechanistic implications. J Biol Chem 272:28455–28460
223. Kataoka K, Furusawa H et al (2000) Functional analysis of conserved aspartate and histidine residues located around the type 2 copper site of copper-containing nitri reductase. J Biochem 127:345–350
224. Suzuki S, Kataoka K, Yamaguchi K (2000) Metal coordination and mechanism of multicopper nitrite reductase. Acc Chem Res 33:728–735
225. Olesen K, Veselov A et al (1998) Spectroscopic, kinetic, and electrochemical characterization of heterologously expressed wild-type and mutant forms of copper-containing nitrite reductase from Rhodobacter sphaeroides 2.4.3. Biochemistry 37:6086–6094
226. Veselov A, Olesen K et al (1998) Electronic structural information from Q-band ENDOR on the type 1 and type 2 copper liganding environment in wild-type and mutant forms of copper-containing nitrite reductase. Biochemistry 37:6095–6105
227. Antonyuk SV, Strange RW et al (2005) Atomic resolution structures of resting-state, substrate- and product-complexed Cu-nitrite reductase provide insight into catalytic mechanism. Proc Natl Acad Sci USA 102:12041–12046
228. Ghosh S, Dey A et al (2007) Resolution of the spectroscopy versus crystallography issue for NO intermediates of nitrite reductase from Rhodobacter sphaeroides. J Am Chem Soc 129:10310–10311
229. Fujisawa K, Tateda A et al (2008) Structural and spectroscopic characterization of mononuclear copper (I) nitrosyl complexes: end-on versus side-on coordination of NO to copper (I). J Am Chem Soc 130:1205–1213
230. Woolum JC, Commoner B (1970) Isolation and identification of a paramagnetic complex from the livers of carcinogen-treated rats. Biochim Biophys Acta 201:131–140
231. Vanin AF, Nalbandian RM (1965) Free radicals of a new type in yeast cells. Biofizika 10:167–168
232. Vanin AF, Nalbandian RM (1966) Free radical states with localization of the unpaired electron on the sulfur atom in yeast cells. Biofizika 11:178–179
233. Maruyama T, Kataoka N et al (1971) Identification of three-line electron spin resonance signal and its relationship to ascites tumors. Cancer Res 31:179–184
234. Palmer RM, Ferrige AG, Moncada S (1987) Nitric oxide release accounts for the biological activity of endothelium-derived relaxing factor. Nature 327:524–526
235. Waldman SA, Rapoport RM et al (1986) Desensitization to nitroglycerin in vascular smooth muscle from rat and human. Biochem Pharmacol 35:3525–3531
236. Ignarro LJ (1999) Nitric oxide: a unique endogenous signaling molecule in vascular biology. Biosci Rep 19:51–71
237. Ignarro LJ (2002) Nitric oxide as a unique signaling molecule in the vascular system: a historical overview. J Physiol Pharmacol 53:503–514
238. Yamamoto T, Bing RJ (2000) Nitric oxide donors. Exp Biol Med 225:200–206
239. Garthwaite J, Boulton CL (1995) Nitric oxide signaling in the central nervous system. Annu Rev Physiol 57:683–706
240. Liu Q, Gross SS (1996) Binding sites of nitric oxide synthases. In: Lester P (ed) Methods in enzymology. Nitric oxide Part A: Sources and detection of NO; NO synthase, vol 268. Academic, London

241. del Río LA, Corp J, Barroso JB (2004) Nitric oxide and nitric oxide synthase activity in plants. Phytochemistry 65:783–792
242. Knowles RG, Moncada S (1994) Nitric oxide synthases in mammals. Biochem J 298 (Pt 2):249–258
243. Martinez MC, Andriantsitohaina R (2009) Reactive nitrogen species: molecular mechanisms and potential significance in health and disease. Antioxid Redox Signal 11:669–702
244. Myers PR, Minor RL et al (1990) Vasorelaxant properties of the endothelium-derived relaxing factor more closely resemble S-nitrosocysteine than nitric oxide. Nature 345:161–163
245. Myers PR, Guerra R, Harrison DG (1992) Release of multiple endothelium-derived relaxing factors from porcine coronary arteries. J Cardiovasc Pharmacol 20:392–400
246. Lancaster JR (1994) Simulation of the diffusion and reaction of endogenously produced nitric oxide. Proc Natl Acad Sci USA 91:8137–8141
247. Wink DA, Mitchell JB (1998) Chemical biology of nitric oxide: insights into regulatory, cytotoxic, and cytoprotective mechanisms of nitric oxide. Free Radic Biol Med 25:434–456
248. Nakamoto K (2009) Infrared and Raman spectra of inorganic and coordination compounds, applications in coordination, organometallic, and bioinorganic chemistry. Wiley, New York
249. Le XC, Xing JZ et al (1998) Inducible repair of thymine glycol detected by an ultrasensitive assay For DNA damage. Science 280:1066–1069
250. Stanbury DM (1989) Reduction potentials involving inorganic free radicals in aqueous solution. In: Sykes AG (ed) Advances in inorganic chemistry, vol 33. Academic, London
251. Bartberger MD, Liu W et al (2002) The reduction potential of nitric oxide (NO) and its importance to NO biochemistry. Proc Natl Acad Sci USA 99:10958–10963
252. Stamler JS, Singel DJ, Loscalzo J (1992) Biochemistry of nitric oxide and its redox-activated forms. Science 258:1898–1902
253. Henry Y, Singel DJ (1996) Metal-nitrosyl interactions in nitric oxide biology probed by electron paramagnetic resonance spectroscopy. In: Feelisch M, Stamler JS (eds) Methods in nitric oxide research. Wiley, Chichester
254. Brown GC (1995) Reversible binding and inhibition of catalase by nitric oxide. Eur J Biochem 232:188–191
255. Bellamy TC, Griffiths C, Garthwaite J (2002) Differential sensitivity of guanylyl cyclase and mitochondrial respiration to nitric oxide measured using clamped concentrations. J Biol Chem 277:31801–31807
256. Craven PA, DeRubertis FR (1978) Restoration of the responsiveness of purified guanylate cyclase to nitrosoguanidine, nitric oxide, and related activators by heme and hemeproteins. Evidence for involvement of the paramagnetic nitrosyl-heme complex in enzyme activation. J Biol Chem 253:8433–8443
257. Ignarro LJ (1990) Haem-dependent activation of guanylate cyclase and cyclic GMP formation by endogenous nitric oxide: a unique transduction mechanism for transcellular signaling. Pharmacol Toxicol 67:1–7
258. Ferrero R, Rodriguez-Pascual F (2000) Nitric oxide-sensitive guanylyl cyclase activity inhibition through cyclic GMP-dependent dephosphorylation. J Neurochem 75:2029–2039
259. Works CF, Jocher CJ et al (2002) Photochemical nitric oxide precursors: synthesis, photochemistry, and ligand substitution kinetics of ruthenium salen nitrosyl and ruthenium salophen nitrosyl complexes. Inorg Chem 41:3728–3739
260. Garbers DL, Lowe DG (1994) Guanylyl cyclase receptors. J Biol Chem 269:30741–30744
261. Karow DS, Pan D et al (2004) Spectroscopic characterization of the soluble guanylate cyclase-like heme domains from Vibrio cholerae and Thermoanaerobacter tengcongensis. Biochemistry 43:10203–10211
262. Gilles-Gonzalez MA, Gonzalez G (2005) Heme-based sensors: defining characteristics, recent developments, and regulatory hypotheses. J Inorg Biochem 99:1–22
263. Zhao Y, Hoganson C et al (1998) Structural changes in the heme proximal pocket induced by nitric oxide binding to soluble guanylate cyclase. Biochemistry 37:12458–12464

264. Paulat F, Berto TC et al (2008) Vibrational assignments of six-coordinate ferrous heme nitrosyls: new insight from nuclear resonance vibrational spectroscopy. Inorg Chem 47:11449–11451
265. Cary SPL, Winger JA et al (2006) Nitric oxide signaling: no longer simply on or off. Trends Biochem Sci 31:231–239
266. Caulton KG (1975) Synthetic methods in transition metal nitrosyl chemistry. Coord Chem Rev 14:317–355
267. Patel RP, Gladwin MT (2004) Physiologic, pathologic and therapeutic implications for hemoglobin interactions with nitric oxide. Free Radic Biol Med 36:399–401
268. Huang Z, Shiva S et al (2005) Enzymatic function of hemoglobin as a nitrite reductase that produces NO under allosteric control. J Clin Invest 115:2099–2107
269. Lancaster JR Jr, Gaston B (2004) NO and nitrosothiols: spatial confinement and free diffusion. Am J Physiol Lung Cell Mol Physiol 287:L465–L466
270. Robinson JM, Lancaster JR Jr (2005) Hemoglobin-mediated, hypoxia-induced vasodilation via nitric oxide: mechanism(s) and physiologic versus pathophysiologic relevance. Am J Respir Cell Mol Biol 32:257–261
271. Sanina NA, Syrtsova LA et al (2007) Reactions of sulfur-nitrosyl iron complexes of "g=2.03" family with hemoglobin (Hb): kinetics of Hb-NO formation in aqueous solutions. Nitric Oxide 16:181–188
272. Brunelli L, Yermilov V, Beckman JS (2001) Modulation of catalase peroxidatic and catalatic activity by nitric oxide. Free Radic Biol Med 30:709–714
273. Giuffre A, Barone MC et al (2000) Reaction of nitric oxide with the turnover intermediates of cytochrome C oxidase: reaction pathway and functional effects. Biochemistry 39:15446–15453
274. Cooper CE (2002) Nitric oxide and cytochrome oxidase: substrate, inhibitor or effector? Trends Biochem Sci 27:33–39
275. Blackmore RS, Greenwood C, Gibson QH (1991) Studies of the primary oxygen intermediate in the reaction of fully reduced cytochrome oxidase. J Biol Chem 266:19245–19249
276. Doyle MP, Herman JG, Dykstra RL (1985) Autocatalytic oxidation of hemoglobin induced by nitrite: activation and chemical inhibition. J Free Radic Biol Med 1:145–153
277. Spagnuolo C, Rinelli P et al (1987) Oxidation reaction of human oxyhemoglobin with nitrite: a reexamination. Biochim Biophys Acta 911:59–65
278. Doyle MP, Pickering RA et al (1981) Kinetics and mechanism of the oxidation of human deoxyhemoglobin by nitrites. J Biol Chem 256:12393–12398
279. Antonini E, Brunori M et al (1966) Preparation and kinetic properties of intermediates in the reaction of hemoglobin with ligands. J Biol Chem 241:3236–3238
280. Gray RD, Gibson QH (1971) The effect of inositol hexaphosphate on the kinetics of CO and O_2 binding by human hemoglobin. J Biol Chem 246:7168–7174
281. Gray RD, Gibson QH (1971) The binding of carbon monoxide to and chains in tetrameric mammalian hemoglobin. J Biol Chem 246:5176–5178
282. Wang QZ, Jacobs J et al (1991) Nitric oxide hemoglobin in mice and rats in endotoxic shock. Life Sci 49:L55–L60
283. Arnold EV, Bohle DS (1996) Isolation and oxygenation reactions of nitrosylmyoglobins. In: Lester P (ed) Methods in enzymology. Nitric oxide Part B: Physiological and pathological processes, vol 269. Academic, London
284. Addison AW, Stephanos JJ (1986) Nitrosyliron (III) hemoglobin: autoreduction and spectroscopy. Biochemistry 25:4104–4113
285. Yonetani T, Yamamoto H et al (1972) Electromagnetic properties of hemoproteins: V. Optical and electron paramagnetic resonance characteristics of nitric oxide derivatives of metalloporphyrin-apohemoprotein complexes. J Biol Chem 247:2447–2455
286. Salerno JC (1996) Nitric oxide complexes of metalloproteins: an introductory overview. In: Lancaster JR Jr (ed) Nitric oxide: principles and actions. Academic, San Diego

287. Le Brun NE, Andrews SC et al (1997) Interaction of nitric oxide with non-haem iron sites of Escherichia coli bacterioferritin: reduction of nitric oxide to nitrous oxide and oxidation of iron (II) to iron (III). Biochem J 326:173–179
288. Lee M, Arosio P et al (1994) Identification of the EPR-active iron-nitrosyl complexes in mammalian ferritins. Biochemistry 33:3679–3687
289. Kim HR, Kim TH et al (2012) Direct detection of tetrahydrobiopterin (BH4) and dopamine in rat brain using liquid chromatography coupled electrospray tandem mass spectrometry. Biochem Biophys Res Commun 419:632–637
290. Nelson MJ (1987) The nitric oxide complex of ferrous soybean lipoxygenase-1. Substrate, pH, and ethanol effects on the active-site iron. J Biol Chem 262:12137–12142
291. Rubbo H, Parthasarathy S et al (1995) Nitric oxide inhibition of lipoxygenase-dependent liposome and low-density lipoprotein oxidation: termination of radical chain propagation reactions and formation of nitrogen-containing oxidized lipid derivatives. Arch Biochem Biophys 324:15–25
292. Kennedy MC, Gan T et al (1993) Metallothionein reacts with Fe^{2+} and NO to form products with a $g = 2.039$ ESR signal. Biochem Biophys Res Commun 196:632–635
293. Flint DH, Allen RM (1996) Iron-sulfur proteins with nonredox functions. Chem Rev 96:2315–2334
294. Brzoska K, Meczynska S, Kruszewski M (2006) Iron-sulfur cluster proteins: electron transfer and beyond. Acta Biochim Pol 53:685–691
295. Cheung PY, Danial H et al (1998) Thiols protect the inhibition of myocardial aconitase by peroxynitrite. Arch Biochem Biophys 350:104–108
296. Hausladen A, Fridovich I (1994) Superoxide and peroxynitrite inactivate aconitases, but nitric oxide does not. J Biol Chem 269:29405–29408
297. Castro L, Rodriguez M, Radi R (1994) Aconitase is readily inactivated by peroxynitrite, but not by its precursor, nitric oxide. J Biol Chem 269:29409–29415
298. Haile DJ, Rouault TA et al (1992) Reciprocal control of RNA-binding and aconitase activity in the regulation of the iron-responsive element binding protein: role of the iron-sulfur cluster. Proc Natl Acad Sci USA 89:7536–7540
299. Rouault TA, Stout CD et al (1991) Structural relationship between an iron-regulated RNA-binding protein (IRE-BP) and aconitase: functional implications. Cell 64:881–883
300. Rouault TA, Haile DJ et al (1992) An iron-sulfur cluster plays a novel regulatory role in the iron-responsive element binding protein. Biometals 5:131–140
301. Drapier JC, Hibbs JB Jr (1996) Aconitases: a class of metalloproteins highly sensitive to nitric oxide synthesis. Methods Enzymol 269:26–36
302. Haile DJ, Rouault TA et al (1992) Cellular regulation of the iron-responsive element binding protein: disassembly of the cubane iron-sulfur cluster results in high-affinity RNA binding. Proc Natl Acad Sci USA 89:11735–11739
303. Gardner PR, Costantino G et al (1997) Nitric oxide sensitivity of the aconitases. J Biol Chem 272:25071–25076
304. Pantopoulos K, Weiss G, Hentze MW (1994) Nitric oxide and the post-transcriptional control of cellular iron traffic. Trends Cell Biol 4:82–86
305. Soum E, Brazzolotto X et al (2003) Peroxynitrite and nitric oxide differently target the iron-sulfur cluster and amino acid residues of human iron regulatory protein 1. Biochemistry 42:7648–7654
306. Weiss G, Goossen B et al (1993) Translational regulation via iron-responsive elements by the nitric oxide/NO-synthase pathway. EMBO J 12:3651–3657
307. Drapier JC, Hirling H et al (1993) Biosynthesis of nitric oxide activates iron regulatory factor in macrophages. EMBO J 12:3643–3649
308. Gardner PR, Fridovich I (1991) Superoxide sensitivity of the Escherichia coli aconitase. J Biol Chem 266:19328–19333
309. Navarre DA, Wendehenne D et al (2000) Nitric oxide modulates the activity of tobacco aconitase. Plant Physiol 122:573–582

310. Gupta KJ, Shah JK et al (2012) Inhibition of aconitase by nitric oxide leads to induction of the alternative oxidase and to a shift of metabolism towards biosynthesis of amino acids. J Exp Bot 63:1773–1784
311. Tortora V, Quijano C et al (2007) Mitochondrial aconitase reaction with nitric oxide, S-nitrosoglutathione, and peroxynitrite: mechanisms and relative contributions to aconitase inactivation. Free Radic Biol Med 42:1075–1088
312. Kobayashi M, Shimizu S (2000) Nitrile hydrolases. Curr Opin Chem Biol 4:95–102
313. Endo I, Nojiri M et al (2001) Fe-type nitrile hydratase. J Inorg Biochem 83:247–253
314. Nakasako M, Odaka M et al (1999) Tertiary and quaternary structures of photoreactive Fe-type nitrile hydratase from Rhodococcus sp. N-771: roles of hydration water molecules in stabilizing the structures and the structural origin of the substrate specificity of the enzyme. Biochemistry 38:9887–9898
315. Nagashima S, Nakasako M et al (1998) Novel non-heme iron center of nitrile hydratase with a claw setting of oxygen atoms. Nat Struct Biol 5:347–351
316. Huang W, Jia J et al (1997) Crystal structure of nitrile hydratase reveals a novel iron centre in a novel fold. Structure 5:691–699
317. Harrop TC, Olmstead MM, Mascharak PK (2004) Structural models of the bimetallic subunit at the A-cluster of acetyl coenzyme a synthase/CO dehydrogenase: binuclear sulfur-bridged Ni-Cu and Ni-Ni complexes and their reactions with CO. J Am Chem Soc 126:14714–14715
318. Murakami T, Nojiri M et al (2000) Post-translational modification is essential for catalytic activity of nitrile hydratase. Protein Sci 9:1024–1030
319. Odaka M, Fujii K et al (1997) Activity regulation of photoreactive nitrile hydratase by nitric oxide. J Am Chem Soc 119:3785–3791
320. Endo I, Odaka M, Yohda M (1999) An enzyme controlled by light: the molecular mechanism of photoreactivity in nitrile hydratase. Trends Biotechnol 17:244–248
321. Voloshin ON, Camerini-Otero RD (2007) The ding protein from Escherichia coli is a structure-specific helicase. J Biol Chem 282:18437–18447
322. Shestakov AF, Shul'ga YM et al (2009) Experimental and theoretical study of the arrangement, electronic structure and properties of neutral paramagnetic binuclear nitrosyl iron complexes with azaheterocyclic thyolyls having 'S-C-N type' coordination of bridging ligands. Inorg Chim Acta 362:2499–2504
323. Nunoshiba T, DeRojas-Walker T et al (1993) Activation by nitric oxide of an oxidative-stress response that defends Escherichia coli against activated macrophages. Proc Natl Acad Sci USA 90:9993–9997
324. D'Autreaux B, Tucker NP et al (2005) A non-haem iron centre in the transcription factor NorR senses nitric oxide. Nature 437:769–772
325. Hidalgo E, Bollinger JM Jr et al (1995) Binuclear[2Fe-2S] clusters in the Escherichia coli SoxR protein and role of the metal centers in transcription. J Biol Chem 270:20908–20914
326. Ding H, Demple B (2000) Direct nitric oxide signal transduction via nitrosylation of iron-sulfur centers in the SoxR transcription activator. Proc Natl Acad Sci USA 97:5146–5150
327. Stamler JS (1994) Cell 78:931
328. Butler AR, Megson IL (2002) Non-heme iron nitrosyls in biology. Chem Rev 102:1155–1166
329. Weinberg JB, Chen Y et al (2009) Inhibition of nitric oxide synthase by cobalamins and cobinamides. Free Radic Biol Med 46:1626–1632
330. Brouwer M, Chamulitrat W et al (1996) Nitric oxide interactions with cobalamins: biochemical and functional consequences. Blood 88:1857–1864
331. Bunn HF, Aster JC (2010) Pathophysiology of blood disorders. McGraw Hill, Boston
332. Sharma VS, Pilz RB et al (2003) Reactions of nitric oxide with vitamin B12 and its precursor, cobinamide. Biochemistry 42:8900–8908
333. Weinberg JB, Chen YC et al (2005) Cobalamins and cobinamides inhibit nitric oxide synthase enzymatic activity. Blood 106:2225

334. Wheatley C (2006) A scarlet pimpernel for the resolution of inflammation? The role of supratherapeutic doses of cobalamin, in the treatment of systemic inflammatory response syndrome (SIRS), sepsis, severe sepsis, and septic or traumatic shock. Med Hypotheses 67:124–142
335. Wheatley C (2007) The return of the scarlet pimpernel: cobalamin in inflammation II-cobalamins can both selectively promote all three nitric oxide synthases (NOS), particularly iNOS and eNOS, and, as needed, selectively inhibit iNOS and nNOS. J Nutr Environ Med 16:181–211
336. Forsyth JC, Mueller PD et al (1993) Hydroxocobalamin as a cyanide antidote: safety, efficacy and pharmacokinetics in heavily smoking normal volunteers. Clin Toxicol 31:277–294
337. Houeto P, Borron SW et al (1996) Pharmacokinetics of hydroxocobalamin in smoke inhalation victims. Clin Toxicol 34:397–404
338. Sharina I, Sobolevsky M et al (2012) Cobinamides are novel coactivators of nitric oxide receptor that target soluble guanylyl cyclase catalytic domain. J Pharmacol Exp Ther 340:723–732
339. Lewandowska H, Brzoska K et al (2010) [Dinitrosyl iron complexes–structure and biological functions]. Postepy Biochem 56:298–304
340. Meczynska S, Lewandowska H et al (2008) Variable inhibitory effects on the formation of dinitrosyl iron complexes by deferoxamine and salicylaldehyde isonicotinoyl hydrazone in K562 cells. Hemoglobin 32:157–163
341. Lo BM, Nuccetelli M et al (2001) Human glutathione transferase P1-1 and nitric oxide carriers; a new role for an old enzyme. J Biol Chem 276:42138–42145
342. Lewandowska H, Meczynska S et al (2007) Crucial role of lysosomal iron in the formation of dinitrosyl iron complexes in vivo. J Biol Inorg Chem 12:345–352
343. Toledo JC Jr, Bosworth CA et al (2008) Nitric oxide-induced conversion of cellular chelatable iron into macromolecule-bound paramagnetic dinitrosyliron complexes. J Biol Chem 283:28926–28933
344. Hickok JR, Sahni S et al (2011) Dinitrosyliron complexes are the most abundant nitric oxide-derived cellular adduct: biological parameters of assembly and disappearance. Free Radic Biol Med 51:1558–1566
345. Pedersen JZ, De Maria F et al (2007) Glutathione transferases sequester toxic dinitrosyl-iron complexes in cells. A protection mechanism against excess nitric oxide. J Biol Chem 282:6364–6371
346. Hidalgo E, Ding H, Demple B (1997) Redox signal transduction via iron-sulfur clusters in the SoxR transcription activator. Trends Biochem Sci 22:207–210
347. Chiang RW, Woolum JC, Commoner B (1972) Biochim Biophys Acta 257:452
348. Pellat C, Henry Y, Drapier JC (1990) IFN-gamma-activated macrophages: detection by electron paramagnetic resonance of complexes between L-arginine-derived nitric oxide and non-heme iron proteins. Biochem Biophys Res Commun 166:119–125
349. Ueno T, Suzuki Y et al (1999) In vivo distribution and behavior of paramagnetic dinitrosyl dithiolato iron complex in the abdomen of mouse. Free Radic Res 31:525–534
350. Ignarro LJ, Ross G, Tillisch J (1991) Pharmacology of endothelium-derived nitric oxide and nitrovasodilators. West J Med 154:51–62
351. Wang YX, Legzdins P et al (2000) Vasodilator effects of organotransition-metal nitrosyl complexes, novel nitric oxide donors. J Cardiovasc Pharmacol 35:73–77
352. Saklayen MG, Mandal AK (1996) Nitric oxide: biological and clinical perspectives. Int J Artif Organs 19:630–632
353. Armstrong RN (1997) Structure, catalytic mechanism, and evolution of the glutathione transferases. Chem Res Toxicol 10:2–18
354. Mannervik B, Alin P et al (1985) Identification of three classes of cytosolic glutathione transferase common to several mammalian species: correlation between structural data and enzymatic properties. Proc Natl Acad Sci USA 82:7202–7206
355. Litwack G, Ketterer B, Arias IM (1971) Ligandin: a hepatic protein which binds steroids, bilirubin, carcinogens and a number of exogenous organic anions. Nature 234:466–467

356. Adler V, Yin Z et al (1999) Regulation of JNK signaling by GSTp. EMBO J 18:1321–1334
357. Kampranis SC, Damianova R et al (2000) A novel plant glutathione S-transferase/peroxidase suppresses Bax lethality in yeast. J Biol Chem 275:29207–29216
358. Dulhunty A, Gage P et al (2001) The glutathione transferase structural family includes a nuclear chloride channel and a ryanodine receptor calcium release channel modulator. J Biol Chem 276:3319–3323
359. Caccuri AM, Antonini G et al (1999) Proton release on binding of glutathione to alpha, mu and delta class glutathione transferases. Biochem J 344(Pt 2):419–425
360. Ford PC (2008) Polychromophoric metal complexes for generating the bioregulatory agent nitric oxide by single- and two-photon excitation. Acc Chem Res 41:190–200
361. Rose MJ, Mascharak PK (2008) Fiat Lux: selective delivery of high flux of nitric oxide (NO) to biological targets using photoactive metal nitrosyls. Curr Opin Chem Biol 12:238–244
362. Silva JJN, Osakabe AL et al (2007) In vitro and in vivo antiproliferative and trypanocidal activities of ruthenium NO donors. Br J Pharmacol 152:112–121
363. Haas KL, Franz KJ (2009) Application of metal coordination chemistry to explore and manipulate cell biology. Chem Rev 109:4921–4960
364. Vanin AF, Vanin AF (2008) P103. Dinitrosyl iron complexes with thiolate ligands as future medicines. Nitric Oxide 19:67
365. Vanin AF, Mokh VP et al (2007) Vasorelaxing activity of stable powder preparations of dinitrosyl iron complexes with cysteine or glutathione ligands. Nitric Oxide 16:322–330
366. Lakomkin VL, Vanin AF et al (2007) Long-lasting hypotensive action of stable preparations of dinitrosyl-iron complexes with thiol-containing ligands in conscious normotensive and hypertensive rats. Nitric Oxide 16:413–418
367. Fujii S, Yoshimura T (2000) Detection and imaging of endogenously produced nitric oxide with electron paramagnetic resonance spectroscopy. Antioxid Redox Signal 2:879–901
368. Yoshimura T, Yokoyama H et al (1996) In vivo EPR detection and imaging of endogenous nitric oxide in lipopolysaccharide-treated mice. Nat Biotechnol 14:992–994
369. Yasui H, Fujii S et al (2004) Spinnokinetic analyses of blood disposition and biliary excretion of nitric oxide (NO)-Fe (II)-N-(Dithiocarboxy)sarcosine complex in rats: BCM-ESR and BEM-ESR studies. Free Radic Res 38:1061–1072
370. Chen YJ, Ku WC et al (2008) Nitric oxide physiological responses and delivery mechanisms probed by water-soluble Roussin's red ester and $\{Fe(NO)_2\}^{10}$ DNIC. J Am Chem Soc 130:10929–10938
371. Dillinger SAT, Schmalle HW et al (2007) Developing iron nitrosyl complexes as NO donor prodrugs. Dalton Trans 3562–3571
372. Huerta S, Chilka S, Bonavida B (2008) Nitric oxide donors: novel cancer therapeutics. Int J Oncol 33:909–927
373. Wecksler SR, Mikhailovsky A et al (2006) Single- and two-photon properties of a dye-derivatized Roussin's red salt ester (Fe_2(mu-RS)$_2$(NO)$_4$) with a large TPA cross section. Inorg Chem 46:395–402
374. Wecksler SR, Mikhailovsky A et al (2006) A two-photon antenna for photochemical delivery of nitric oxide from a water-soluble, dye-derivatized iron nitrosyl complex using NIR light. J Am Chem Soc 128:3831–3837
375. Wecksler SR, Hutchinson J, Ford PC (2006) Toward development of water soluble dye derivatized nitrosyl compounds for photochemical delivery of NO. Inorg Chem 45:1192–1200
376. Wecksler S, Mikhailovsky A, Ford PC (2004) Photochemical production of nitric oxide via two-photon excitation with NIR light. J Am Chem Soc 126:13566–13567
377. Zheng Q, Bonoiu A et al (2008) Water-soluble two-photon absorbing nitrosyl complex for light-activated therapy through nitric oxide release. Mol Pharm 5:389–398
378. Fry NL, Rose MJ et al (2010) Ruthenium nitrosyls derived from tetradentate ligands containing carboxamido-N and phenolato-O donors: syntheses, structures, photolability, and time dependent density functional theory studies. Inorg Chem 49:1487–1495

379. Fry NL, Mascharak PK (2011) Photoactive ruthenium nitrosyls as NO donors: how to sensitize them toward visible light. Acc Chem Res 44:289–298
380. Fry NL, Mascharak PK (2012) Photolability of NO in designed metal nitrosyls with carboxamido-N donors: a theoretical attempt to unravel the mechanism. Dalton Trans 41:4726–4735
381. Afshar RK, Patra AK, Mascharak PK (2005) Light-induced inhibition of papain by a {Mn-NO}6 nitrosyl: identification of papain-SNO adduct by mass spectrometry. J Inorg Biochem 99:1458–1464
382. Eroy-Reveles AA, Leung Y et al (2008) Near-infrared light activated release of nitric oxide from designed photoactive manganese nitrosyls: strategy, design, and potential as NO donors. J Am Chem Soc 130:4447–4458
383. Szundi I, Rose MJ et al (2006) A new approach for studying fast biological reactions involving nitric oxide: generation of NO using photolabile ruthenium and manganese NO donors. Photochem Photobiol 82:1377–1384
384. Ghosh K, Eroy-Reveles AA et al (2004) Reactions of NO with Mn (II) and Mn (III) centers coordinated to carboxamido nitrogen: synthesis of a manganese nitrosyl with photolabile NO. Inorg Chem 43:2988–2997
385. Madhani M, Patra AK et al (2006) Biological activity of designed photolabile metal nitrosyls: light-dependent activation of soluble guanylate cyclase and vasorelaxant properties in rat aorta. J Med Chem 49:7325–7330
386. Patra AK, Rose MJ et al (2004) Photolabile ruthenium nitrosyls with planar dicarboxamide tetradentate N (4) ligands: effects of in-plane and axial ligand strength on NO release. Inorg Chem 43:4487–4495
387. Rose MJ, Fry NL et al (2008) Sensitization of ruthenium nitrosyls to visible light via direct coordination of the dye resorufin: trackable NO donors for light-triggered NO delivery to cellular targets. J Am Chem Soc 130:8834–8846
388. Rose MJ, Olmstead MM, Mascharak PK (2007) Photosensitization via dye coordination: a new strategy to synthesize metal nitrosyls that release NO under visible light. J Am Chem Soc 129:5342–5343
389. Rose MJ, Mascharak PK (2008) A photosensitive $\{Ru\text{-}NO\}^6$ nitrosyl bearing dansyl chromophore: novel NO donor with a fluorometric on/off switch. Chem Commun 3933–3935
390. Lim MH, Lippard SJ (2007) Metal-based turn-on fluorescent probes for sensing nitric oxide. Acc Chem Res 40:41–51
391. Soh N, Imato T et al (2002) Ratiometric direct detection of nitric oxide based on a novel signal-switching mechanism. Chem Commun 2650–2651
392. Hilderbrand SA, Lippard SJ (2004) Nitric oxide reactivity of fluorophore coordinated carboxylate-bridged diiron (II) and dicobalt (II) complexes. Inorg Chem 43:5294–5301
393. Hilderbrand SA, Lippard SJ (2004) Cobalt chemistry with mixed aminotroponiminate salicylaldiminate ligands: synthesis, characterization, and nitric oxide reactivity. Inorg Chem 43:4674–4682
394. Lim MH, Lippard SJ (2004) Fluorescence-based nitric oxide detection by ruthenium porphyrin fluorophore complexes. Inorg Chem 43:6366–6370
395. Lim MH, Kuang C, Lippard SJ (2006) Nitric oxide-induced fluorescence enhancement by displacement of dansylated ligands from cobalt. Chembiochem 7:1571–1576
396. Smith RC, Tennyson AG, Lippard SJ (2006) Polymer-bound dirhodium tetracarboxylate films for fluorescent detection of nitric oxide. Inorg Chem 45:6222–6226
397. Hilderbrand SA, Lim MH, Lippard SJ (2004) Dirhodium tetracarboxylate scaffolds as reversible fluorescence-based nitric oxide sensors. J Am Chem Soc 126:4972–4978
398. Lim MH (2007) Preparation of a copper-based fluorescent probe for nitric oxide and its use in mammalian cultured cells. Nat Protoc 2:408–415
399. Lim MH, Lippard SJ (2006) Fluorescent nitric oxide detection by copper complexes bearing anthracenyl and dansyl fluorophore ligands. Inorg Chem 45:8980–8989

400. Smith RC, Tennyson AG et al (2005) Conjugated polymer-based fluorescence turn-on sensor for nitric oxide. Org Lett 7:3573–3575
401. Lim MH, Lippard SJ (2005) Copper complexes for fluorescence-based NO detection in aqueous solution. J Am Chem Soc 127:12170–12171
402. Ford PC, Fernandez BO, Lim MD (2005) Mechanisms of reductive nitrosylation in iron and copper models relevant to biological systems. Chem Rev 105:2439–2455
403. Smith RC, Tennyson AG et al (2006) Conjugated metallopolymers for fluorescent turn-on detection of nitric oxide. Inorg Chem 45:9367–9373
404. Xing C, Yu M et al (2007) Fluorescence turn-on detection of nitric oxide in aqueous solution using cationic conjugated polyelectrolytes. Macromol Rapid Commun 28:241–245
405. Do L, Smith RC et al (2006) Luminescent properties of water-soluble conjugated metallopolymers and their application to fluorescent nitric oxide detection. Inorg Chem 45:8998–9005
406. Franz KJ, Singh N et al (2000) Aminotroponiminates as ligands for potential metal-based nitric oxide sensors. Inorg Chem 39:4081–4092
407. Lim MH, Wong BA et al (2006) Direct nitric oxide detection in aqueous solution by copper (II) fluorescein complexes. J Am Chem Soc 128:14364–14373
408. Lim MH, Xu D, Lippard SJ (2006) Visualization of nitric oxide in living cells by a copper-based fluorescent probe. Nat Chem Biol 2:375–380
409. Ouyang J, Hong H et al (2008) A novel fluorescent probe for the detection of nitric oxide in vitro and in vivo. Free Radic Biol Med 45:1426–1436
410. Vanin AF (2009) Dinitrosyl iron complexes with thiolate ligands: physico-chemistry, biochemistry and physiology. Nitric Oxide 21:1–13
411. Keese MA, Bose M et al (1997) Dinitrosyl-dithiol-iron complexes, nitric oxide (NO) carriers in vivo, as potent inhibitors of human glutathione reductase and glutathione-S-transferase. Biochem Pharmacol 54:1307–1313
412. Vasilieva SV, Moshkovskaya EY et al (2004) Genetic signal transduction by nitrosyl-iron complexes in Escherichia coli. Biochemistry 69:883–889
413. Tran NG, Kalyvas H et al (2011) Phenol nitration induced by an $\{Fe(NO)_2\}^{10}$ dinitrosyl iron complex. J Am Chem Soc 133:1184–1187
414. Bellota-Anton C, Munnoch J et al (2011) Spectroscopic analysis of protein Fe-NO complexes. Biochem Soc Trans 39:1293–1298